

Department of Environment, Land and Infrastructure Engineering Master Thesis in Georesources and Geoenergy Engineering

Capillary Breakthrough Pressure Measurement of Hydrogen and Development of a Laboratory Protocol

By

Temurbek Ismoilov

Student number: s316149

Supervisor: Prof. Francesca Verga

Nacer Benlalam

Nicolo' Santi Vasile

This page intentionally left blank

Abstract

This thesis addresses the critical challenge of secure and efficient underground hydrogen storage (UHS), a key component in the global transition to clean energy and the achievement of carbon neutrality goals under the Paris Agreement. Hydrogen, as a zero-emission energy carrier, holds vast potential across multiple sectors; however, its small molecular size and high diffusivity pose significant leakage risks during storage. Ensuring the integrity of caprocks that seal underground reservoirs is therefore essential.

The core focus of this research is the assessment of experimental methods dedicated to evaluating caprock sealing efficiency through representative measurement of capillary threshold pressure a fundamental parameter that determines a caprock's hydraulic ability to prevent hydrogen migration. A comprehensive review of existing laboratory methods was conducted, with emphasis on the most widely adopted practices for experimentally evaluating different types of threshold pressure.

Building on this foundation, a standardized laboratory protocol was developed and implemented using a customized experimental setup capable of measuring breakthrough pressure for hydrogen as well as other gases such as CO₂, CH₄ and N₂. The laboratory system components were described. Based on which, the adopted breakthrough pressure measurement protocol, namely step-by-step test, was outlined. To this end, targeted technical recommendations are proposed to enhance measurement reliability and repeatability, including improvements in temperature control, pressure stability and system automation.

The developed protocol provides a robust, repeatable and accurate methodology for assessing caprock sealing efficiency, which is important for selecting suitable UHS sites, defining maximum operational pressures and minimizing storage-related risks. The outcomes of this work contribute significantly to advancing safe and efficient UHS technologies, supporting the broader deployment of hydrogen as a clean energy solution and facilitating sustainable energy transition.

Table of Contents

Abstra	ct	3
List of	figures	4
List of	tables	6
1. In	ntroduction	7
1.1.	The Scope of the Thesis	10
2. U	Inderground Hydrogen Storage and Caprock Sealing Efficiency	11
2.1.	Hydrogen properties	12
2.2.	Caprock characterizations	15
2.3.	Trapping mechanisms of hydrogen	16
2.4.	Caprock sealing efficiency	20
2.5.	Factors affecting caprock sealing efficiency	21
2.6.	Stages of gas capillary breakthrough	28
3. L	aboratory tests	31
3.1.	Mercury injection porosimeter test	32
3.2.	Step-by-step test (Standard test)	35
3.3.	Residual capillary pressure test (Snap-off test)	37
3.4.	Dynamic threshold pressure test	40
3.5.	Comparison of the laboratory tests	44
4. R	eview of best practices of step-by-step test	45
4.1.	Case study 1	45
4.2.	Case study 2	48
4.3.	Case study 3	52
5. L	aboratory work to measure threshold pressure	54
5.1.	Detailed description of laboratory setup components	56
5.2.	Test procedure	61
5.3.	Recommendations	73
6. C	onclusion	74
Bibliog	graphy	76
List	of figures	
_	1. The key technologies for the energy transition in the oil and industry [2]	
_	2. Global hydrogen projects and investment overview in 2024 [3]	
-	3. Hydrogen storage in porous reservoir rocks [3]4. Aquifer schematic (a) before H2 injection, and (b) after H2 injection [7]	
	5. Phase diagram and density of hydrogen [8]	

Figure 6. Geologic challenges to UHS [9]	.14
Figure 7. Underground hydrogen storage mechanisms [14]	.17
Figure 8. Hydrogen solubility as function of pressure (a), brine salinity (b), temperature (c). Hydrogen	
solubility in diesel (d) [14]	.18
Figure 9. Schematic of capillary sealing mechanism in a pore throat of caprock [15]	
Figure 10. (a) Hydrogen density as a function of pressure and temperature; (b) densities of hydrogen,	
methane, carbon dioxide and water as a function of pressure and temperature [16]	22
Figure 11. Hydrogen and water viscosities as a function of pressure and temperature [16]	22
Figure 12. Interfacial tension of gas-water system as a function of pressure and temperature [16]	23
Figure 13. Diffusivity of hydrogen in (a) water and (b) different hydrocarbons as a function of pressure	;
and temperature [16]	
Figure 14. Contact angles of (a) hydrogen-brine quartz and (b) hydrogen-brine-aged quartz systems as	a
function of pressure, temperature and stearic acid concentration [16]	
Figure 15. Hydrogen-rock interfacial tension as a function of (a) pressure and temperature, (b) stearic a	cid
concentration at 323 K [16]	.25
Figure 16. Hydrogen-water-sandstone and carbon dioxide – water-sandstone capillary pressures in	
drainage as a function of water saturation [16]	.25
Figure 17. (a) hydrogen-water-sandstone drainage relative permeability curves as a function of water	
saturation. (b) water-sandstone drainage relative permeability curves for various gases as a function of	
water saturation [16]	.26
Figure 18. Gas-water-sandstone drainage mobility ratio curves for hydrogen and carbon dioxide as a	
function of water saturation [16]	.27
Figure 19. Drainage and Imbibition curves [19]	.28
Figure 20. Drainage and Imbibition phenomena in caprocks [18]	.29
Figure 21. Definitions of breakthrough pressure, capillary entry pressure and snap-off pressure given by	У
Hildenbrand et al. [19]	.30
Figure 22. Apparatus for Mercury Capillary Pressure measurement [22]	.33
Figure 23. Interpretation of the Mercury injection porosimeter test data [23]	.34
Figure 24. Interpretation of the data from Mercury injection porosimeter test to obtain the capillary enti-	ry
pressure of the caprock [23]	.34
Figure 25. Schematic flow diagram of the high-pressure core holder apparatus [24]	.36
Figure 26. Cross section of the high-pressure core holder used for standard test [24]	.36
Figure 27. Data obtained from a standard test [15]	.37
Figure 28. Scheme of the two experimental modes. A) constant upstream pressure mode; B) introduction	on
of gas into a fixed upstream volume mode; downstream volume fixed in both instances. P1, P2 are	
pressures at upstream and downstream respectively [20]	.38
Figure 29. Gas breakthrough curve for methane including the permeability curve calculated [20]	.39
Figure 30. Scheme of the experimental parameters recorded and their interpretation in terms of capillar	У
processes. A) pressure history of a gas breakthrough experiment; B) capillary pressure of the gas phase	as
a function of water saturation; C) relative permeability curve for the gas phase as a function of water	
saturation during drainage (I) and imbibition (II) [20]	.39
Figure 31. Conceptual model of Darcy's law	.40
Figure 32. The experimental setup of the dynamic threshold pressure test, modified from [25]	.41
Figure 33. Schematic diagram illustrating pressure zones during gas injection phase	.42
Figure 34. on the left: typical production curve recorded at the outlet; on the right: typical production	
curve recorded at the outlet when the pressure drop applied is lower than the capillary entry pressure	.43
Figure 35. Diagram of the laboratory apparatus used for the standard test [26]	.45
Figure 36. Schematic representation of gas permeability measurement setup and Klinkenberg Effect,	
modified from [27]	
Figure 37. Schematic of apparatus for breakthrough pressure measurement [15]	.49

Figure 38. Modified schematic of apparatus for improved clarity in breakthrough pressure m	
Figure 39. Schematic of apparatus with recommended optimizations for breakthrough pressu	
measurements	52
Figure 40. Schematic of Lab Setup (Left) and Hassler-Type Coreholder (Right)	52
Figure 41. Experimental laboratory setup	55
Figure 42. Schematic diagram of the laboratory setup	56
Figure 43. Schematic of the coreholder: 1) Inlet tubing 2) Sample seats 3) Confining fluid 4)	Heating
plates 5) Core sample 6) Rubber sleeve 7) Confining pressure line 8) Outlet tubing	57
Figure 44. Receptacle with downstream line port and ventilation line port	58
Figure 45. User interface of the customized software	
Figure 46. Pump filament with brine phase. Red valve is closed, green valve is open, and blu	
indicate the presence of brine	•
Figure 47. Sample saturation phase. Red valves are closed, green valves are open and blue tu	bing lines
indicate the presence of brine	•
Figure 48. Use of tissue paper to detect brine leakage at inaccessible void spaces within the cand at tubing joints during the saturation phase	oreholder
Figure 49. Brine removal phase. Red valves are closed, green valves are open and blue tubin	
indicate the presence of brine	_
Figure 50. Pump filament with hydrogen phase. Red valve is closed, green valve is open, and tubing lines indicate the presence of hydrogen	l purple
Figure 51. Applying initial reservoir conditions, bypass line is open.	
Figure 52. At time 0, the system at initial reservoir conditions, inlet and outlet pressures equa	
pressure. BPR set to reservoir pressure. Delta P is zero, bypass line is closed	
Figure 53. Hydrogen leak detection using the bubble method and gas detector at high-risk loc	
including coreholder inlet and outlet, pump joints and tubing connections	
Figure 54. Gas bubble appearance at the receptacle indicating gas breakthrough	
Figure 55. Modified diagram of the laboratory setup	
List of tables	
Table 1. Comparison of UHS types [3]	11
Table 2. Physicochemical properties of H2, CH4 and CO2 [7]	13
Table 3. Composition of Hastelloy B and Hastelloy C and their compatibility with different g	gases, data
taken from [12]	
Table 4. Main physical and mechanical properties of shale caprocks relevant to UHS [13]	
Table 5. Overview of the potential impacts of adsorption and desorption processes on various	
properties of caprocks relevant to UHS [13]	
Table 6. Overview of different terminologies of capillary pressures found in literature [20]	30
Table 7. Comparison of the laboratory tests	44
Table 8. Specifications of the laboratory setup	56

1. Introduction

Because of the serious consequences of global warming and climate change, the world energy systems are changing significantly, with an energy transition focused on moving from fossil fuels to renewable energy sources. Around 200 countries signed the Paris Agreement which establishes an ambitious and necessary goal to take immediate action against climate change to secure the planet's future. According to its article 2 (a), the objective of this agreement is to "Holding the increase in the global average temperature to well below 2°C above pre-industrial levels and pursuing efforts to limit the temperature increase to 1.5°C above pre-industrial levels, recognizing that this would significantly reduce the risks and impacts of climate change" [1].

Fossil fuels, such as oil, gas and coal currently serve as the main energy sources. To reduce carbon footprint or emissions, the oil and gas industry is undergoing an energy transition that integrates artificial intelligence (AI), renewable energy, hydrogen and carbon capture utilization and storage (CCUS), as shown in Figure 1.

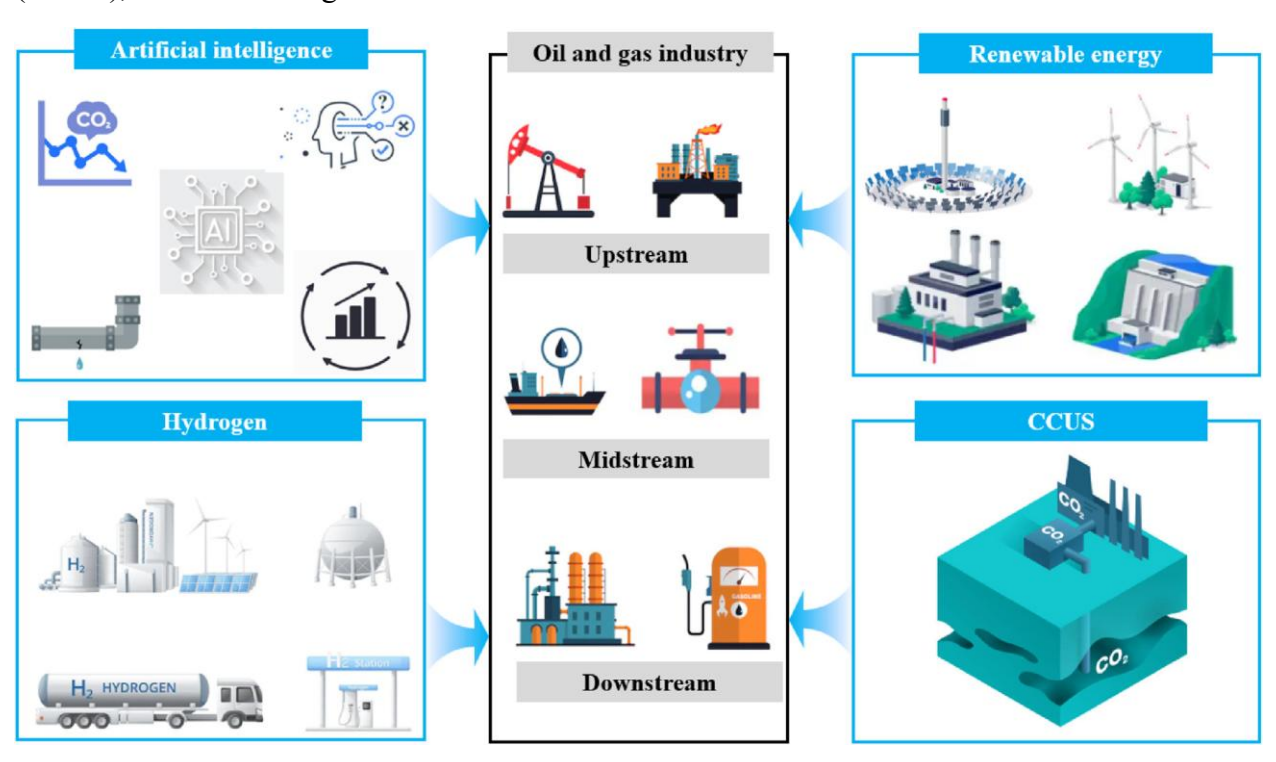


Figure 1. The key technologies for the energy transition in the oil and industry [2]

Hydrogen can be derived from both renewable and non-renewable sources, its production can be categorized into three main types based in its energy source and production method: grey, blue and green hydrogen. Grey hydrogen is derived from hydrocarbons through processes like coal gasification, steam methane reforming, or methane pyrolysis without CCUS. Blue hydrogen is produced similarly to grey hydrogen but incorporates CCUS to mitigate emissions. Green hydrogen is generated through water electrolysis powered by renewable electricity. Combining CCUS with hydrogen production offers a practical method to reduce CO2 emissions in the oil and gas industry. Captured CO2 can be utilized for enhanced oil recovery (EOR) or stored in subsurface saline aquifers [2].

Renewable energy sources such as solar and wind are influenced by seasonal variations, wind intensity and geographic conditions. These factors, combined with fluctuating annual energy demands, can lead to either surpluses or shortages of renewable energy. Because of the unpredictable nature of renewable sources, hydrogen offers a reliable alternative that is not

dependent on seasons. Hydrogen can be stored and utilized during periods of high demand, aligning with the Power-to-X (PtX) concept. As the most abundant and lightest element in nature, it has the highest energy content. Hydrogen can be seen as a key replacement for fossil fuels because it can be burned, stored and used similarly. This makes hydrogen an attractive option for decarbonizing high-demand energy intensive industries such as shipping, aviation and steel and iron production [3]. Interest in hydrogen production projects is growing globally, according to Statista, hydrogen storage capacity is projected to reach 10 terawatt-hours (TWh) by 2035, with announced projects indicating a potential capacity of 40 TWh [4]. As of 2024 there are 1572 clean hydrogen projects worldwide (Figure 2). For instance, the NEOM green hydrogen production project, biggest in the world and located in Saudi Arabia, which will be in operation by the end of 2030 and will produce 600 tonnes of green hydrogen per day using renewable wind and solar energy [5].



Figure 2. Global hydrogen projects and investment overview in 2024 [3]

The smooth operation of large-scale hydrogen value chains requires adequate storage capacity and performance. Geological storage is considered as the most effective method for large-scale, long-term hydrogen storage. Hydrogen can be stored in underground geological formations such as aquifers, salt caverns and depleted oil and gas reservoirs (Figure 3). Underground Hydrogen Storage (UHS) plays an important role in enhancing electricity system stability, integrating renewable energy sources and supporting decarbonization goals. Underground natural gas storage (UGS) shares several similarities with UHS, and knowledge gained in UGS (methane) and CCUS (CO2) can be applied to UHS projects such as site selection, storage techniques, monitoring and managing injection and withdrawal cycles. A key difference is that hydrogen exhibits higher chemical reactivity compared to natural gas (methane), meaning that hydrogen can participate in

biological, microbial and chemical activities. By 2050 hydrogen may become a major energy vector supplementing or replacing coal and natural gas [3].

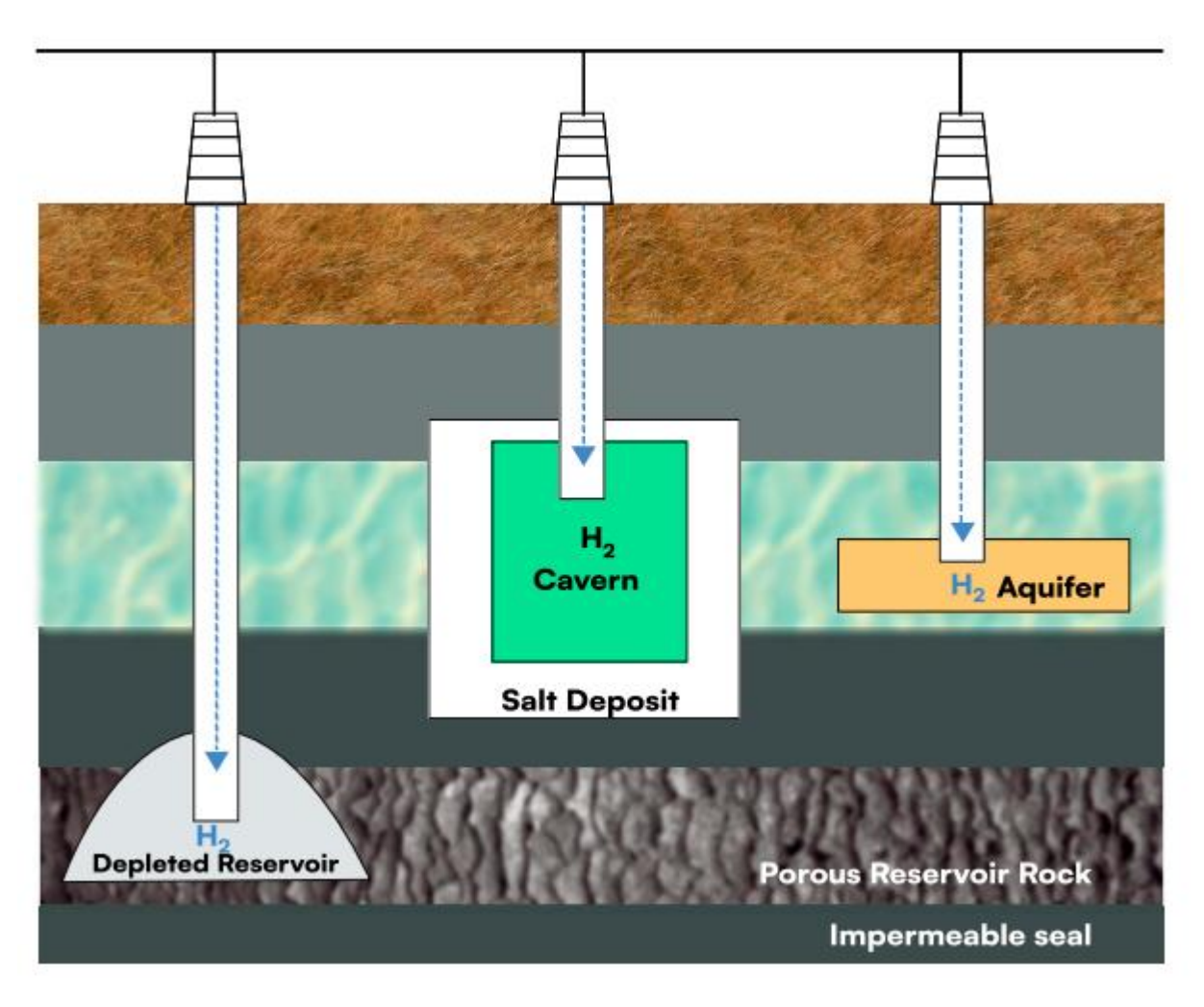


Figure 3. Hydrogen storage in porous reservoir rocks [3]

The caprock, an impermeable seal overlying the reservoir rock, is critical for safely storing fluids in UHS, UGS and CCUS systems, ensuring containment for required time durations. Thorough characterization of the caprock is essential for the success of these projects. The caprock's ability to retain gas depends on its capacity to withstand overpressure beyond the reservoir's discovery pressure without exceeding its structural limits. Gas retention in a water-saturated caprock is driven by capillary forces at the gas-water interface, which prevent gas leakage. In the absence of water saturation in the caprock, gas could escape at a rate determined by the caprock's permeability to gas. For the UGS, UHS and CCUS, accurately predicting the overpressure that reservoir can sustain before gas displaces water from the caprock is crucial, as this directly impacts storage capacity. The maximum sealing efficiency of the caprock is denoted as the breakthrough pressure which defines the pressure at which gas fully penetrates the caprock compromising its sealing capacity. Underestimation of breakthrough pressure can result in injecting a smaller fluid volume than the reservoir can safely accommodate, leading to inefficient use of the storage site (reduced storage capacity) and higher cost per unit of stored fluid (economic feasibility). Overestimation of breakthrough pressure can lead to gas leakage, reducing storage efficiency and posing environmental, safety and regulatory risks. Therefore, accurate measurement of breakthrough pressure is important and laboratory measurements remain the most reliable method, as it is difficult to obtain accurate values of breakthrough pressure in the field. Additionally, hydrogen unique properties, such as high diffusivity, leakage potential and risk of hydrogen embrittlement

necessitate rigorous caprock assessment to ensure safe and efficient storage, minimizing economic and environmental risks. Understanding the caprock properties and its sealing efficiency is important for ensuring safe and effective UHS.

This thesis first reviews underground hydrogen options and properties of the caprock, then compares laboratory methods for threshold pressure measurement, analyzes best practices from case studies, and finally develops a standardized laboratory protocol for breakthrough pressure measurement using a customized setup.

1.1. The Scope of the Thesis

This thesis evaluates the sealing efficiency of caprock for Underground Hydrogen Storage (UHS) to ensure reliable hydrogen containment. This study focuses on the following:

- Comprehensive analysis of petrophysical and geomechanical properties of the caprock and factors affecting its sealing efficiency
- Review of laboratory test methods available in the literature for caprock sealing evaluation, analyzing their procedures, experimental setups, strengths and limitations.
- Comparison of test methods to determine the most accurate and reliable for caprock sealing assessment
- Analysis of three case studies from the literature to identify best practices for conducting step-by-step test.
- Development of standardized laboratory protocol for a step-by-step test using a customized laboratory setup and providing recommendations to improve the setup

2. Underground Hydrogen Storage and Caprock Sealing Efficiency

Underground gas storage (UGS) offers several advantages, including:

- larger capacity and safer storage than above-ground storage facilities
- efficient use of surface space
- cost-effectiveness
- availability of suitable geological formations worldwide.

In the energy industry, the common practice is to store methane during summer months (approximately seven months) when production exceeds demand and withdraw it in winter (about five months) when demand surpasses production. Currently out of 642 UGS projects, nearly 75% are depleted oil and gas reservoirs, 13 % are aquifers and 12% are caverns [6]. UHS is possible in depleted reservoirs, aquifers and salt caverns, each option has unique characteristics that influence the hydrogen storage efficiency and suitability. A comparison of storage sites for UHS is presented in Table 1.

Storage Type Depleted Gas Aquifer Salt Cavern Geographical availability High in most countries High in most countries Limited Small to medium Storage capacity Medium to large Large to very large Suitability for hydrogen Pure hydrogen under Experience from Proven depleted field still under study, hydrogenmethane proven study 45-80% 20-33% Cushion gas requirement 50-60% Number of cycles per year 1-2 1-2 10 High Low **Chemical conversion rate** Average **Operational pressures** 15-285 bar 30-315 bar 35-270 bar Seasonal **Operational type** Seasonal Frequent Seismic risk High Low Average Withdrawal rate High Average Low Leakage risk High High Low **Development** / operation Average Average High cost **Key considerations / factors** Microbial activity, Microbial activity, fluid-Salt domes are fluid-rock rock composition, gas favored over bedded composition, tightness (new storage salt operational conditions development) deposits

Table 1. Comparison of UHS types [3]

Caverns are artificially created chambers within saltdomes or bedded salt deposits through a controlled process of injection of freshwater from the surface to dissolve salt, resulting in a large cylindrical cavity. A typical salt cavern may extend up to 2000 m in depth, with a volume of around 1 million m3, a height of 300 to 500 m and a diameter of 50 to 100 m. These caverns are often considered the optimal choice for UHS due to their low gas permeability, favorable rheological properties that ensure good sealing and their capacity to manage stresses through viscous-plastic deformation. The sealing properties of evaporite minerals (such as anhydrite, gypsum and rock salt) and the mechanical stability of salt caverns make them well-suited for medium-term and short-term storage. Additionally, the high salinity of these environments typically inhibits in-situ

microbial activity, as microorganisms struggle to thrive in such conditions. Key factors in the UHS design in salt caverns include the depth and thickness of the salt beds, the composition of surrounding rock in the reservoir and the solubility of the salt [7].

Aquifer is a subsurface formation of porous, water-saturated rock, commonly found in sedimentary basins worldwide, presenting a feasible option for UHS. The storage mechanism for aquifer and depleted hydrocarbon reservoirs are similar because they both rely on porous and permeable rock formations. For effective UHS in aquifers, following geological features are required: a porous rock matrix to store hydrogen, an impermeable caprock to prevent buoyancy-driven upward migration and an anticlinal trap to limit lateral hydrogen flow, ensuring stable plume development around the injection well (Figure 4). Aquifers require a larger cushion gas volume (cushion gas is the non-recoverable gas left in the reservoir to maintain pressure for efficient gas injection and withdrawal). Due to the limited availability of geological data the use of aquifers for hydrogen storage is often more costly than that of depleted hydrocarbon reservoirs [7].

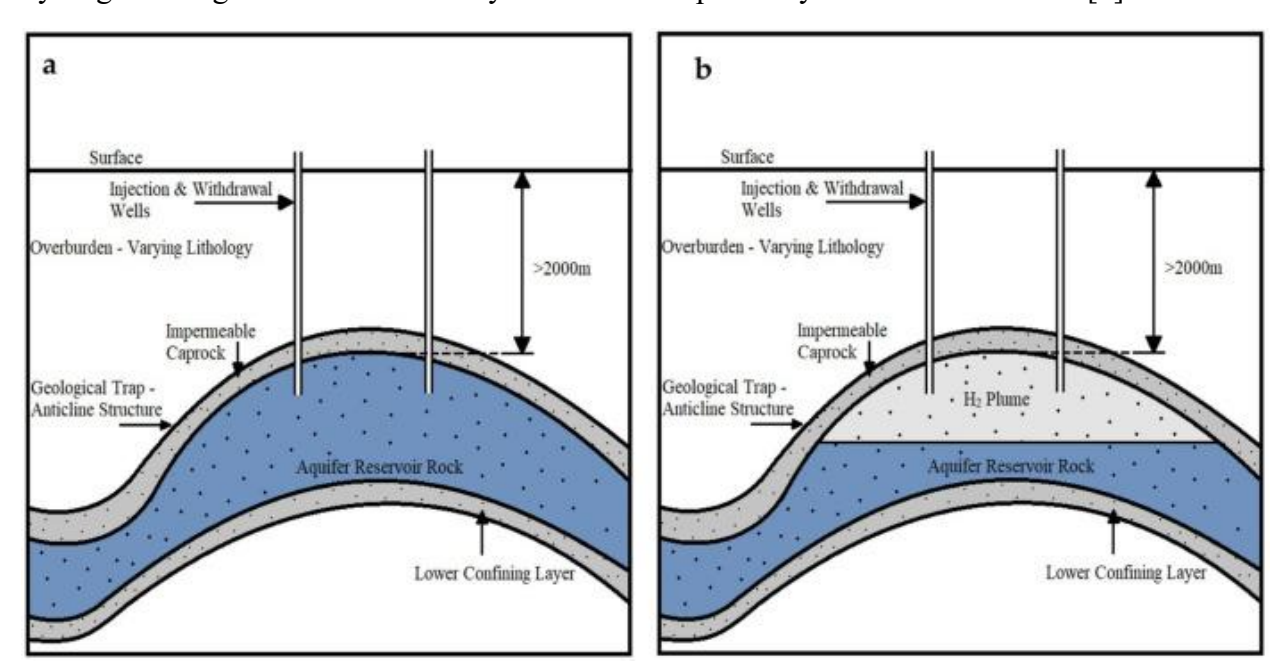


Figure 4. Aquifer schematic (a) before H2 injection, and (b) after H2 injection [7].

Depleted hydrocarbon reservoirs can be considered as a portion of an aquifer, where only residual water saturation exists within the pore which are predominantly occupied with trapped hydrocarbons (oil and gas). These reservoirs are simpler to develop, manage and sustain due to existing infrastructure with proven reliability. In contrast to aquifer based UHS, depleted gas reservoirs benefit from residual gas, which minimizes the need for large volumes of cushion gas to maintain operational pressure. However, if the residual gas mixes with the injected hydrogen, it may reduce the purity of the stored gas during withdrawal.

2.1. Hydrogen properties

Hydrogen is the lightest gas in nature and it has no color and odor. Hydrogen is about 8 times less dense than methane and 22 times less dense than carbon dioxide necessitating greater storage volume and pressure to contain an equivalent mass of gas. The low viscosity and molecular weight of hydrogen increase its potential for leakage. In a hydrogen-methane-brine system, hydrogen's lower solubility compared to methane reduces losses from dissolution, but its high diffusivity increases losses through diffusion and dispersion. The high diffusivity of hydrogen poses

challenges for UHS in caverns because cavern rocks are less effective at sealing compared to aquifers and depleted oil and gas reservoirs. The solubility of hydrogen in water increases with pressure but decreases with increasing **temperature and salinity**. The solubility of hydrogen is similar to that of methane and significantly lower than that of carbon dioxide. As shown in Table 2 hydrogen's physical properties differ significantly from those of methane and carbon dioxide and conclusions obtained from UGS and CCS cannot be directly applied to UHS [7].

Properties	H ₂	CH ₄	CO ₂
Molecular weight, g/mol	2.016	16.043	44.09
Density at standard conditions, kg/m ³	0.089	0.657	1.98
Viscosity at standard conditions, Pa*s	0.89*10 ⁻⁵	1.1*10 ⁻⁵	1.49*10 ⁻⁵
Solubility in pure water at standard conditions, g/l	16*10 ⁻⁴	22.7*10 ⁻³	1.45*10 ⁻³
Boiling point, ⁰ C	-253	-162	-78.44
Critical temperature, ⁰ C	-239.95	-82.3	-31
Critical pressure, atm	12.8	45.79	72.79
Heating value range, kJ/g	120 - 142	50 - 55.5	-
Diffusion in pure water at standard conditions, m ² /s	5.13*10 ⁻⁹	1.85*10 ⁻⁹	1.60*10 ⁻⁹
Flash point, ⁰ C	-253	-188	-
Flammability range, ⁰ C	4 - 75	5 - 15	-

Table 2. Physicochemical properties of H2, CH4 and CO2 [7]

The density of hydrogen strongly depends on temperature and pressure conditions. At atmospheric pressure and temperature below -259.14 °C hydrogen has a density of 76 kg/m3 and it has solid state, while under other conditions hydrogen is in gaseous state (above -252.87 °C) with a density of only 0.089 kg/m3. Its liquid state with a density of 70.8 kg/m³ exists at narrow temperature range. As a consequence, hydrogen is typically stored underground in its gaseous state. As pressure increases its density will rapidly increase (Figure 5). To maximize the storage capacity, selecting a storage site with low temperature and high pressure is the most suitable [8].

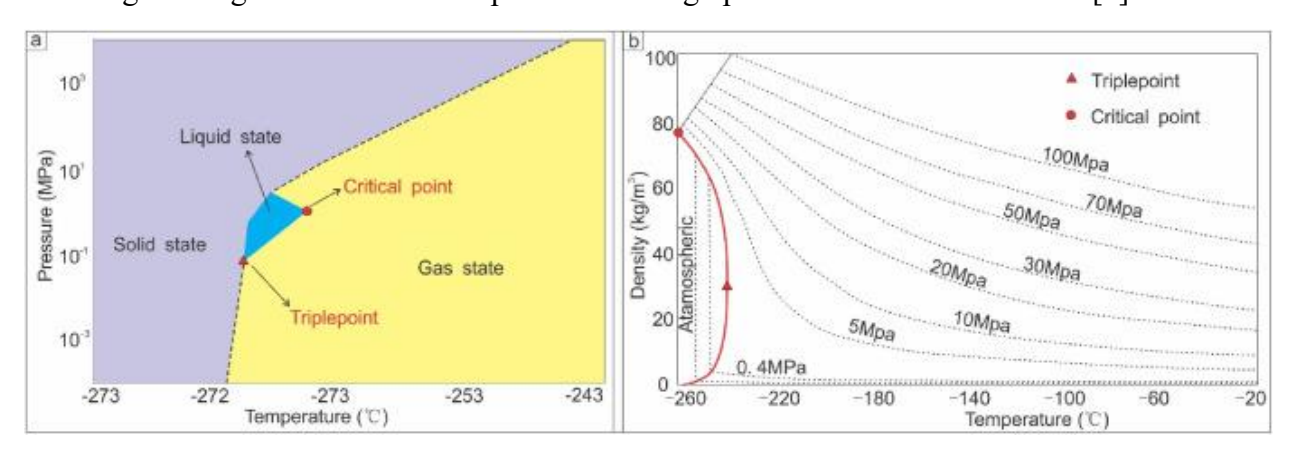


Figure 5. Phase diagram and density of hydrogen [8]

UHS encounters numerous uncertainties and technical challenges. Ensuring the integrity of the reservoir is crucial to prevent hydrogen leakage and maintain storage volume and purity. This is primarily related to storage integrity, which depends on the integrity of the reservoir, wellbore components and caprock. The geological uncertainties associated with UHS are shown in Figure 6.

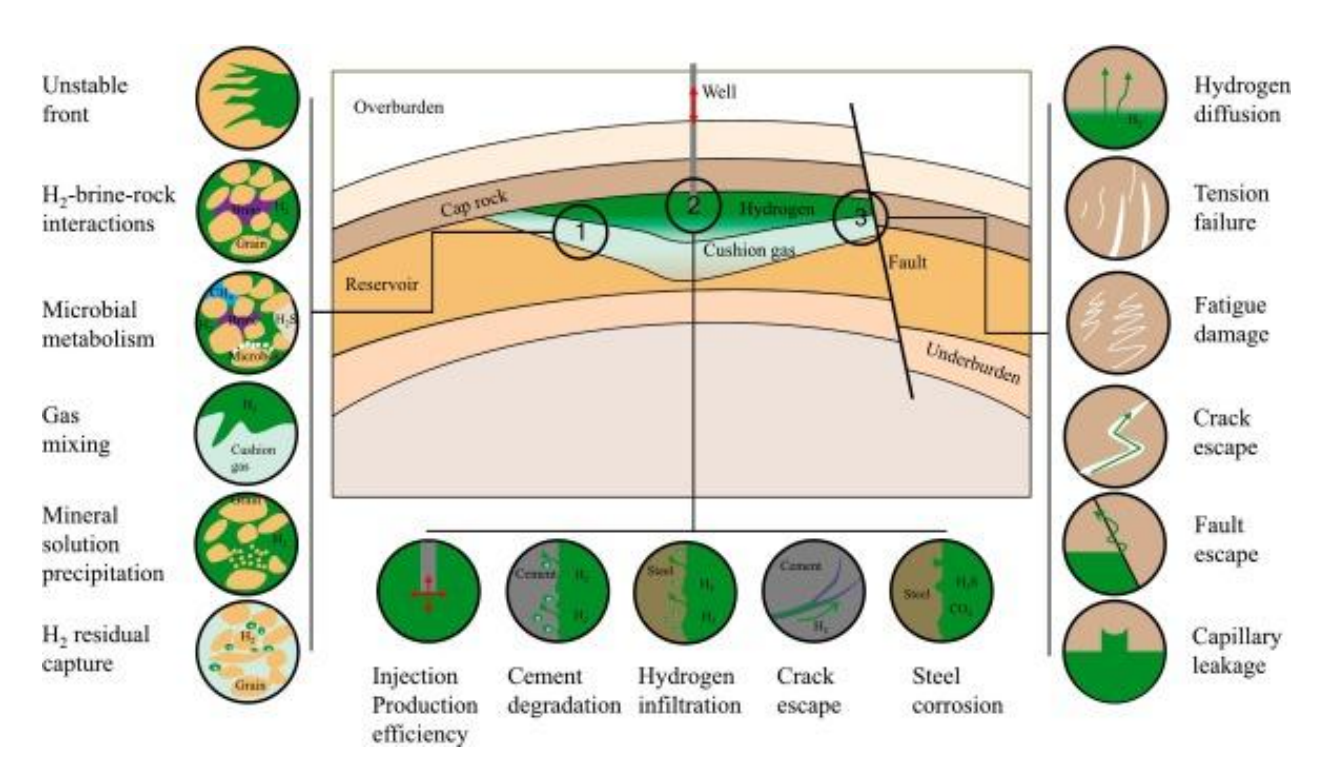


Figure 6. Geologic challenges to UHS [9]

UHS involves complex fluid interactions, with the injected hydrogen pushing out existing brine or hydrocarbons. These interactions are influenced by fluid properties, reservoir rock characteristics and phase interactions. Hydrogen has low density and viscosity and these properties can lead to issues like **gravity segregation**, **unstable flow and lateral spreading** making the recovery of the injected hydrogen difficult. In depleted oil and gas reservoir injected hydrogen is prone to mixing with cushion gases and any remaining hydrocarbons. Whether hydrogen flow is miscible or immiscible depends on the reservoir type:

- In aquifer, the absence of a cushion gas can create conditions where **capillary trapping** and **viscous fingering** occur, which can trap hydrogen and reduce the efficiency during withdrawal.
- In depleted oil and reservoirs, where the miscible flow is present, hydrogen can mix with existing gases and this reduces the purity of hydrogen.

Viscous fingering is a phenomenon where hydrogen moves unevenly and this increases the risk of residual trapping and hydrogen dissolution in the brine. The capillary fingering is more dominant in multiphase hydrogen-brine systems mainly due to significant interfacial tension between brine and hydrogen at low flowrates [10].

Hydrogen embrittlement refers to the process by which hydrogen due to small molecular size and high diffusivity penetrate metal lattices, reducing ductility and stiffness and increasing the risk of material failure under high pressure conditions. Material selection for UHS wellbores demands more rigorous standards and requirements than for UGS and CCS. Studies recommend deploying **polyethylene tubing, cathodic protection and coated tubing** for wellbores used in hydrogen injection. A comprehensive assessment of sealing integrity, alloying elements, steel grades and tubing types along with the development of low-cost high-strength, hydrogen embrittlement resistant materials is crucial for preventing leakage and ensuring cost-effective, long-term sealing integrity. High-strength carbon steels may also perform well in hydrogen environments, especially in hydrogen sulfide rich sour natural gases. All surface and subsurface equipment and casing

strings for UHS facilities must meet hydrogen compatibility standards and withstand mechanical load variations over multiple injection and withdrawal cycles [10].

Hastelloy

Hastelloy is a family of nickel-based superalloys and it is an ideal material for UHS applications due to its exceptional corrosion resistance and mechanical stability. Depending on the chemical composition, Hastelloy is classified into various grades: B and C. Hastelloy C276 is a nickelmolybdenum-chromium alloy with additions of tungsten and cobalt, designed to provide superior performance in corrosive and high-temperature conditions. Its chemical composition: approximately 57% nickel, 14.5–16.5% chromium, 15–17% molybdenum, 3–4.5% tungsten, 4– 7% iron, up to 2.5% cobalt, and trace amounts of silicon (0.08%), manganese (1%), carbon (0.01%), vanadium (0.35%), phosphorus (0.025%), and sulfur (0.01%) [11]. The high nickel content ensures excellent resistance to a wide range of corrosive substances, while molybdenum and chromium enhance resistance to pitting, crevice corrosion and stress-corrosion cracking as well as high-temperature stability. The addition of tungsten and cobalt further improves the mechanical properties of the alloy, enabling it to withstand high temperatures up to 1040 C without significant loss of mechanical strength. Hastelloy is compatible with hydrogen, methane, carbon dioxide, hydrogen sulfide and other gases as indicated in Table 3. By selecting Hastelloy for wellbore pipelines and equipment, we can improve the safety, operational efficiency and long-term reliability of UHS systems.

Table 3. Composition of Hastelloy B and Hastelloy C and their compatibility with different gases, data taken from [12]

Material	Composition, %							Compatibility					
	Cr	Fe	С	Si	Co	Mn	V	Mo	P	S	Ni	W	with H ₂ , CO ₂ ,
													H ₂ S, CH ₄
Hastelloy B	1	4 -	0.12	1	2.5	1	0.2-	26 -	0.04	0.03	Remainder	0	Recommended
		6					0.6	30					
Hastelloy C	15.5 -	4.5	0.12	1	2.5	1	0.2-	16 -	0.04	0.03	Remainder	3.75-	Recommended
	17.5	-					0.4	18				5.25	
		7.5											

2.2. Caprock characterizations

Reservoir rocks like sandstones or limestones store gas within their pore volume, where its buoyancy causes it to rise and be trapped beneath an overlying caprock, typically tight shale. Shale caprocks are characterized by a range of physical and mechanical properties that make them suitable for UHS, including porosity, permeability and mechanical strength. Understanding these properties is critical not only for assessing the caprock's response to stresses induced by hydrogen injection and withdrawal, but also for evaluating its long-term sealing efficiency (Table 4).

Table 4. Main physical and mechanical properties of shale caprocks relevant to UHS [13]

Property	Definition	Typical
		Range/Values
Porosity	Measure of the void spaces in the rock	2% to 15%
Permeability	Ability of the rock to transmit fluids	10 ⁻¹⁸ to 10 ⁻¹² m ²
Compressive	The maximum compressive stress the rock can withstand	10 to 100 MPa
Strength		
Tensile Strength	The maximum tensile stress the rock can withstand	<10 Mpa
Young' Modulus	The measure of the stiffness of the rock	5 to 50 GPa
Poisson's Ratio	Ratio of lateral strain to axial strain	0.1 to 0.3
Anisotropy	Variation in properties in different directions due to the layered	Significant
	structure	

Wettability	Tendency of the rock surface to be wetted by a fluid	Water-wet
Capillary Pressure	Pressure difference across the interface of two immiscible fluids in the	High
	pores	

Shale caprocks contain various minerals such as clays, calcite, quartz and pyrite, with calcite being more abundant, while pyrite is found in smaller amounts (2-8 %). Depending on the mineral composition and degree of compaction the porosity of shale caprocks may range from 2 % to 15 %. Permeability of shale caprocks is generally very low, varying from 10⁻¹⁸ to 10⁻¹² m² [13].

The mechanical strength of shale caprocks is determined by their mineral composition and the presence of natural fractures, shales with higher clay mineral content typically show lower mechanical strength compared to those with higher quartz content. Higher carbonate content in shales increases brittleness, reducing plastic deformation capacity, whereas shales with higher clay mineral content are highly sensitive to stress variations. Due to layered structure nature shale caprocks exhibit significant anisotropy which affects their mechanical behavior and fluid flow properties. Clay minerals like smectite and illite can undergo swelling or shrinkage when exposed to water or other fluids, altering porosity and permeability. This response can cause fatigue damage over time, promoting microcracking and fracture development. Over extended periods, thermal maturation of organic matter can increase brittleness, making the caprock formation more prone to mechanical failure and elevating the risk of wellbore instability. Creep deformation may occur in more ductile shales, leading to long-term subsidence or changes in porosity and permeability. Pressure solution can induce further compaction of shales rich in clay or carbonate minerals, reducing porosity and permeability over time. Recent research shows that hydrogen does not undergo geochemical reactions with calcite, exhibiting negligible alteration to its pore structure even after a year. Geochemical concerns during hydrogen injection include crack initiation and fault reactivation, and these concerns can trigger induced seismicity, threatening storage site integrity and nearby infrastructure. The injection of hydrogen into the reservoir increases the pore pressure within the rock and this elevated pore pressure reduces the effective stress acting on fault planes (Terzaghi's principle). Mitigation strategies for fault reactivation and induced seismicity in UHS projects mainly focus on the control of gas injection flow rates to manage reservoir pressure and minimize associated risks. Continuous monitoring of pressure and real-time adjustment of injection parameters are important in maintaining pressure below thresholds that could trigger seismicity [13].

2.3. Trapping mechanisms of hydrogen

The trapping mechanisms for hydrogen in UHS vary depending on the reservoir type. Unlike CCS, solubility, residual and mineral trapping are less desirable for hydrogen storage. Instead, hydrogen trapping is primarily controlled by displacement forces (viscous, capillary and gravitational), operational parameters (injection and withdrawal cycles) and site-specific conditions (mineralogy, pressure and temperature). In aquifers, gravitational forces predominantly influence fluid distribution due to the significant density difference between water and hydrogen. In viscous-dominated regimes, instability from the high mobility ratio may cause fingering. Fingering refers to the unstable finger-like patterns of fluid displacement that occur when less viscous fluid (hydrogen) displaces a more viscous fluid (water) in porous medium. When hydrogen is injected into UHS sites, its behavior is governed by the following trapping mechanisms: structural, residual, dissolution/solubility, mineral, adsorption/absorption as shown in Figure 7 [10] [14].

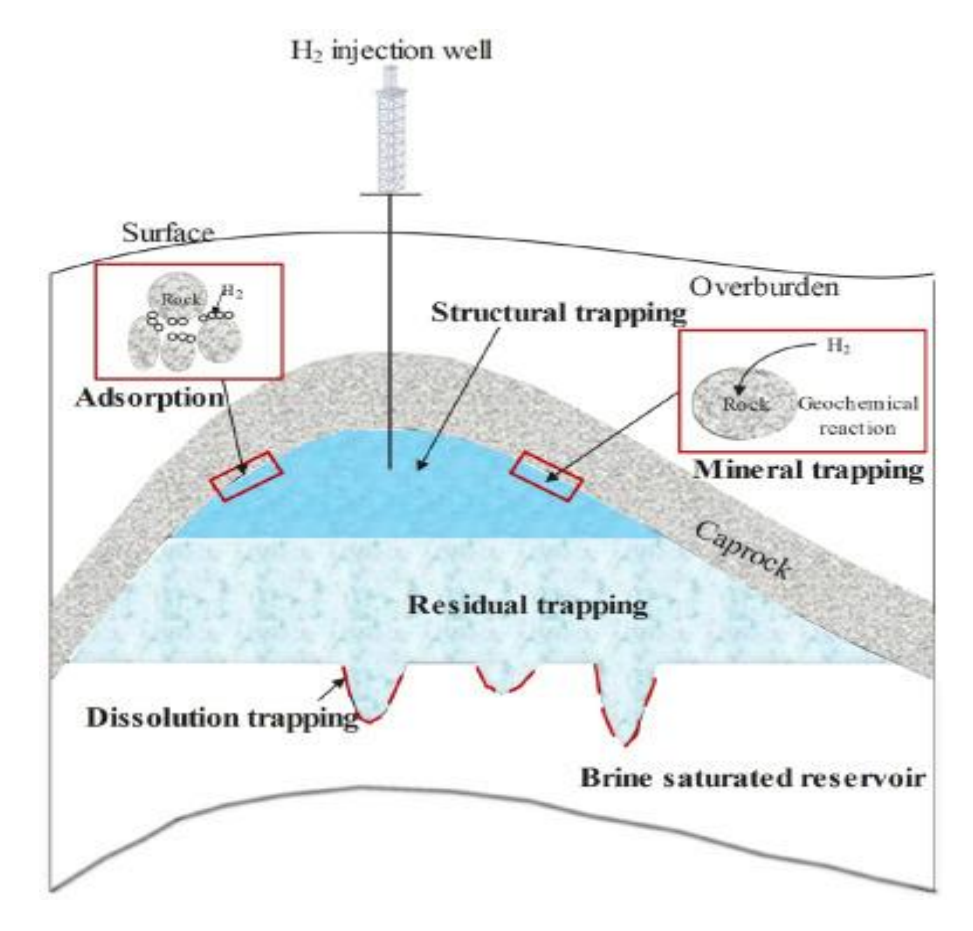


Figure 7. Underground hydrogen storage mechanisms [14]

<u>Structural trapping</u> is a primary mechanism for trapping hydrogen in geological formations. It occurs when injected hydrogen accumulates below the impermeable caprock. The column height of trapped gas beneath the caprock is determined by the balance between buoyancy and capillary forces, which in turn depend on:

- hydrogen-water interfacial tension and contact angle (both depend on water salinity, operating pressure and temperature);
- pore throat radius;
- density difference between water and hydrogen (the higher is the density difference the higher is the buoyancy force)

If the balance between buoyancy and capillary forces is compromised the risk of hydrogen leak arises. Another critical phenomenon **Buoyant microseepage** influences hydrogen migration through caprock pore networks. This phenomenon occurs when gas molecules overcome capillary forces at localized weak points in the caprock or along microfractures and diffuse upward by buoyancy. Buoyant microseepage has been observed in CCS projects due to prolonged overpressure in reservoir, cyclic gas injection and withdrawal, and it must be taken seriously in UHS [13].

Residual trapping is a secondary mechanism where hydrogen is entrapped in porous media by capillary forces. This process depends on rock wettability which is characterized by the contact angle. According to Young-Laplace law, small pores and poorly connected pore systems generate high capillary pressures and residual saturation, leading to significant hydrogen loss within the reservoir as it becomes unrecoverable. However, some residual trapped hydrogen may be recoverable during subsequent injection and withdrawal cycles, depending on **capillary forces**, **pore geometry and wettability** [14].

<u>Dissolution or solubility trapping</u> involves the dissolution of injected hydrogen into saline formation water in the aquifers, which increases trapping capacity but leads to hydrogen loss during withdrawal. **Hydrogen dissolution depends on the brine salinity, pressure and temperature conditions.** Under UHS conditions, hydrogen solubility in water increases with pressure but decreases with salinity, temperature has negligible impact on hydrogen solubility. The effects of pressure, salinity and temperature on hydrogen solubility are shown in Figure 8 (a), (b) and (c), respectively. In the hydrogen-methane-brine system, hydrogen loss due to dissolution is minimal, however the solubility of hydrogen in hydrocarbon liquids (diesel) is one order of magnitude higher than in water (Figure 8 (d)). This emphasizes the importance of considering hydrogen dissolution losses in depleted oil and gas reservoirs [14].

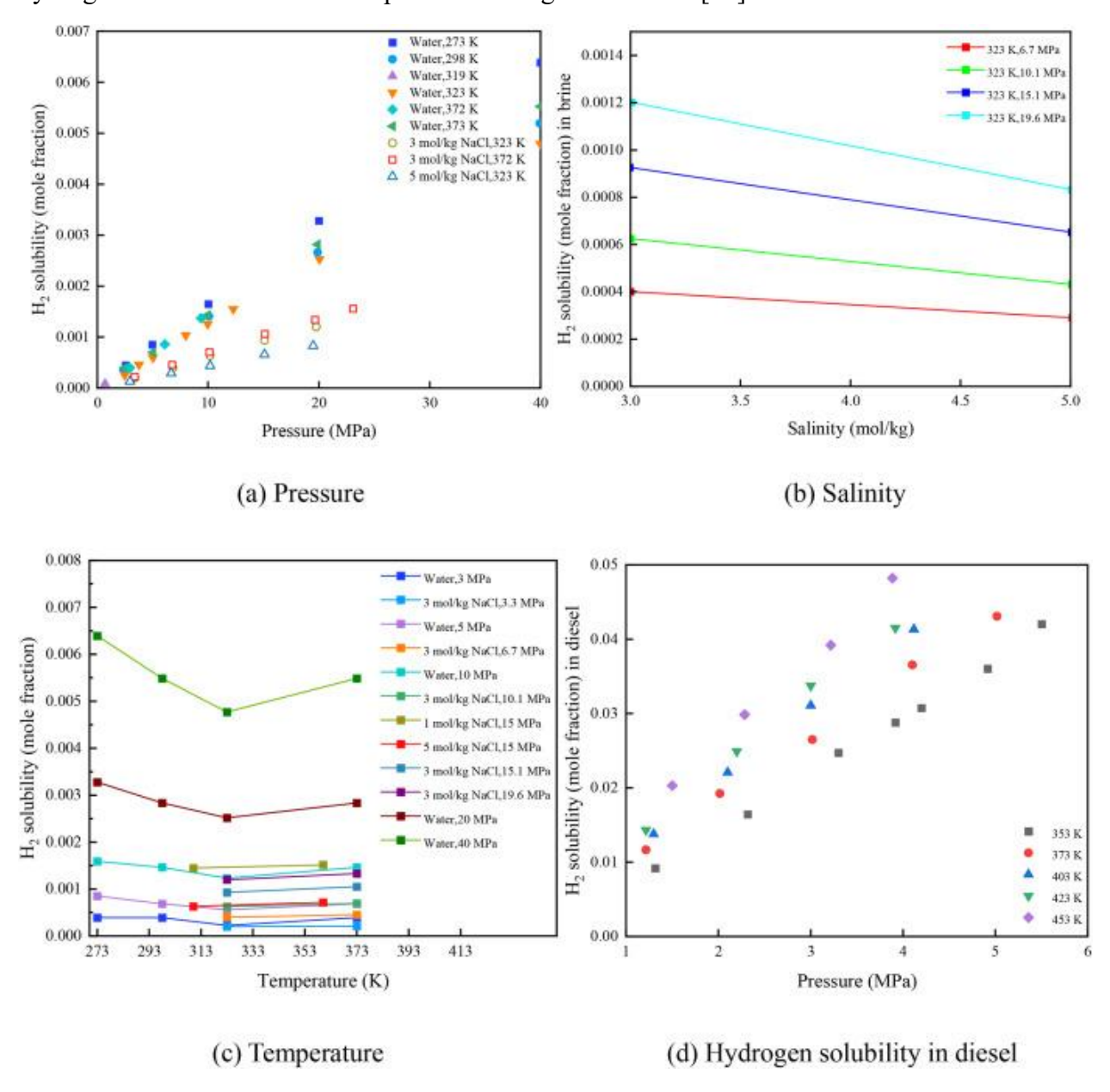


Figure 8. Hydrogen solubility as function of pressure (a), brine salinity (b), temperature (c). Hydrogen solubility in diesel (d) [14]

<u>Mineral trapping</u> occurs when injected hydrogen interacts with formation minerals and fluids, altering petrophysical properties and geomechanical stability. In CCS, mineral trapping is considered the safest carbon capture mechanism, but in UHS context it reduces both hydrogen content and hydrogen recovery. This process is affected by temperature, salinity and the chemical

composition of the formation rocks. Rock rich in quartz, potash feldspar, silicates and clay minerals exhibit minimal reactivity with hydrogen and formations mainly composed by these minerals are suitable sites for UHS [14].

Adsorption and absorption are influenced by the physical and chemical properties of the caprock, including its mineral composition, pore structure and organic matter content. Adsorption involves the process where hydrogen molecules adhere to the surface of the rock's pores. This process is mainly governed by van der Waals forces. In contrast to adsorption, absorption involves the penetration of hydrogen molecules into the bulk matrix of the shale caprock. Absorption can lead to swelling and structural changes in the shale matrix, particularly in clay-rich caprocks. Hydrogen reaction with certain minerals and organic materials in the caprock affect absorption. Understanding the processes of adsorption and absorption in shale caprocks is important for optimizing hydrogen storage, as these processes can significantly impact the geomechanical behavior of caprocks. For example, hydrogen absorption may cause swelling, whereas desorption could trigger shrinkage cracking in the caprock, potentially increasing the pore pressure and reducing the effective stress in shale caprocks. This can potentially lead to changes in the mechanical stability of the formation. Swelling reduces the permeability of shale, hindering fluid flow through caprock and thus enhancing its sealing efficiency. Moreover, changes in pore pressure and mechanical stress from adsorption and absorption can influence the initiation and propagation of fractures within the shale. General overview of the effects of adsorption and desorption processes on caprock properties is provided on Table 5.

Table 5. Overview of the potential impacts of adsorption and desorption processes on various mechanical properties of caprocks relevant to UHS [13]

Property	Adsorption impact	Desorption impact	Additional notes
Swelling	Increases due to hydrogen uptake, leading to higher pore	Decreases as hydrogen is released, potentially	Swelling can affect the mechanical stability of the caprock, impacting UHS
	pressure and reduced stress	causing shrinkage	integrity
Permeability	Reduces due to reduction in pore space and fluid flow pathways	Increases as shrinkage opens up pore spaces	Critical for fluid transport and gas extraction efficiency, influencing UHS performance
Fracture Propagation	Increases in pore pressure can initiate and propagate fractures	Reduces pore pressure can stabilize existing fractures	Important for hydraulic fracturing operations and maintaining UHS geomechanical strength
Mechanical Strength	Decreases due to swelling and increased pore pressure	Potentially increases as desorption reduces internal stress	Mechanical strength is crucial for the integrity of storage formations and UHS stability
Chemical Interactions	Hydrogen adsorption can lead to chemical alterations in minerals and organic matter	Desorption may reverse some chemical changes	Chemical interactions can affect long- term stability and storage capacity, impacting UHS
Thermal Conductivity	May decrease due to changes in pore structure and mineral composition	Can increase as desorption restores the original pore structure	Thermal properties are important for temperature management in UHS sites
Elastic Modulus	Reduces as swelling affects the rigidity of the caprock	Can be restored partially as desorption reduces swelling	Elastic modulus impacts the deformation behavior under stress, affecting UHS geomechanical strength
Porosity	Decreases due to swelling and pore space reduction	Increases as desorption opens pore spaces	Porosity is a key factor in determining storage capacity and fluid flow in UHS
Hydraulic Conductivity	Reduces as swelling decreases pore connectivity	Increases as desorption improves pore connectivity	Hydraulic conductivity affects the movement of fluids through the caprock, impacting UHS efficiency
Capillary Pressure	Increases due to reduced pore sizes and increased surface tension effects	Decreases as pore sizes increase with desorption	Capillary pressure influences fluid distribution and retention in the caprock, crucial for UHS

The study of trapping mechanisms in UHS faces significant technical challenges, including geological complexities, variable injection rates, caprock integrity uncertainties, data availability and modeling techniques.

2.4. Caprock sealing efficiency

The injected gas in the reservoir, being less dense than brine or oil, is trapped under hydrostatic conditions, where an equilibrium exists between the buoyant forces driving the gas upward and the capillary forces within the caprock that resist gas migration (structural trapping). The caprock, fully saturated with brine, creates a barrier that impedes upward gas movement. Sealing capacity of caprock is determined by the capillary forces at the interface between the wetting phase (brine water), which fully saturates the caprock and the nonwetting phase (gas) in the reservoir. This capillary sealing mechanism is given in Figure 9, which shows a pore throat with a curved interface separating water and gas within caprock. Pn is pressure of gas, Pw is pressure of water and Pc is the capillary pressure across the gas and water meniscus in a pore throat. It is the capillary pressure that prevents the penetration of gas into the caprock through slow Darcy flow. When the pressure difference between the gas and water exceeds the capillary pressure at a pore throat, gas will advance along the channel until it reaches the next smaller pore throat. When the differential pressure across the caprock overcomes the capillary pressures of a series of interconnected pore throats of arbitrarily large sizes, a continuous flow of gas will be formed and consequently a slow Darcy flow will occur. This differential pressure is regarded as the capillary breakthrough pressure or breakthrough pressure of the caprock and it is important parameter for assessing the sealing efficiency of the caprock.

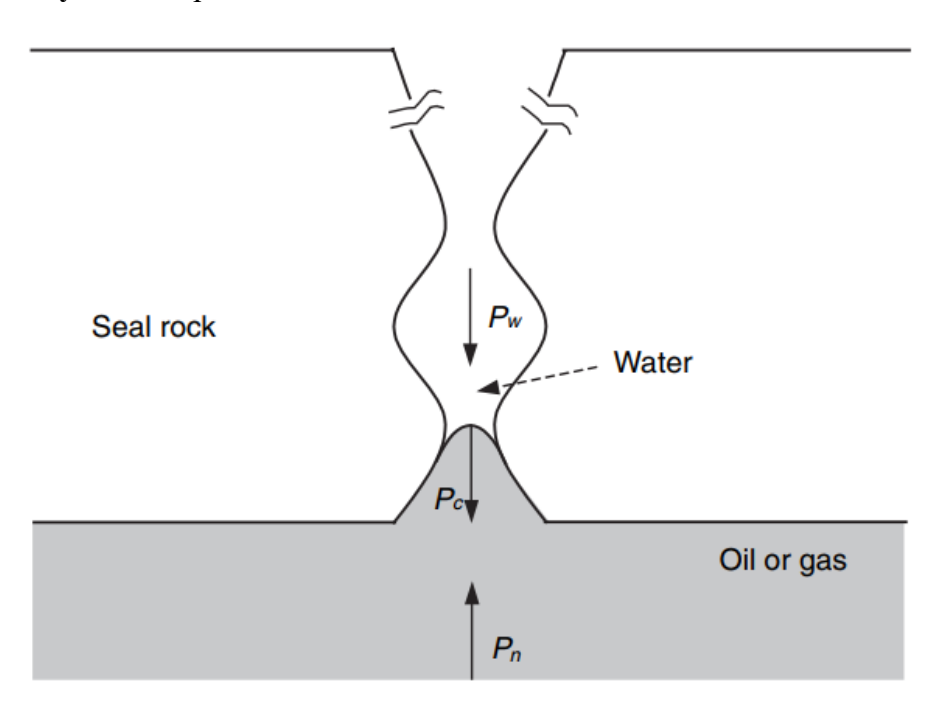


Figure 9. Schematic of capillary sealing mechanism in a pore throat of caprock [15]

The capillary pressure (Pc) across a single pore throat can be described by the Young-Laplace equation (1):

$$P_c = P_n - P_w = \frac{2\sigma}{r} \cos\theta$$
 Equation 1

where:

- σ is the interfacial tension (IFT) between the nonwetting phase (hydrogen gas) and wetting phase (water),
- r is the equivalent radius of the pore throat,
- θ is the contact angle.

From equation 1, it is clear that capillary pressure is directly proportional to interfacial tension between the two phases and inversely proportional to the pore throat radius. The contact angle, which indicates the wettability of the solid surface, also plays an important role in determining the magnitude of the capillary pressure.

Breakthrough pressure has applications in many areas including oil and gas reservoir evaluation prior to exploration, basin analysis, hydrocarbon secondary migration assessment, selection of suitable geological formations for gas storage. In UHS and CCS, the sealing efficiency of the caprock must be carefully evaluated to prevent gas leakage. This involves determining an injection pressure that keeps the differential pressure across the caprock below its breakthrough pressure. If this threshold is exceeded, the injected gas may permeate the caprock, establish a continuous gas phase within interconnected pore networks and migrate upward through Darcy flow. To mitigate this risk, selecting an appropriate injection pressure is important. Additionally, quantifying the migration rate due to such flow is crucial for assessing potential risks and understanding the behavior of the system if the caprock's integrity is compromised. In UGS, the common practice for safe storage is to keep pressure of the injected gas below the original reservoir pressure. The assumption is that the caprock, which originally contained oil and gas, has sufficiently high sealing capacity to prevent gas leakage through it. However, when hydrocarbons (methane and oil) are replaced by the injected hydrogen, the lower interfacial tension of the injected hydrogen/brine system relative to that of the original hydrocarbon/brine system results in a lower capillary pressure of the caprock. Consequently, the sealing capacity of the same caprock is compromised in hydrogen storage and needs to be re-evaluated. Another factor for choosing storage injection pressure is the **fracture pressure** of the caprock. The assumption is that injection remains safe as long as the pressure stays below this fracture pressure threshold. This is risky in practice when the breakthrough pressure of the caprock is lower than the fracture pressure. In such cases, the injected hydrogen may penetrate the caprock and escape into overlying formations before reaching fracture pressure. Therefore, accurate determination of caprock sealing efficiency is important for designing UHS systems and mitigating associated risks [15].

2.5. Factors affecting caprock sealing efficiency

The sealing efficiency of caprock is governed by fluid properties, fluid-rock interactions and other factors. In this section we will briefly study each property and factor influencing sealing efficiency From Young-Laplace equation it is clear that capillary pressure depends on wettability, pore structure, interfacial tension of rock-fluid. All these parameters depend on other parameters like pressure, temperature, salinity, mineral composition of the caprock.

- Density

Pressure and temperature increase with formation depth due to the geothermal and hydrostatic gradients. Hydrogen density drastically increases with pressure and decreases slightly with temperature as shown in Figure 10.

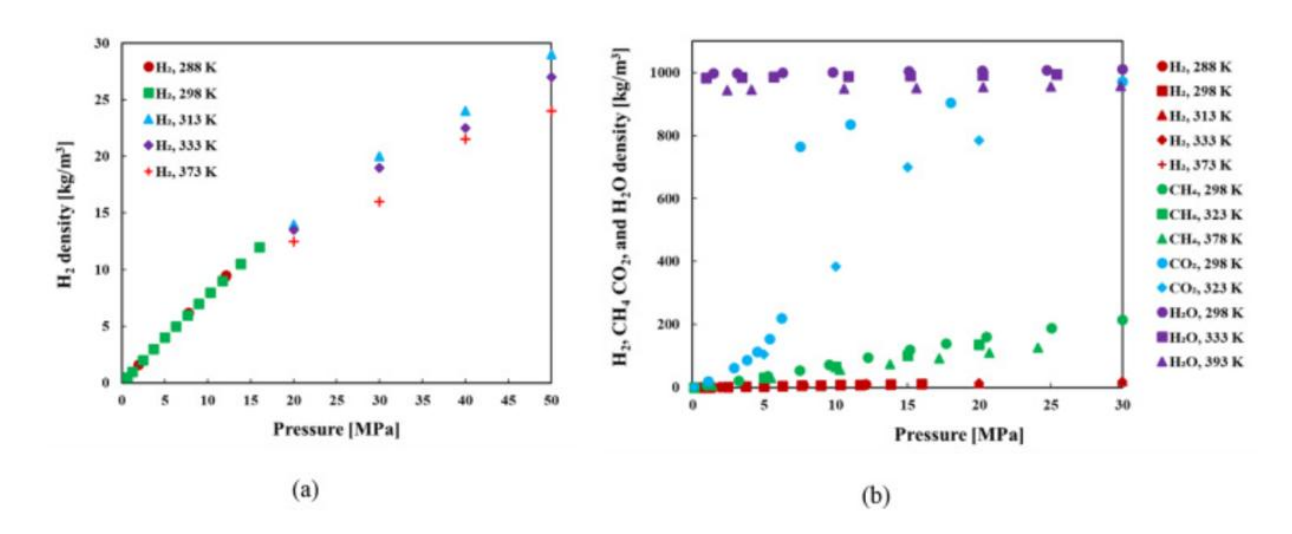


Figure 10. (a) Hydrogen density as a function of pressure and temperature; (b) densities of hydrogen, methane, carbon dioxide and water as a function of pressure and temperature [16]

Hydrogen density is significantly smaller than water density at the same thermobaric conditions, as a result this large hydrogen water difference will lead to strong gravity segregation (buoyancy) and more rapid hydrogen upward migration, when compared with other gases.

- Viscosity

Viscosity quantifies the ability of a fluid to flow, thus important parameter for hydrogen injection and withdrawal. Hydrogen viscosity is slightly influenced by temperature and pressure. With increasing pressure and temperature, the hydrogen viscosity increases. However, the viscosity of water is almost constant with pressure and temperature change (Figure 11)

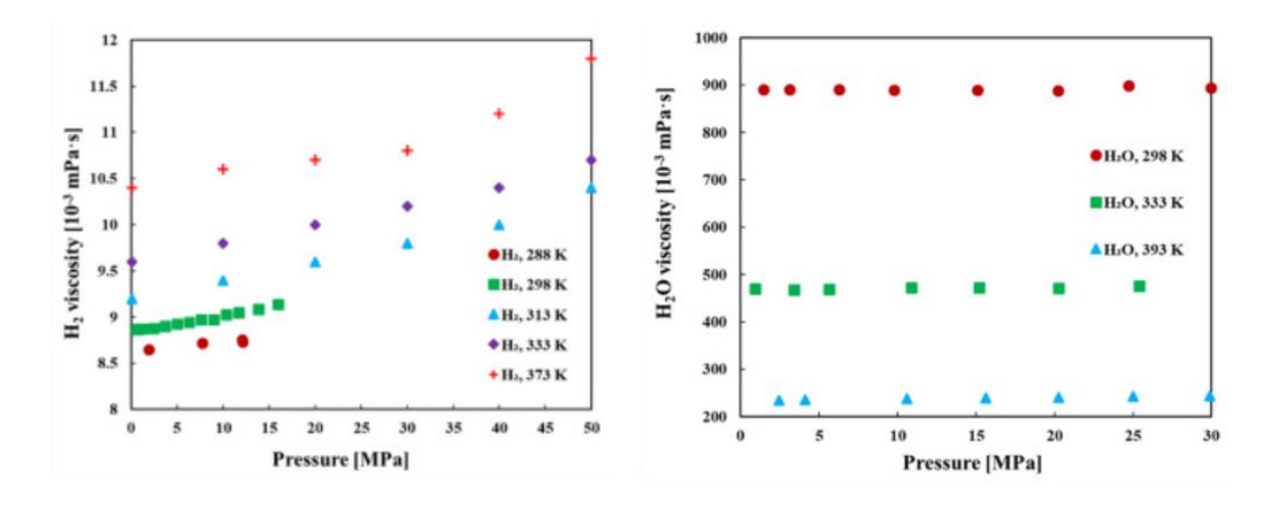


Figure 11. Hydrogen and water viscosities as a function of pressure and temperature [16]

- Interfacial tension

Interfacial tension is a force that exists at the boundary between two immiscible fluids (water and gas). It represents the force per unit length that must be applied to overcome the attractive forces between molecules of the same fluid and create a new surface. Interfacial tension determines the capillary pressures and it is a function of pressure, temperature and fluid composition.

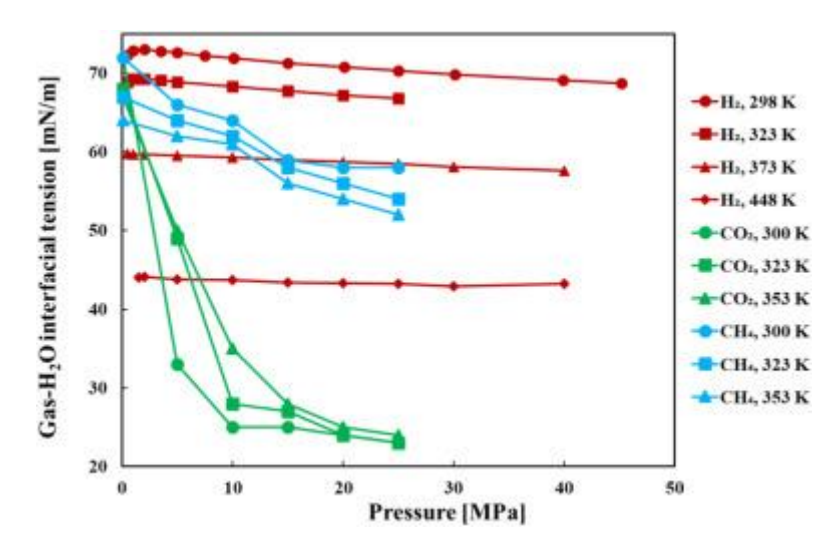


Figure 12. Interfacial tension of gas-water system as a function of pressure and temperature [16]

As shown Figure 12, hydrogen-water interfacial tension is almost independent of pressure, but it decreases strongly with increasing temperature. However, this behavior is quasi opposite to that of carbon dioxide and methane. Interfacial tension of carbon dioxide-water strongly decreases with pressure, but only slightly increases with temperature, while methane-water interfacial tension decreases with both pressure and temperature.

- Solubility

As discussed previously in chapter 2.3 hydrogen solubility or dissolution depends on the brine salinity, pressure and temperature conditions. Hydrogen solubility in water is much smaller at ambient conditions than at underground storage conditions. With increasing salinity and pressure at the same temperature the salinity of hydrogen decreases.

- Diffusivity

Diffusivity of hydrogen in water increases with increasing temperature and decreasing pressure strongly as shown in Figure 13 (a) and in hydrocarbons it decreases with carbon number as shown in Figure 13 (b). This means that hydrogen loss due to hydrogen diffusion could be significant in deep aquifers and depleted hydrocarbon reservoirs

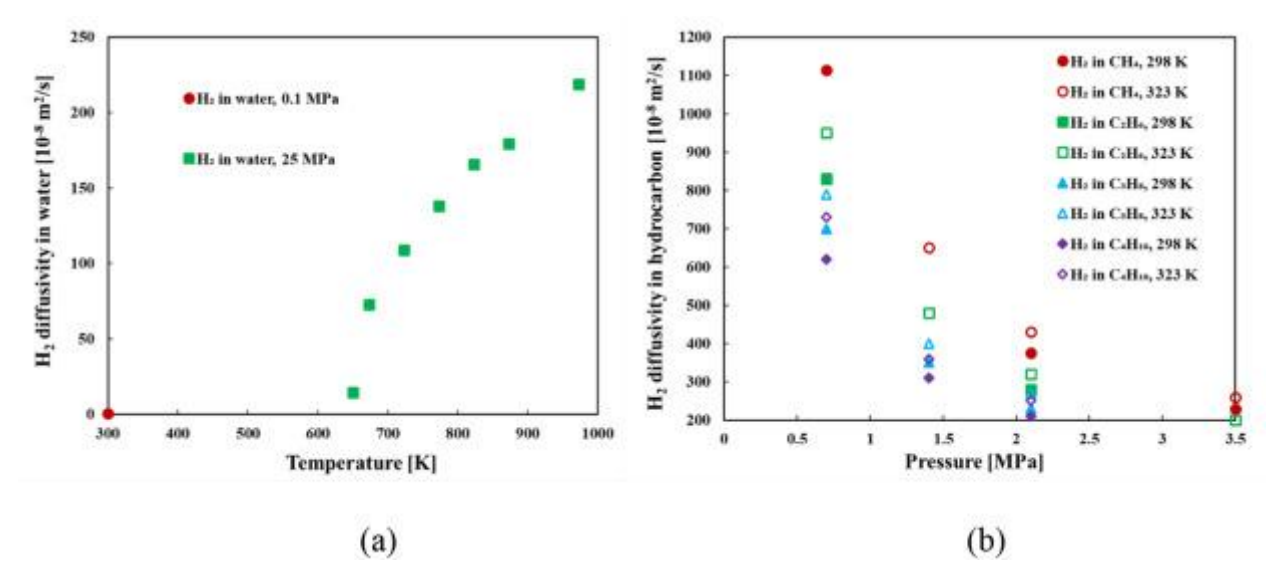


Figure 13. Diffusivity of hydrogen in (a) water and (b) different hydrocarbons as a function of pressure and temperature [16]

- Wettability

Wettability is the relative affinity of one fluid to a solid surface in the presence of another immiscible fluid. Wettability is a function of interfacial tension and contact angle. Hydrogen-rock wettability is heterogeneously distributed in the subsurface because of the heterogeneous rock surface chemistry, mineral composition and pore geometry. Hydrogen-rock wettability is important parameter that determines formation storage capacity, capillary pressure (sealing efficiency), hydrogen saturation (thus permeability) and residual hydrogen saturation and hydrogen injectivity. Contact angle strongly depends on pressure and temperature and is increasing with increasing pressure and temperature (Figure 14a) and stearic acid concentration (Figure 14b). Changes in pressure and temperature will affect gas density and intermolecular forces between gas (hydrogen) and rock, and thus also contact angle.

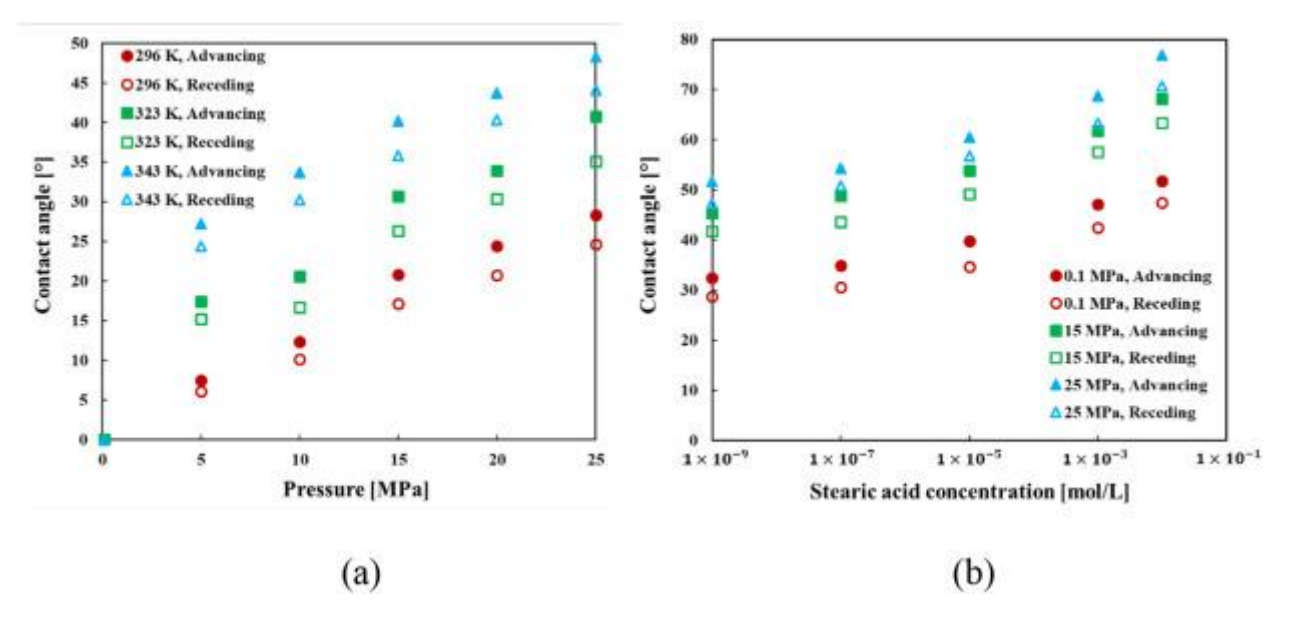


Figure 14. Contact angles of (a) hydrogen-brine quartz and (b) hydrogen-brine-aged quartz systems as a function of pressure, temperature and stearic acid concentration [16]

- Hydrogen-rock interfacial tension

Hydrogen-rock interfacial tension decreases with pressure and temperature for cleaned quartz and basaltic rock, and it increases with increasing stearic acid concentration (Figure 15). As clean quartz does not exist in the subsurface, stearic acid aged quartz-hydrogen interfacial tension is used to represent more realistic UHS conditions.

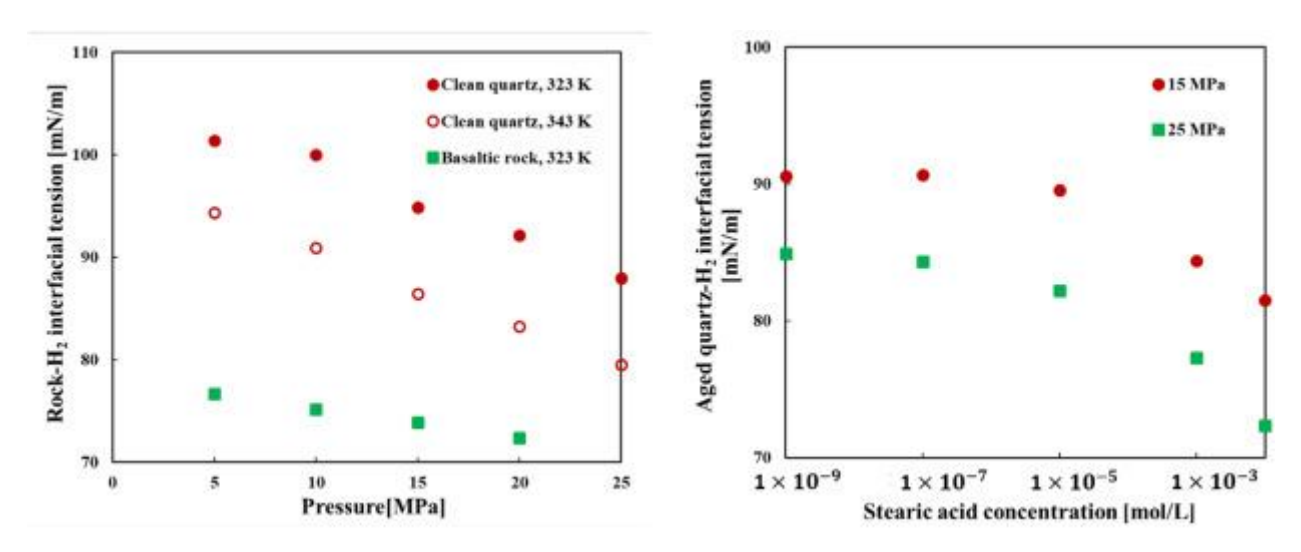


Figure 15. Hydrogen-rock interfacial tension as a function of (a) pressure and temperature, (b) stearic acid concentration at 323 K [16]

- Capillary pressure

Capillary pressure is determined by capillary forces and is key parameter that characterizes multiphase flow in geological porous media. It corresponds to pressure difference existing at the interface between two immiscible fluids (water and gas). Capillary pressure determines pore-scale fluid configurations and fluid movement, and thus reservoir scale flow, which is implemented by capillary pressure and relative permeability curves measured as a function of water saturation. Prior to hydrogen injection, the pore spaces are occupied by formation brine. during injection hydrogen displaces the in-situ brine and the amount of brine displaced (and thus hydrogen injected) and the pressure required for this process are controlled by capillary pressure. Ideally, achieving higher hydrogen saturation with reduced water saturation would maximize storage capacity. Capillary pressure decreases increasing water saturation. The impact of pressure and temperature on capillary pressure is minimal for hydrogen, in contrast to carbon dioxide, where these factors significantly affect capillary pressure (Figure 16).

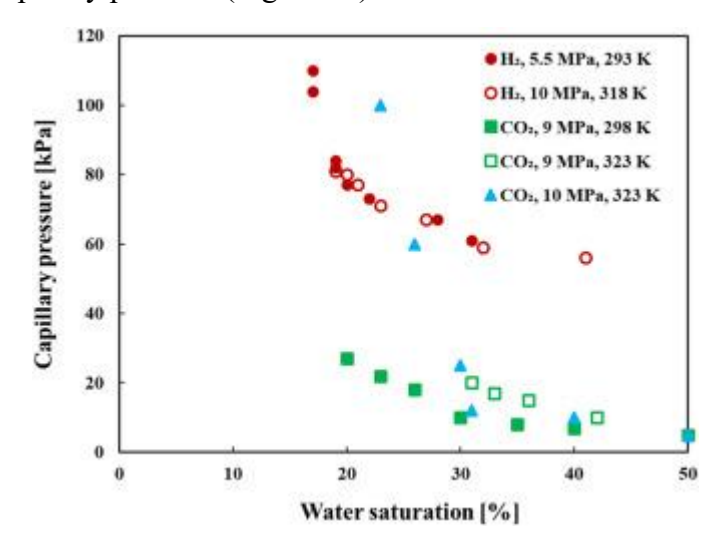


Figure 16. Hydrogen-water-sandstone and carbon dioxide – water-sandstone capillary pressures in drainage as a function of water saturation [16]

- Relative permeability

Relative permeability is defined as the ratio of effective permeability to absolute permeability, where effective permeability refers to the conductance of a specific fluid in the presence of other

fluids. Multi-phase fluid flow in porous media is strongly governed by relative permeability, which is influenced by water saturation and rock wettability. For example, at pressure of 5.5 MPa and temperature of 293 K hydrogen relative permeability increases from 0 to 0.04 when water saturation decreases from 90% to 40%, and at higher pressure of 10 MPa and temperature of 318 K hydrogen relative permeability increases from 0 to 0.03 when water saturation decreases from 80% to 40% (Figure 17 a). In contrast, at 9 MPa and 323 K relative permeability of carbon dioxide increases from 0 to 0.4 when water saturation decreases from 97% to 45%, and at 8.3 MPa and 298 K, relative permeability of methane increases from 0.05 to 0.8 when water saturation decreases from 70% to 30% (Figure 17 b). These comparisons indicate that hydrogen exhibits significantly lower flow capacity through brine-saturated sandstone compared to carbon dioxide and methane. Relative permeability strongly influences the sealing efficiency of the caprock. Low gas permeability in the caprock indicates that brine occupies most of the pores, thus limiting gas flow within the pores and enhancing sealing efficiency. In contrast, higher gas relative permeability reduces the caprock ability to retain injected gas. Therefore, lower gas permeability corresponds to higher sealing efficiency.

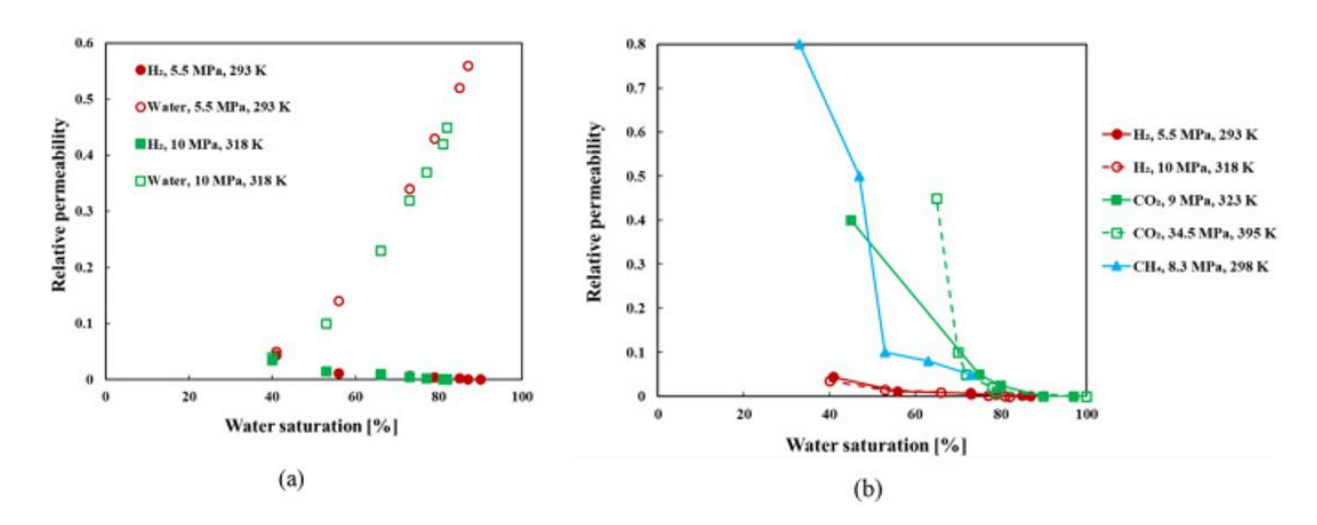


Figure 17. (a) hydrogen-water-sandstone drainage relative permeability curves as a function of water saturation. (b) water-sandstone drainage relative permeability curves for various gases as a function of water saturation [16]

- Mobility ratio

Mobility ratio (M) is the ratio between mobility of displacing fluid (hydrogen) and mobility of displaced fluid (water) defined as (Equation 2):

$$M = \frac{\frac{k_{rH2}}{\mu_{H2}}}{\frac{k_{rw}}{\mu_{w}}}$$
 Equation 2

where:

 k_{rH2} , k_{rw} are relative permeabilities of hydrogen and water respectively

 μ_{H2} , μ_w are viscosities of hydrogen and water respectively

Mobility ratio is a critical factor influencing the efficiency of hydrogen injection and withdrawal as well as the stability of hydrogen-formation brine interface. A high mobility ratio promotes viscous fingering, resulting in reduced hydrogen sweep efficiency and ineffective displacement of formation brine. Mobility ratio depends on water saturation, pressure and temperature conditions,

displacing fluid type (hydrogen, methane, carbon dioxide). Specifically in sandstone mobility ratio increases sharply with decreasing water saturation. With increasing pressure and temperature mobility ratio for hydrogen decreases as shown in Figure 18.

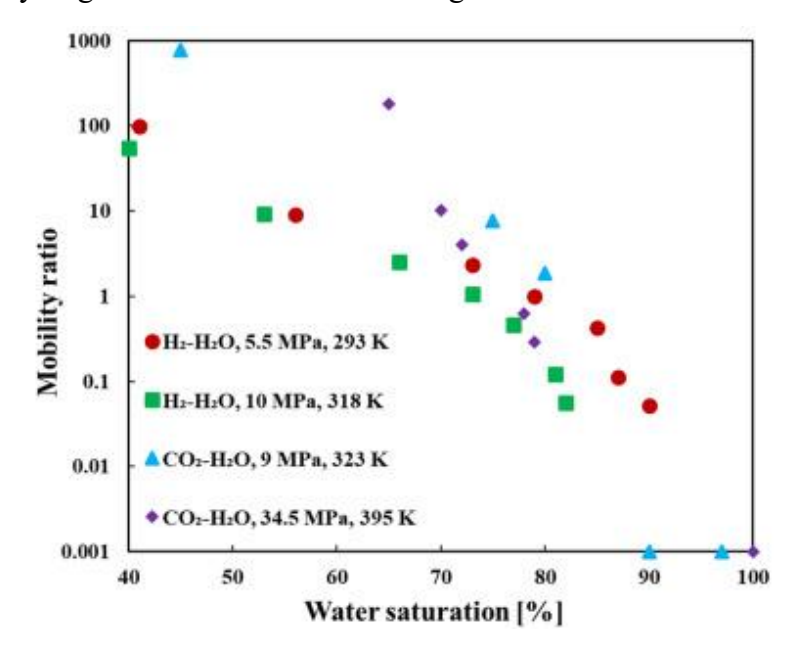


Figure 18. Gas-water-sandstone drainage mobility ratio curves for hydrogen and carbon dioxide as a function of water saturation [16]

- chemical reactions

Chemical reactions in UHS can be divided into:

- inorganic hydrogen-brine-rock reactions or geochemical reactions
- biochemical or organic reactions (where bacteria utilize hydrogen for metabolic processes)

Inorganic reactions between hydrogen, brine and rock can alter permeability, porosity, pore structure, mineral composition and mechanical stability of the rock. Alterations in porosity, permeability directly influence capillary pressure thereby affecting the sealing efficiency of the caprock. The impacts of geochemical reaction were briefly discussed earlier in section 2.2. The pH level is another parameter that governs chemical reactions between hydrogen, brine and caprock minerals. Variations in pH significantly affect mineral dissolution and precipitation processes, which in turn influence the porosity, permeability, sealing efficiency of caprock. pH and temperature dictates the geochemical reactions occurring between water (brine), hydrogen and caprock minerals. As temperature increases, reactions occur more rapidly, significantly altering the mineral composition and structural properties of the UHS formations. Acidic environments promote enhanced geochemical reactivity, resulting in significant porosity changes that could potentially compromise the integrity of the caprock. Alkaline conditions exhibit reduced reactivity, which contributes to greater stability in UHS, although localized dissolution-precipitation process may still occur. Organic reactions are inhibited in high-salinity environments, but are enhanced in alkaline environments. Hydrogen redox reactions are slow in acidic aqueous aquifers and depleted oil and gas reservoir, where high salinity conditions prevail. However, in depleted oil and gas reservoirs reactions between hydrogen and hydrocarbons are also possible for example conversion of ethane with hydrogen into methane, resulting in hydrogen loss. Furthermore, if sulphur is present at these storage sites, reactions between hydrogen and sulphur may generate hydrogen sulfide (a toxic and corrosive gas) and this can accelerate material degradation, particularly in

wellbores and subsurface equipment, leading to increased risks of structural failure and compromised sealing integrity [17].

2.6. Stages of gas capillary breakthrough

During the injection and withdrawal cycles in underground hydrogen storage, two key physical processes occur in the reservoir: **drainage and imbibition**. In the drainage process, injected hydrogen, a nonwetting fluid, displaces the wetting fluid (water) during the injection phase. Conversely, in the imbibition process, water displaces the injected hydrogen during the withdrawal phase. Due to variations in the behavior of wetting and nonwetting fluids in porous media, influenced by capillary forces and pore structure, hysteresis arises in drainage and imbibition phases. During drainage, the nonwetting fluid (hydrogen) displaces the wetting fluid (water), requiring higher pressure to overcome capillary resistance in smaller pores. In imbibition, the wetting fluid re-enters the pores, but the process follows a different pressure path due to contact angle variations, pore geometry and trapped gas, leading to lower capillary pressure. This irreversible behavior, influenced by pore size distribution and fluid-rock interactions, causes the hysteresis loop between the drainage and imbibition pressure curves (Figure 19).

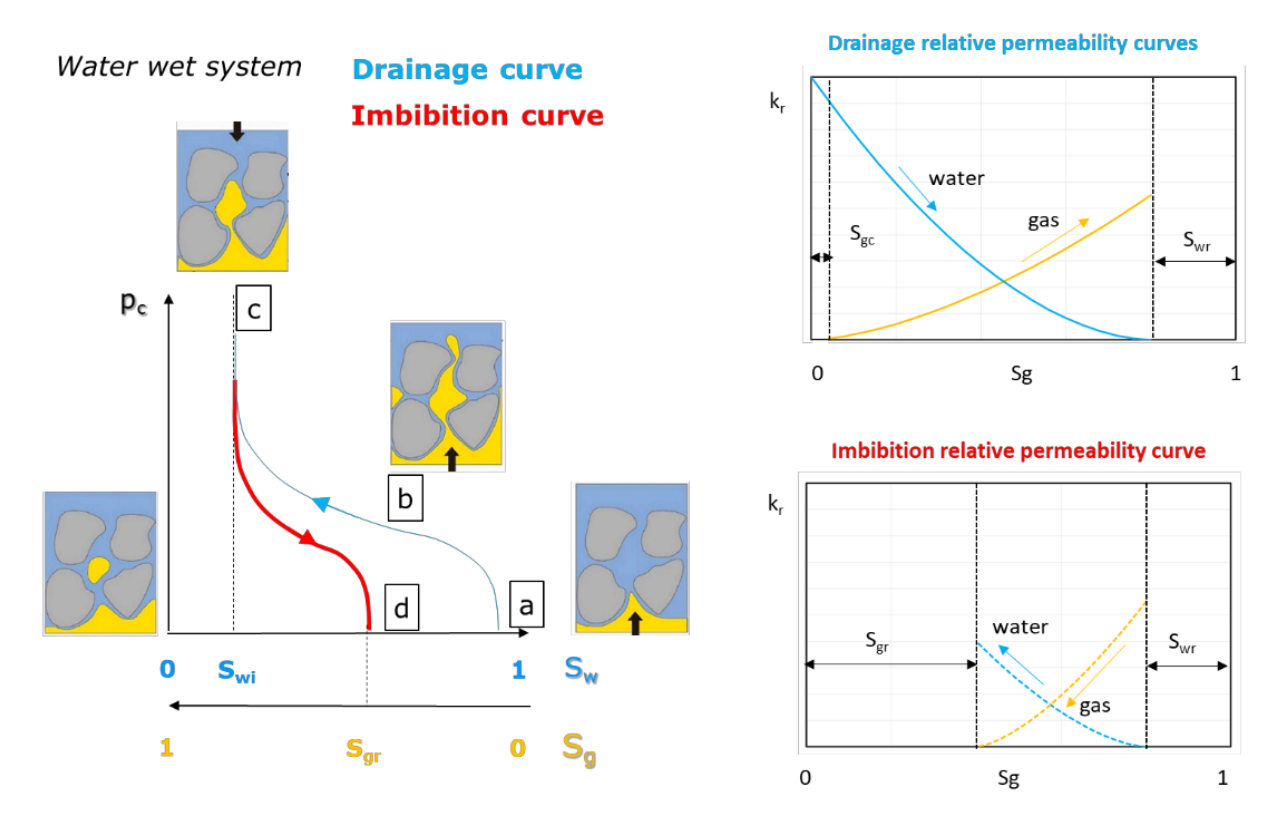


Figure 19. Drainage and Imbibition curves [19]

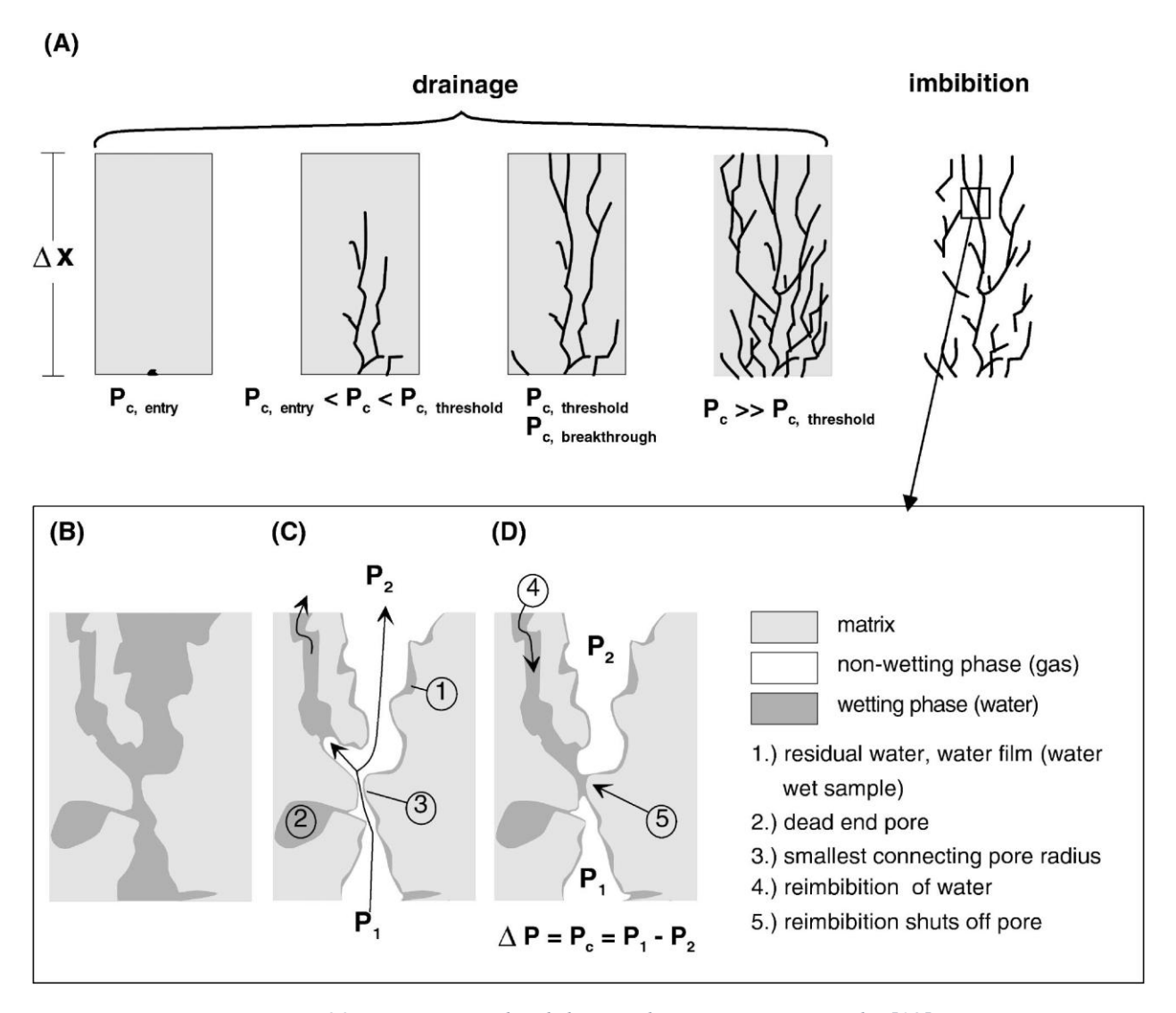


Figure 20. Drainage and Imbibition phenomena in caprocks [18]

The stages of the capillary breakthrough process of nonwetting phase through porous medium is shown in Figure 20.

Before the drainage process starts, the caprock is fully saturated with formation brine. The drainage process starts when the pressure of nonwetting phase exceeds the capillary entry pressure (Figure 20). At this stage, gas saturation in the caprock remains below the critical gas saturation (the minimum gas saturation required for gas to flow continuously in a porous medium). Consequently, gas accumulates in the largest non-interconnected pores without flowing, as the relative permeability to gas is zero (Figure 19). In the next stage of the drainage process, the pressure of gas is still greater than the entry pressure but lower than the breakthrough pressure. Gas saturation becomes greater than the critical gas saturation (saturation of gas at which gas becomes movable), enabling gas to flow through the caprock in continuous flow paths. During this phase, gas saturation increases, the flow is capillary dominated and there is no flow of gas in the downstream. The relative permeability to water decreases, while the relative permeability to gas increases as shown in Figure 19. In the third stage, when the pressure of gas reaches breakthrough pressure, gas reaches the downstream part of the system through the largest of the narrowest capillary pore throats, representing the easiest flow path. In the final stage, when the pressure of gas exceeds breakthrough pressure, flow becomes viscous-dominated and the gas flows continuously downstream.

A further reduction of the gas pressure below the breakthrough pressure will lead to re-imbibition of the water, starting with the smallest pores and proceeding to larger pores. As a consequence, the relative permeability to gas will decrease due to the loss of interconnected flowpaths. When the last interconnected flowpath is shut-off, the relative permeability to gas will drop to zero and due to this loss of connectivity, a pressure difference will persist between the gas phases below and above the seal. This remaining pressure difference is called residual pressure or snap-off pressure (Figure 21).

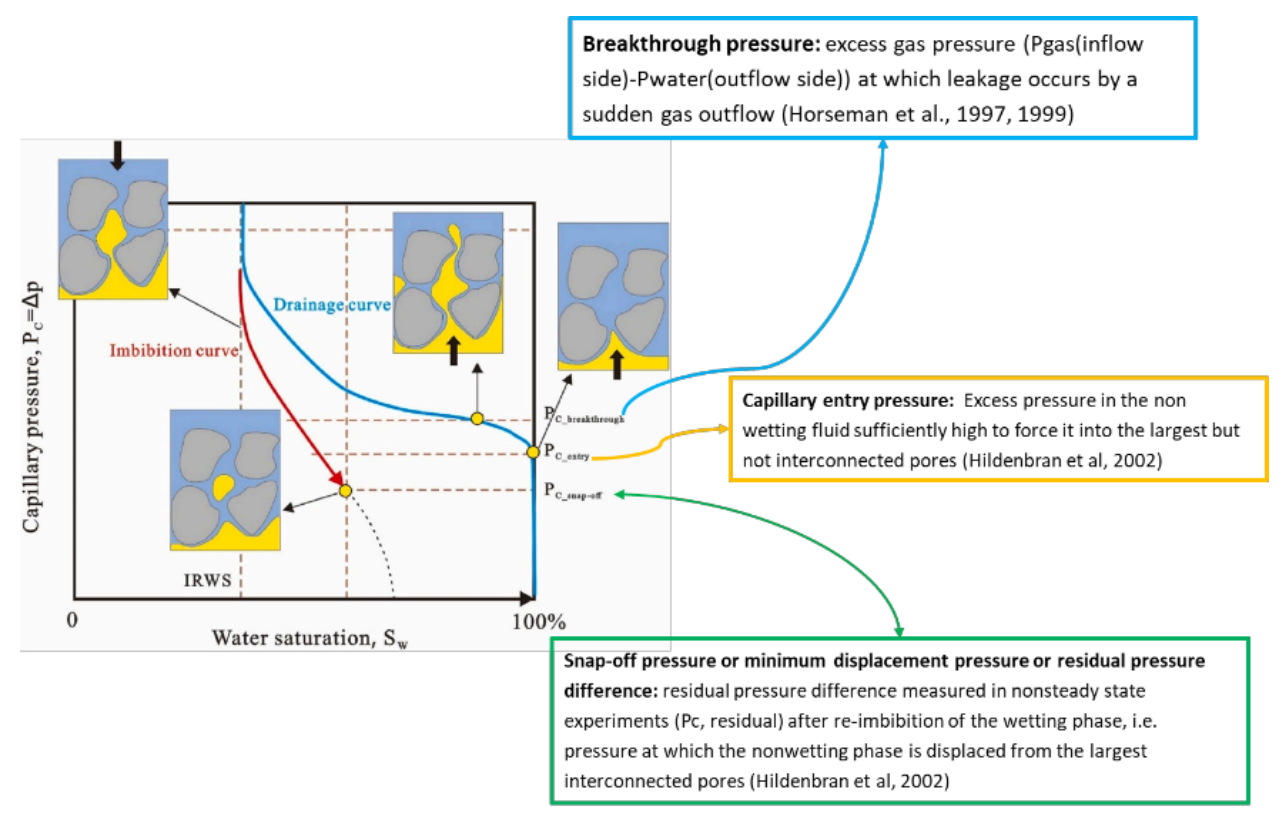


Figure 21. Definitions of breakthrough pressure, capillary entry pressure and snap-off pressure given by Hildenbrand et al. [19]

Several studies have investigated the capillary sealing efficiency of caprocks by using gas to displace the water from fully saturated caprock sample in the laboratory. Depending on the experimental procedures, interpretations and evaluations, different terminologies have been used by authors to describe capillary sealing efficiency. Table 6 gives an overview of those different terminologies.

T.11. ()	C 1:00	4			C 1 .	1:4	$\Gamma 2 \Omega 7$
Table 6. Overview	oi aimerent	terminologies	s ot cabilları) bressures	тоипа і	n iiterature	1201

Terminology	Definitions	Author
Minimum	Residual pressure difference measured in nonsteady state	Hildenbrand et
displacement	experiments after reimbibition of the water. Pressure at which	al. (2002)
pressure	the gas is displaced from the largest interconnected pores	
Threshold	Minimum differential pressure between the gas and the water at	Ibrahim et al.
displacement	which the gas starts to move continuously through the caprock	(1970)
pressure		
Threshold pressure	Injection pressure at which a continuous flow of water resulted,	Thomas et al.
	and if enough time was allowed gas finally appeared at the outlet	(1968)
	end of the core	
Displacement or	The minimum gas injection pressure required to establish a	Schowalter
breakthrough	continuous filament of gas through the largest interconnected	(1979). Smith
pressure	pore throats of rock fully saturated with water	(1966)

Critical pressure	Denoting a sudden gas bubble release through the outlet tubing	Pusch et al.
	gas flow is already detectable below this pressure	(1985)
Pore entry pressure	Pressure at which gas flow is detected on the downstream side,	Galle & Tanai
or critical pressure	below this pressure no gas flow is possible	(1998), Galle
_	- · · ·	(2000)
Breakthrough	Second threshold pressure at which gas flow at the downstream	Galle & Tanai
pressure	side increases suddenly	(1998), Galle
	-	(2000)
Breakthrough	Excess gas pressure ((P gas(inflow) – Pwater(outflow)) at which	Horseman et
pressure	leakage occurs by a sudden gas outflow.	al. 1997

The term "threshold pressure" or "displacement pressure" do not provide a precise definition of the caprock sealing efficiency. This may be attributed to the fact that different authors have conducted tests under different conditions and used their own definitions to characterize the same phenomenon. In this study, to ensure better clarity we adopted the following terms and definitions:

<u>Capillary entry pressure or entry pressure</u> is the pressure difference between gas and water at which gas starts to enter the pore spaces of the caprock sample by displacing water from the largest but not interconnected pores, followed by the production of displaced water at the outlet.

So, one solid indication of entry pressure is when we see some water production at the outlet.

<u>Capillary breakthrough pressure or breakthrough pressure</u> is the pressure difference between gas and water at which gas flows continuously through the largest interconnected pore throats of the caprock. At this point, gas leakage becomes detectable at the outlet, indicating the gas has formed a continuous flowpath within the pore network.

<u>Snap-off pressure</u> is the capillary pressure at which the gas becomes discontinuous in the caprock pore network during imbibition, as the water spontaneously re-enters and surrounds gas in pore throats, trapping it as isolated volume. Or snap-off pressure is capillary pressure corresponding to residual gas saturation after water re-imbibition.

Snap-off pressure and entry pressure are used as reference values to evaluate sealing capacity, however they don't fully characterize sealing efficiency. Snap-off pressure it relates to the imbibition process and represents the residual pressure difference between nonwetting and wetting phases after snap-off occurs. For snap-off to take place, the nonwetting phase must break through the caprock, which is undesirable for maintaining sealing integrity of the caprock in UHS. Similarly, entry pressure alone does not fully represent the sealing efficiency of the caprock, as it only indicates the minimum pressure required for the gas to begin displacing the water without ensuring breakthrough. Therefore, breakthrough pressure is considered as more representative parameter for evaluating caprock sealing efficiency, as it defines the pressure at which the gas fully penetrates the caprock, compromising its sealing capacity. Laboratory measurement is the most important means to obtain breakthrough pressure as it is difficult to be measured in the field.

3. Laboratory tests

Many experimental methods have been proposed to proposed the previously defined pressure in order to evaluate the hydraulic sealing efficiency. They can be divided into two categories: **direct** and **indirect methods** [21].

Direct methods involve physical displacement of brine by gas (preferably same composition as the one intended for storage), they are more representative of the gas-water-rock system.

Indirect methods do not involve the physical displacement of the fluids (gas and water) in the porous medium but instead use a proxy fluid or alternative measurement technique to infer the capillary properties. These methods are less representative of the actual gas-water-rock system, and often used due to their simplicity or ability to provide complementary data. The most widely used indirect method is mercury injection porosimeter test.

In this section, different tests are presented and explained, each one try to reproduce a particular phenomenon that may occur in the caprock. Starting from the **mercury injection porosimeter test** that can be used to obtain a quick estimation of the entry pressure of the caprock, continuing with the **standard test (step by step test)** that reproduce the displacement of water by gas in the fully saturated caprock sample, then the **residual capillary pressure test** that, reproducing the drainage and reimbibition phenomena, gives the snap-off pressure, and finally, the **dynamic threshold pressure** test, an innovative method introduced to obtain the entry pressure in a rapid way. Standard test (step-by-step test), residual capillary pressure test and dynamic threshold pressure test are direct methods.

3.1. Mercury injection porosimeter test

This test was introduced by W. R. Purcell [22] and it focuses on measuring capillary pressures at each saturation using mercury as nonwetting phase with a contact angle higher than 90°. As explained later in this section, the interpretations available in the literature for this test allow to give a first approximation of the **capillary entry pressure**. The experimental apparatus is shown in Figure 22.

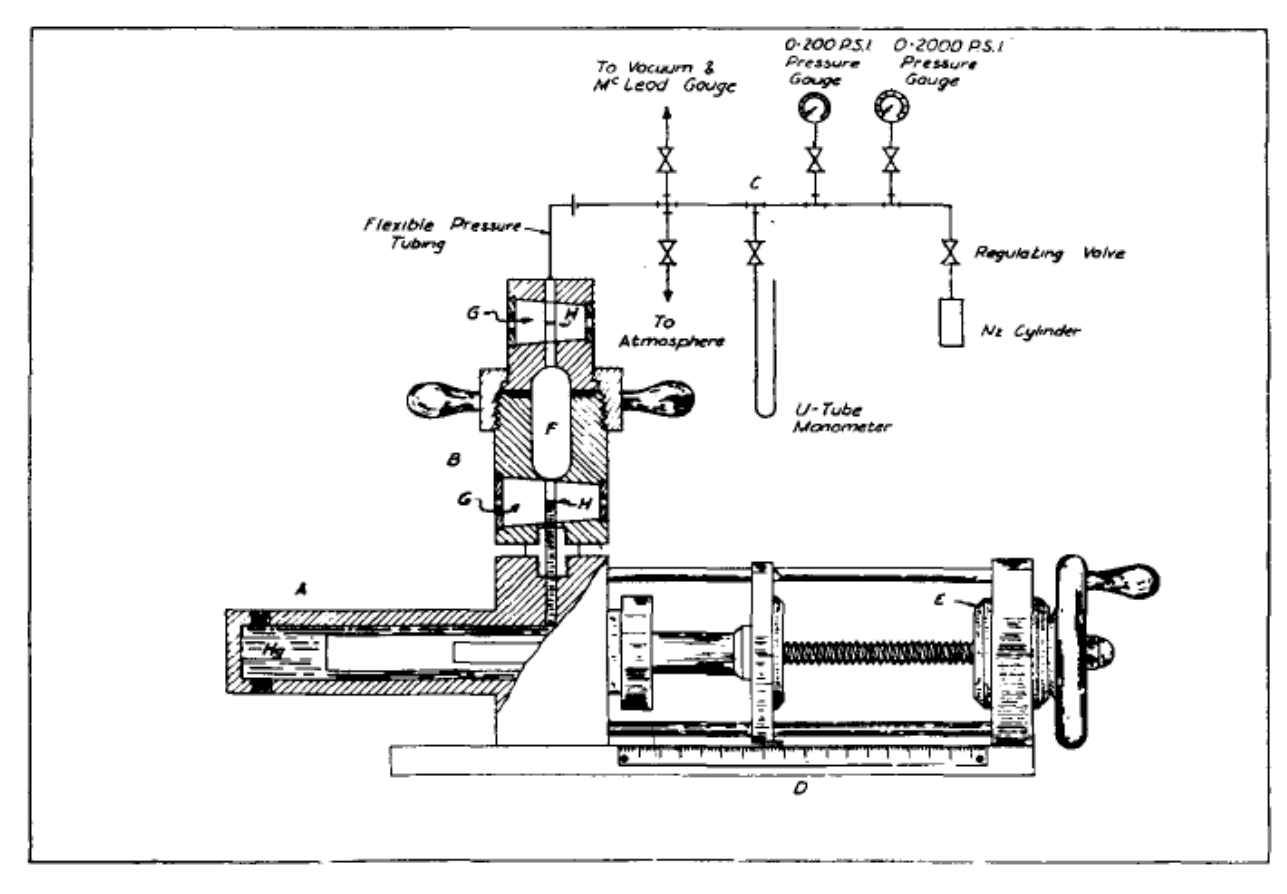


Figure 22. Apparatus for Mercury Capillary Pressure measurement [22]

It consists of the following components: A-mercury displacement pump; B – sample holder; C – manifold system, D – Scale; E – vernier; F – cavity of the sample holder; G – Lucite window; H – reference marks

Test procedure:

- Test starts placing the plugs (or drill cuttings) previously dried in the cavity of the sample holder. Then the sample holder is filled with mercury and the bulk volume of the sample is obtained.
- No confining pressure is applied
- Subsequently, the pressure inside the sample holder is incrementally increased, allowing mercury to penetrate the pores, with saturation values recorded at each pressure increment (or pressure step).
- The entire saturation curve can be obtained (within 30 to 60 minutes according to author).

A curve of capillary pressure vs. mercury saturation is obtained from the test data. To adapt this curve from the mercury-air system to the target system (gas-brine), a correction is applied using the Young-Laplace equation:

$$\frac{\sigma_{(Hg-air)}cos\theta_{(Hg-air)}}{P_c^{(Hg-air)}} = \frac{\sigma_{(gas-brine)}cos\theta_{(gas-brine)}}{P_c^{(gas-brine)}}$$
 Equation 3

Special attention should be taken to the values obtained using this test since, as the procedure employs a mercury-air system under specific pressure and temperature conditions. The correction applied via the Young-Laplace equation relies on theoretical values of interfacial tension and contact angle available in the literature. This method is commonly used as a first estimation rather than a precise value. Some interpretations of the data are available in the literature. The tangent method states that the **capillary entry pressure** is given by the tangent to the plateau of the

mercury intrusion curve, as shown in Figure 23, another interpretation defines the capillary entry pressure as the pressure corresponding to 10% of mercury saturation, as shown in Figure 24.

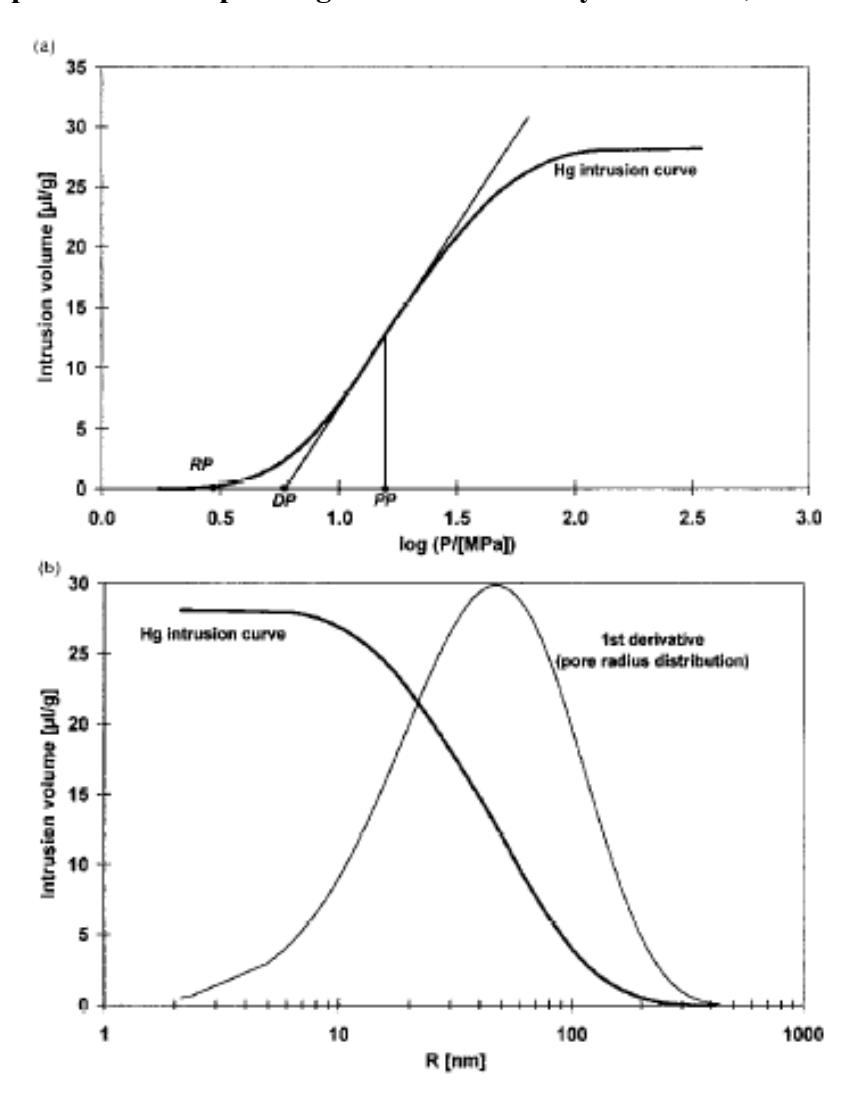


Figure 23. Interpretation of the Mercury injection porosimeter test data [23]

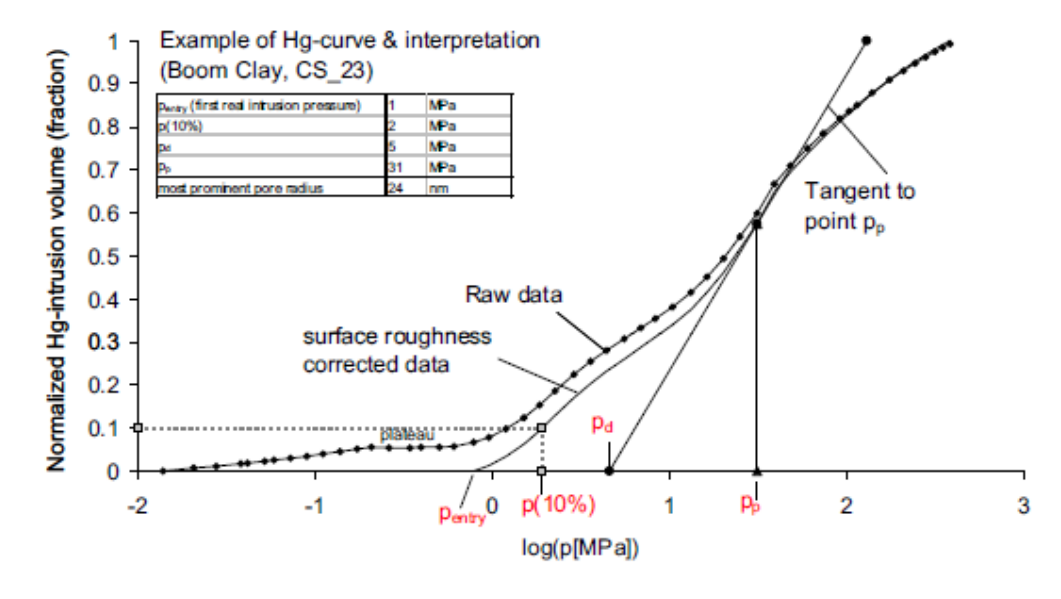


Figure 24. Interpretation of the data from Mercury injection porosimeter test to obtain the capillary entry pressure of the caprock [23]

Advantages:

- Rapid test (results can be obtained a few days after the sampling)
- Enables analysis of irregularly shaped samples and rock cuttings
- Provides an **indirect estimation of capillary entry pressure** of gas-brine system without requiring direct gas-liquid displacement tests

Disadvantages:

- The interfacial tension and contact angles of gas-brine systems are influenced by several factors including fluid properties, porous media characteristics, pressure and temperature. These factors require dedicated lab analysis, reliance on literature data may be inaccurate.
- The test does not simulate in-situ conditions (confining pressure and temperature). Petrophysical properties of low-permeability rock samples are very sensitive to the confining pressure stress either on tight reservoir rock or on shale samples.
- Samples must be completely dry. This is impossible to achieve in the laboratory, as there always be some saturation of water in the pore structure due to capillary forces and water wet nature of the rocks. Moreover, drying procedures can alter pore structure and affect porosity and permeability of the core sample.
- Inaccurate method

3.2. Step-by-step test (Standard test)

Step-by-step test, also called the standard test in the literature, was introduced by Thomas et al. [24], the procedure is to simulate the drainage process within the caprock, **directly** measuring **capillary breakthrough pressure** from core samples and under in-situ conditions.

Test procedure:

- Saturation of sample with brine
- Fully saturated sample is placed inside the coreholder
- The sample is confined with a pressure higher than the expected breakthrough pressure
- Apply in-situ stress, pressure and temperature conditions:
 - Temperature is reservoir temperature and water bath is used to maintain temperature constant during the test
 - The sample is confined with a pressure higher than the expected breakthrough pressure (to reproduce **in-situ stress conditions**, to avoid lateral flow and hydrofracturing of the sample)
- The gas inlet pressure is increased step-by-step and maintained constant for a certain time duration to achieve pressure equilibrium at each step. Pressure step is determined by the permeability of the caprock sample. The lower the permeability, the larger the pressure increment.
- Read the water flow in the outlet in each pressure increment
- The breakthrough pressure is reached when a <u>continuous flow of water appears in the outlet</u> and, <u>if enough time is allowed, gas finally appears</u>. The last recorded pressure gradient is the breakthrough pressure (Figure 27).

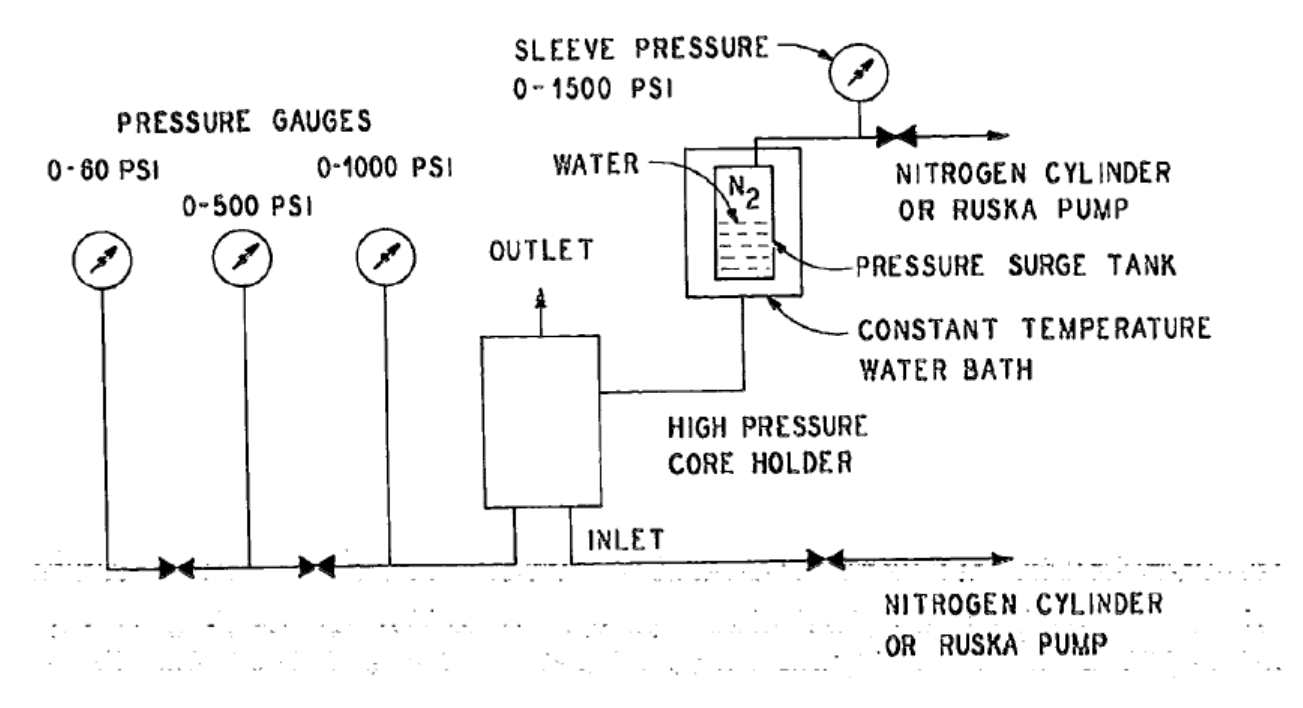


Figure 25. Schematic flow diagram of the high-pressure core holder apparatus [24]

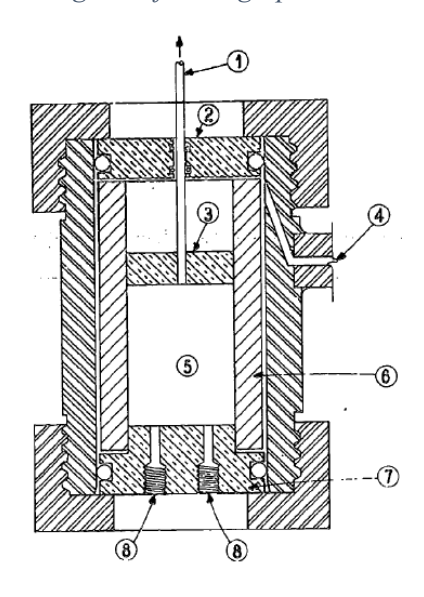


Figure 26. Cross section of the high-pressure core holder used for standard test [24]

The parts of the apparatus: 1) outlet stem; 2) top core holder end plate; 3) top core sample end plate; 4) pressure inlet for rubber sleeve; 5) core sample; 6) rubber sleeve; 7) bottom core holder and sample end plate; 8) gas or water inlets

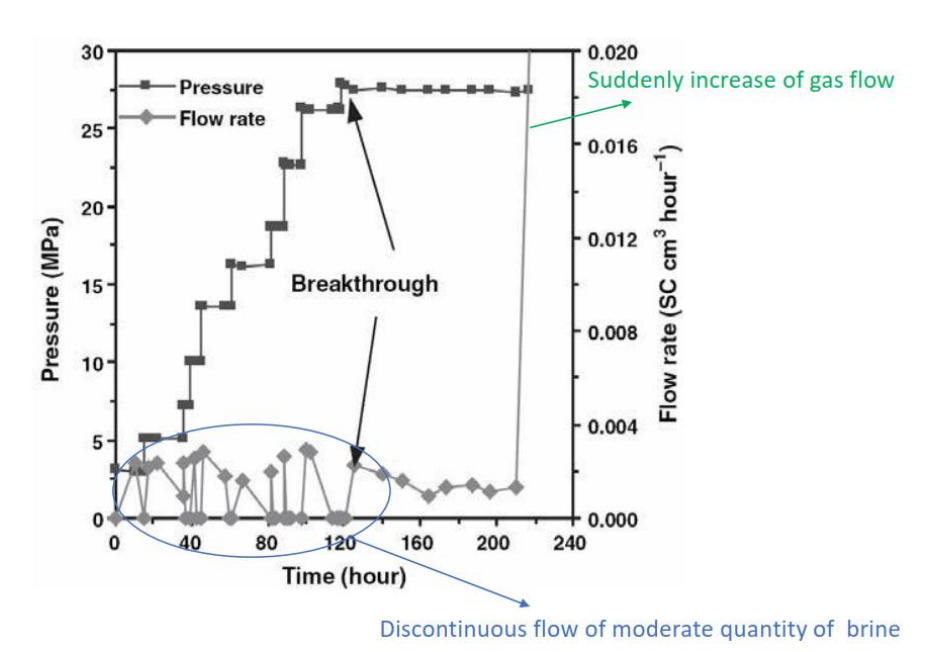


Figure 27. Data obtained from a standard test [15]

Advantages:

- Reproduces the drainage phenomena
- In situ conditions (confining pressure and temperature conditions)
- **Direct measurement of capillary breakthrough pressure** for different gas-brine systems (hydrogen, methane, carbon dioxide, nitrogen etc.)
- high accuracy affected by magnitude of pressure step increment

Disadvantages:

- Time consuming (since the permeability of caprock sample is usually in the order of micro/nano Darcy, it takes long time for pressure equilibrium to be established).
- Pressure step increment size (the magnitude of pressure increments directly affects both accuracy and test duration. Smaller pressure step increments improve accuracy but prolong the test, while larger pressure step increments may reduce precision and lead to overestimation of capillary breakthrough pressure)
- Sample saturation (the sample must be 100% saturated with brine to ensure representativeness of the wetting phase, if sample is not fully saturated, we can obtain unreliable results)
- Low brine production rates (the brine outflow rates are very small, especially in tight caprocks, making detection challenging and requiring sensitive measurement equipment)

3.3. Residual capillary pressure test (Snap-off test)

The residual capillary pressure test was conducted by Hildebrand et al. [20] and it simulates the drainage (displacement of water by gas) and reimbibition (displacement of gas by water) in the caprock to **directly** measure <u>residual capillary pressure</u> or <u>snap-off pressure</u>.

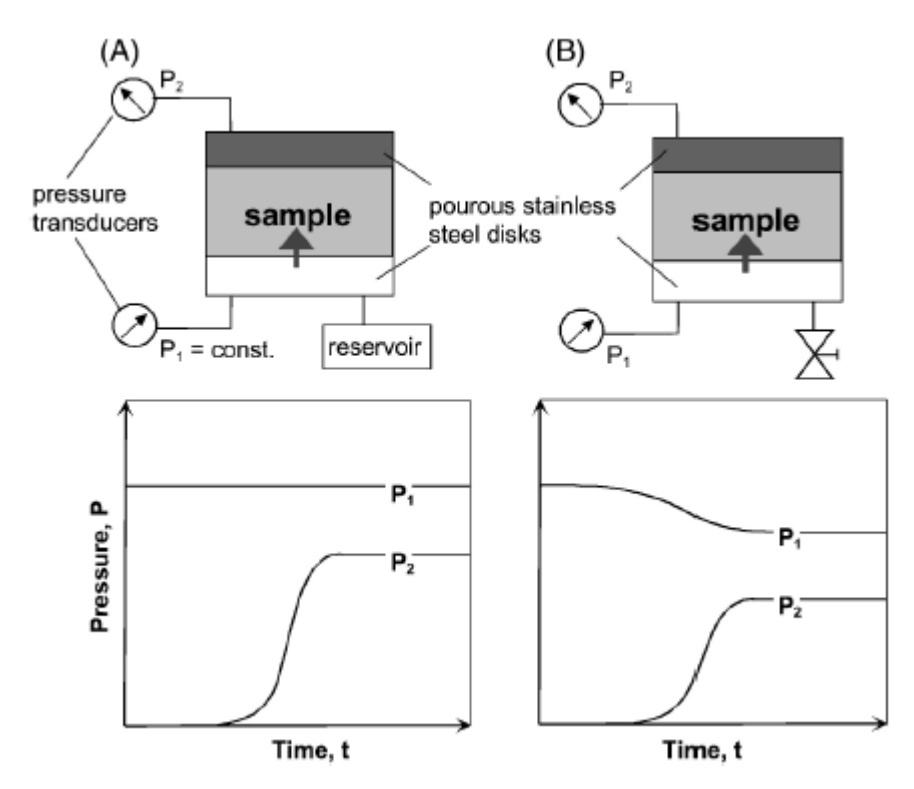


Figure 28. Scheme of the two experimental modes. A) constant upstream pressure mode; B) introduction of gas into a fixed upstream volume mode; downstream volume fixed in both instances. P1, P2 are pressures at upstream and downstream respectively [20]

Test procedure:

- Fully brine-saturated sample is placed inside the coreholder
- The sample is confined with a pressure higher than the expected breakthrough pressure
- The sample is subjected to a confining pressure exceeding the expected breakthrough pressure to replicate in-situ stress conditions, prevent lateral flow and avoid hydrofracturing.
- In-situ reservoir temperature is maintained throughout the test
- Apply an instantaneous high-pressure gradient (exceeding the expected gas breakthrough pressure), across the rock sample and monitoring the resulting gas (gas breakthrough) by means of the pressure changes (nonsteady state, capillary controlled experiments)
- Then, as shown in Figure 28, the experiment follows one of two procedures:
 - Procedure A: the upstream (high-pressure) side of the cell is maintained at constant pressure by using pressure regulator
 - Procedure B: the upstream (high-pressure) side of the cell is filled with gas at high pressure and then sealed
- In this closed system, the pressure difference across the sample decreases over time until gas flow stops completely as shown in Figure 28. This reduction allows the wetting phase to re-enter pore space, starting with the smaller pores, until the gas phase is fully trapped within the pore network.
- The final pressure difference after stabilization is the **residual pressure or snap-off** pressure

Data obtained from the residual capillary pressure test is shown in Figure 29. The conceptual flow of capillary processes in the experiment is shown in Figure 30.

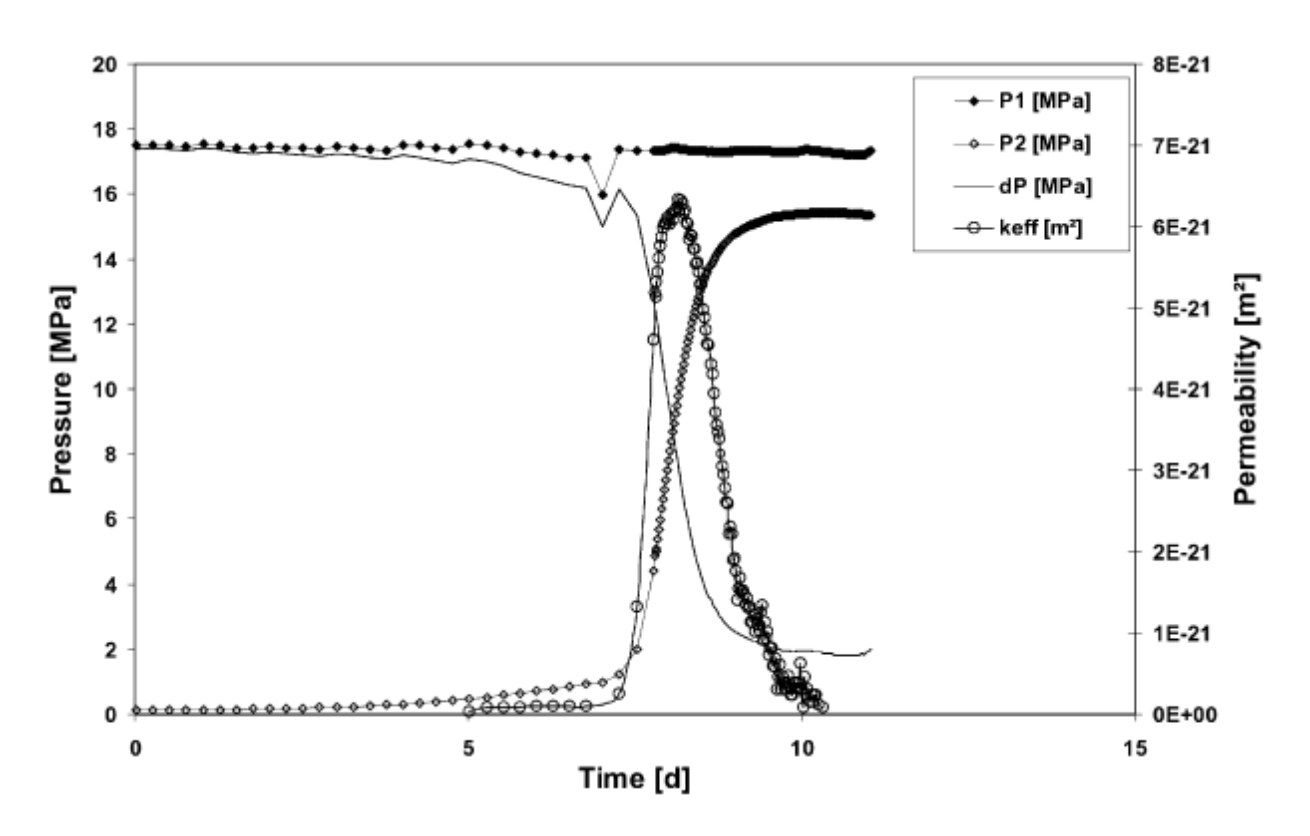


Figure 29. Gas breakthrough curve for methane including the permeability curve calculated [20]

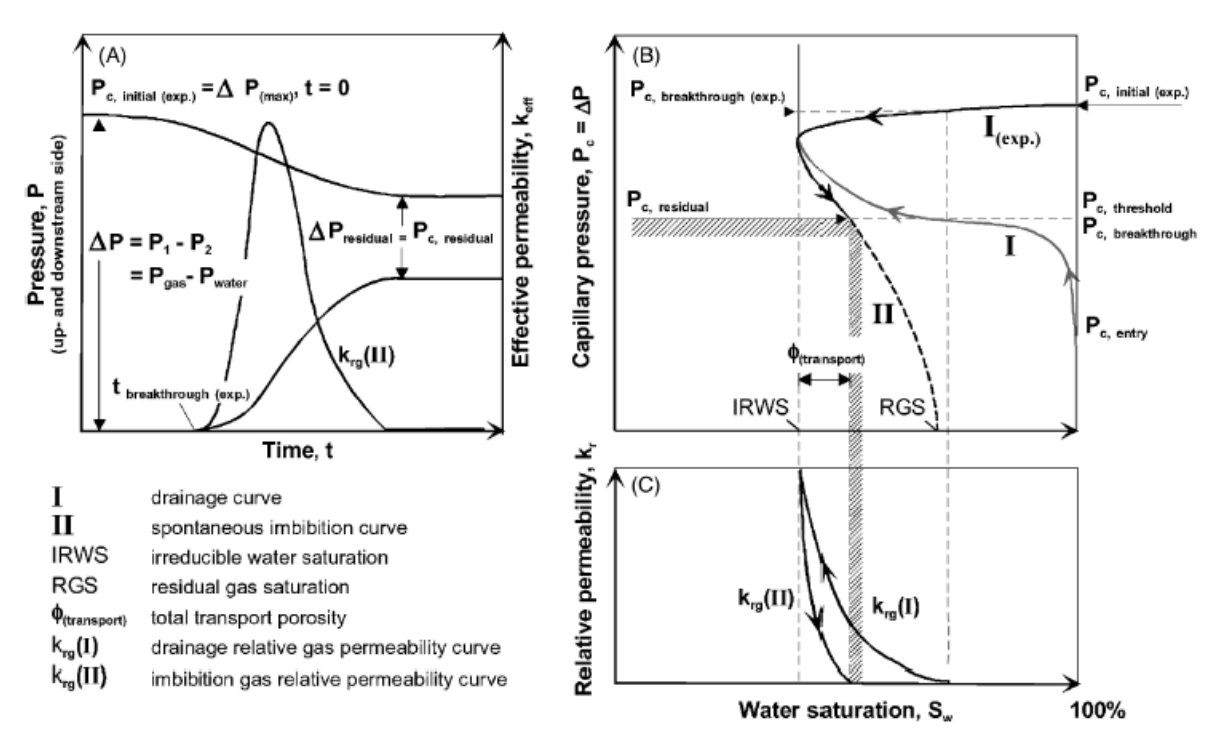


Figure 30. Scheme of the experimental parameters recorded and their interpretation in terms of capillary processes. A) pressure history of a gas breakthrough experiment; B) capillary pressure of the gas phase as a function of water saturation; C) relative permeability curve for the gas phase as a function of water saturation during drainage (I) and imbibition (II) [20]

Advantages:

- It replicates the drainage and imbibition phenomena potentially occurring in the caprock under reservoir conditions

- In-situ confining pressure and temperature condition to represent reservoir storage conditions
- Direct measurement of snap-off pressure for different gas-brine system (hydrogen, carbon dioxide, methane, nitrogen, etc)
- Enables calculation of effective gas permeability after gas breakthrough has occurred, as continuous gas flux develops from upstream to downstream until the residual pressure gradient is reached. The effective permeability can be calculated from the pressure change in the downstream using Darcy' law for compressible media (Equation 4), (Figure 31)
- Fast (test requires less time than standard test, however it may still require weeks for low permeability rocks, as a final quasi-constant pressure difference needs to be built for imbibition process)
- The experimental time depends on the initial pressure difference (the higher is the pressure difference the lower is the time)
- The snap-off pressure is reproducible and independent of the initial pressure difference applied to the caprock sample

Disadvantages:

- It has been found out that snap-off pressure is consistently lower and sometimes significantly lower than breakthrough pressure for the same caprock sample

$$k_{eff} = -\frac{2V_2\mu\Delta x}{A({P_2}^2 - {P_1}^2)}\frac{dP_2}{dt}$$
 Equation 4
$$V_2 - \text{volume of gas at the downstream [m}^3], P_1 \text{ and } P_2 - \text{pressures at the upstream and downstream}$$

 V_2 – volume of gas at the downstream [m³], P_1 and P_2 – pressures at the upstream and downstream [Pa], k – effective permeability to the gas phase [m²], A – cross section area of the core sample [m²], μ – viscosity of gas [Pa*s], Δx – the length of the sample [m],

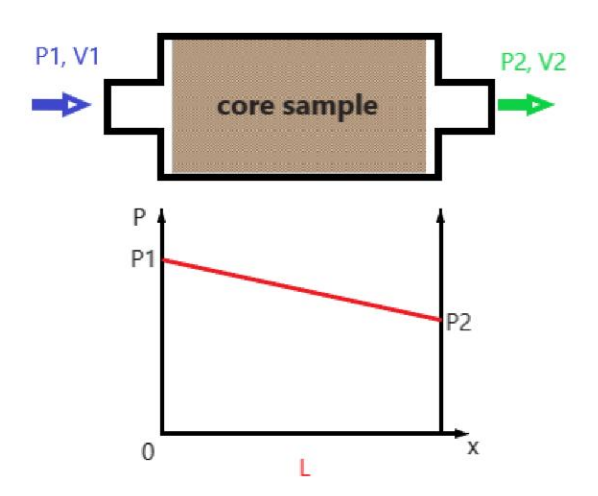


Figure 31. Conceptual model of Darcy's law

3.4. Dynamic threshold pressure test

This test was proposed by Egermann et al [25] and this test allows to measure **capillary entry pressure** under in-situ conditions. From dynamic point view, capillary entry pressure is the pressure difference between nonwetting phase and wetting phase that does not contribute to the flow. To have displacement of wetting phase by nonwetting phase within the caprock saturated with brine we apply constant pressure drop which is higher than capillary entry

pressure (Figure 32). The innovativeness of this method lies in the author's assumption that the total pressure drop consists of three distinct components, each corresponding to one of the following regions:

- the upstream invaded region
- the front region
- the downstream virgin region

In the sample's pore system, the upstream region of the caprock sample is occupied by gas that has displaced the brine, as the applied pressure drop exceeds the capillary entry pressure. The front region serves as a transition region, featuring pressure jump associated with capillary entry pressure. The virgin region refers to the portion of the caprock at downstream that remains fully saturated with brine, as the pressure drop has not reached this part yet, meaning the brine saturation stays constant and unchanged, just as it was in its initial state. This explains why this region is called "virgin". Schematically it is shown in Figure 33.

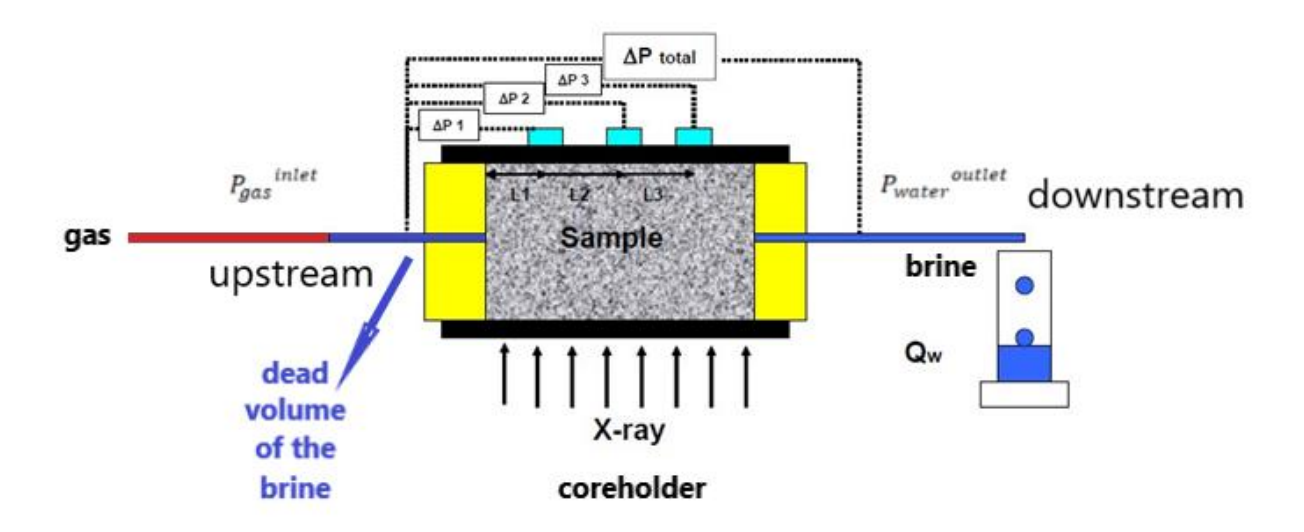


Figure 32. The experimental setup of the dynamic threshold pressure test, modified from [25]

Total pressure drop can be written as:

$$\Delta P_{total} = P_{nonwetting\ phase} - P_{wetting\ phase} = P_{gas}^{inlet} - P_{water}^{outlet}$$

$$\Delta P_{total} = \left(\Delta P_{gas}\right) + \left(\Delta P_{front}\right) + \left(\Delta P_{water}\right) =$$

$$\left(P_{gas}^{inlet} - P_{gas}^{front}\right) + \left(P_{gas}^{front} - P_{water}^{front}\right) + \left(P_{water}^{front} - P_{water}^{outlet}\right) \text{ Equation 5}$$
 where:

 ΔP_{aas} - the pressure drop in the nonwetting phase (gas) invaded region

 ΔP_{front} – the pressure drop in the front region

 ΔP_{water} – the pressure drop in the virgin region

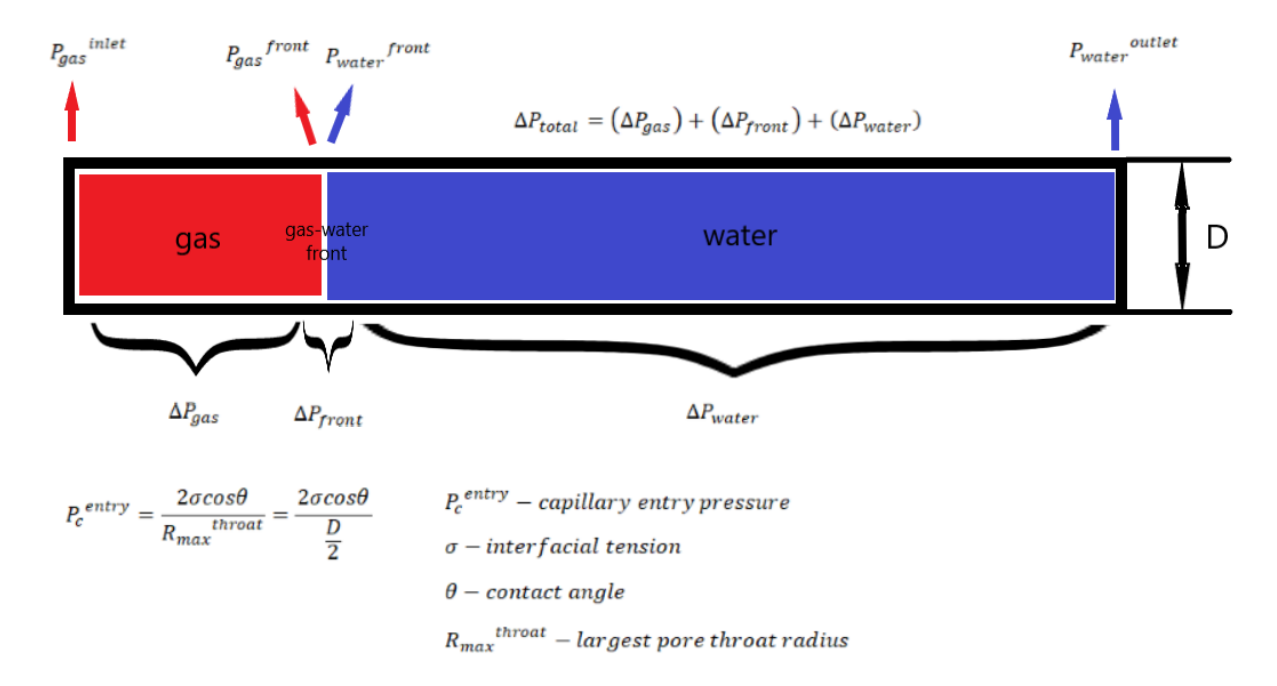


Figure 33. Schematic diagram illustrating pressure zones during gas injection phase

At the start of the test (time = 0), when gas injection gas begins, the authors have made **two** assumptions:

- The pressure drop in the nonwetting phase invaded region can be neglected ($\Delta P_{gas} = 0$). This arises from the limited extent (L1 is very small, approximately zero) of this region at the start of the injection. The pressure drop in the front region (ΔP_{front}) is equal to capillary entry pressure (P_c^{entry})
- The pressure drop in the virgin region can be calculated with Darcy's formula for incompressible fluids (water).

$$\Delta P_{water} = \frac{\mu_w L}{kA} Q_w$$
 Equation 6

where:

 Q_w – water flowrate at the downstream [m³/s], μ_w – water viscosity [Pa*s], L – length of the core sample [m], k – permeability of the core sample [m²], A – cross sectional area of the core sample [m²]

It is then possible to determine directly the capillary entry pressure using following equations:

$$\Delta P_{total} = (\Delta P_{gas}) + (\Delta P_{front}) + (\Delta P_{water}) = 0 + P_c^{entry} + \frac{\mu_w L}{kA} Q_w$$

$$P_c^{entry} = \Delta P_{total} - \frac{\mu_w L}{kA} Q_w$$
Equation 7

Test procedure:

- Preparation:
 - Put core sample fully saturated with brine in the coreholder and apply in-situ conditions (confining pressure and temperature)
 - The nonwetting fluid (gas) is injected into the brine core sample at constant pressure drop (ΔP_{total}) which is higher than expected capillary entry pressure.

Then we have two periods:

- First period: at the beginning of the injection, we have some dead volume of brine in the inlet. Then we apply constant pressure drop and gas starts to push that dead volume into the pore space, as a result we will see droplets of water at the outlet. This procedure continues until gas reaches the inlet of the coreholder. We measure water volume at each time and convert it to flowrate and then calculate absolute permeability of the water by using Darcy 'law. It is very important to have sufficient amount of dead brine volume at the inlet of the coreholder, to see slope on the diagram of recorded volume brine versus time. The slope corresponds to absolute water flowrate and absolute water permeability.
- Second period: Once the gas reaches the inlet of the coreholder, gas starts to enter the pore network and displaces water from the largest interconnected pore throats, as a consequence the water flow rate at the outlet will change, because of pressure gradient at existing at the interface gas-water in the pore throat, corresponding to the capillary entry pressure. The slope on diagram of recorded volume brine versus time will decrease and the slope will characterize the effective water flowrate and effective water permeability, because we don't have one phase flow in the pore network anymore. When we increase the injection pressure the pressure drop will decrease and when it is below the capillary entry pressure, the production of water at the outlet will stop. The indication of this phenomenon can be sudden change in slope. When applied pressure drop is lower than entry pressure, we have horizontal slope on the diagram meaning that there is no water flow. As soon as pressure drop exceeds the entry pressure the slope of the diagram starts to increase from zero as shown in Figure 34.

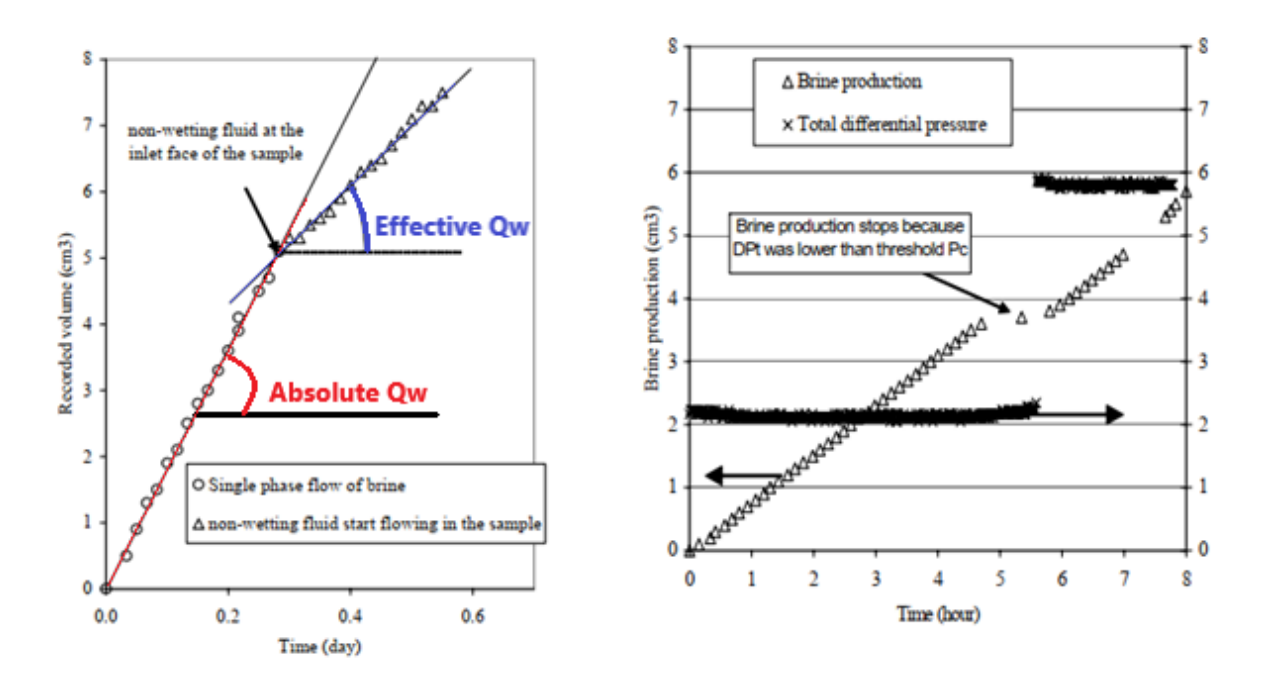


Figure 34. on the left: typical production curve recorded at the outlet; on the right: typical production curve recorded at the outlet when the pressure drop applied is lower than the capillary entry pressure

The authors also proposed the implementation of local pressure drop measurements across the core sample ($\Delta P1$, $\Delta P2$ and $\Delta P3$) as shown in Figure 32 and apply the same procedure to each pressure drop to measure of local capillary entry pressure taking into account the heterogeneity of the core sample.

Advantages:

- Reproduces the drainage phenomena
- In-situ confining pressure and temperature condition to represent reservoir storage conditions
- **Direct measurement of capillary entry pressure** for different gas-brine systems (hydrogen, methane, carbon dioxide, nitrogen etc.)
- Fast (the test is faster than standard test)
- Enables calculation of effective water permeability and absolute water permeability by using Darcy' law.
- Takes into account the anisotropy of the caprock (local measurement of pressure drop across the caprock to evaluate capillary entry pressure takes into account heterogeneities of the core sample)

Disadvantages:

- This test is good for fine graded core samples, but for very low permeability and ultra-low permeability rocks it cannot give reliable results because it becomes difficult to detect water production at the outlet. Water production will be very low, requiring highly sensitive volume measurement equipment. The wrong measurement of the water volume will lead to the wrong measurement of entry pressure. Underestimation of the first will lead to overestimation of the second.
- The applied pressure drop can overestimate the entry pressure. Since the test is dynamic and allows no time for pressure equilibration within the caprock, there is a risk of overestimating capillary entry pressure. For very low permeability rocks and ultra-low permeability rocks the test requires higher pressure drops which may alter the petrophysics of the core sample (porosity and permeability)

3.5. Comparison of the laboratory tests

The comparison of different laboratory tests is given in Table 7.

Table 7. Comparison of the laboratory tests

Test	Parameter measured	Advantages	Disadvantages
Mercury	Entry pressure	- Fast	- No in-situ conditions
injection		- Use of irregularly shaped samples	- Not representative of gas-
porosimeter test		and rock cuttings	water-rock system
			- Not accurate
Standard Test	Breakthrough pressure	- High accuracy	- Slow
(Step-by-step		- In-situ conditions	
test)		- Representative of gas-water-rock	
		system	
Residual	Snap-off pressure	- High accuracy	- The snap-off pressure is
capillary		- Relatively Fast	lower than the breakthrough
pressure test		- In-situ conditions	pressure [21]
		- Reproduce the drainage and	
		reimbibition phenomena	
Dynamic	Entry pressure	- Fast	- Complex experimental
threshold		- In-situ conditions	system
pressure test		- Representative of gas-water-rock	- Can overestimate entry
		system	pressure, since it relies on
			the MIP data for the initial
			pressure approximation (not
			reliable)

From Table 7 we can understand that the only test that gives an accurate value of breakthrough pressure and good representativeness is the step-by-step test. The residual test also offers certain advantages, it is faster than step-by-step test, but it only measures residual pressure which corresponds to imbibition process. In contrast, step-by-step test accurately measures breakthrough pressure which corresponds to the maximum sealing efficiency of the caprock (maximum capillary pressure before gas starts flowing through the caprock). This accuracy and good representativeness of drainage phenomena are main advantages of the step-by-step test, despite its main disadvantage - the time to conduct the test which is dependent on the pressure step.

4. Review of best practices of step-by-step test

Step-by step test (Standard test) demonstrates clear advantage in terms of representativeness, reliability and accuracy. In this chapter we will study best practices of conducting step-by-step test and focus on the experimental setup and procedures taken by different researchers whose works are available in the literature. The insights taken from their laboratory experiments will be implemented to develop standard laboratory protocol for conducting step-by-step test. The procedure of the step-by-step tests conducted by different researchers are almost the same and general procedure is well explained previously in chapter 3.2. Here we will mainly focus on the experimental setup, its components, functionality of each component, steps taken by researchers to accurately replicate drainage phenomena and measure breakthrough pressure.

4.1. Case study 1

Amirsaman et al [26] performed a standard test using their laboratory setup (Figure 35) to measure the capillary breakthrough pressure of methane, nitrogen and carbon dioxide in shale and anhydrite caprock samples from Iran.

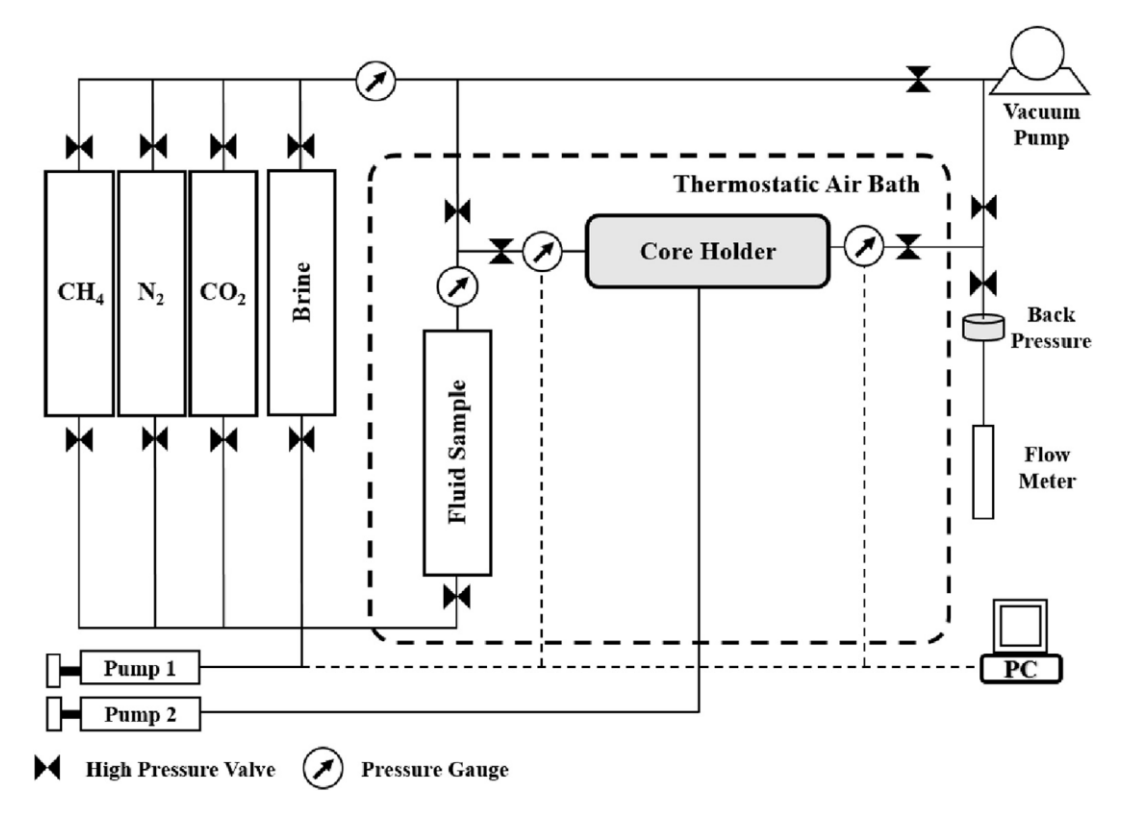


Figure 35. Diagram of the laboratory apparatus used for the standard test [26]

The apparatus consists of:

- Thermostatic air bath is used to keep temperature constant during the test
- Tri-axial high pressure coreholder with an elastic sleeve, sealing the core plug
- Pressure gauges/sensors (inlet and outlet pressures)
- **High pressure piston-cylinder** like accumulator is used to transport fluid sample to the coreholder through high pressure lines
- Four normal pressure accumulators are used to contain fluid samples (methane, nitrogen, carbon dioxide) and brine
- Accumulator in the thermostatic bath chamber which is feed with fluid samples
- **Pump 1** is high pressure syringe pump, equipped to the setup and used to pressurize the fluid sample.
- **Pump 2** is high pressure syringe pump disconnected from the setup to supply the confining pressure in the coreholder. Both pump 1 and pump 2 can operate at pressures up to 9500 psi (or 655 bar), have capacity of 266 ml and flowrate accuracy of 0.001 ml/min.
- Vacuum pump is used to expel air from the tubing system
- Backpressure regulator is used to maintain the outlet pressure of the coreholder
- Pressure gauges are used to monitor the pressure
- **Digital differential pressure gauge (PC)** is used to record the difference between the two sides (inlet and outlet) of the coreholder
- Flow meter is used to measure the gas flow rate
- **High pressure 2-way straight body needle valves** made of stainless steel are used to regulate flowrate and pressure during the test. They can handle pressures up to 10000 psi (or 690 bar).

Test procedure:

Sample Preparation

For the experiment, they used shale and anhydrite caprock samples with a diameter of 3.8 cm and a length of 2.9 cm. They mercury injection porosimetry method was used to determine average pore diameter, bulk density, porosity and first approximation of capillary entry pressure. Additionally, quantitative X-Ray Diffraction (XRD) analysis was used to determine the mineral composition of the core samples.

Then they measured absolute permeabilities of dried samples using different gases (carbon dioxide, nitrogen, methane) under specific mean pressure conditions. Klinkenberg correction was then applied to determine the average absolute permeabilities for the core samples. This correction accounts for gas slippage or slip flow phenomena when gas permeability increases at low mean pressures in porous media due to gas molecules colliding with pore walls. Conceptually this is represented in Figure 36.

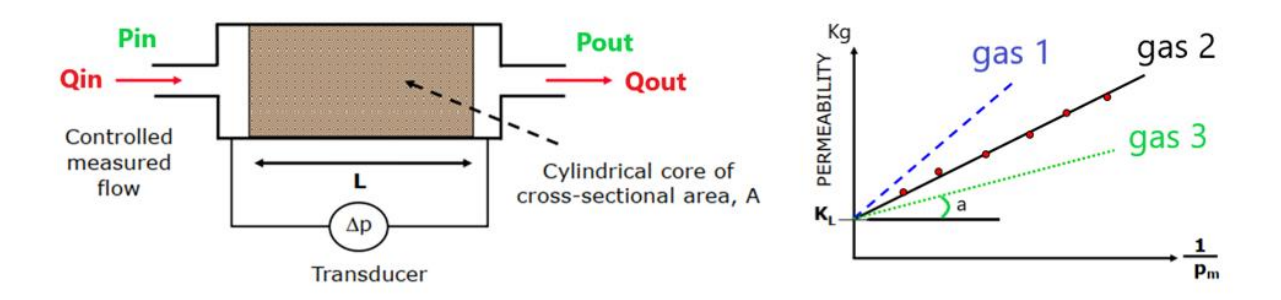


Figure 36. Schematic representation of gas permeability measurement setup and Klinkenberg Effect, modified from [27]

$$K_{g} = \frac{2V_{out}\mu L}{At} \frac{P_{out}}{P_{in}^{2} - P_{out}^{2}} = \frac{2Q_{out}\mu L}{A} \frac{P_{out}}{P_{in}^{2} - P_{out}^{2}}$$

$$K_{g} = K_{L} \left(1 + \frac{b}{P_{m}}\right) = K_{L} + \frac{K_{L}b}{P_{m}} = K_{L} + \alpha \cdot \frac{1}{P_{m}}$$

$$Equation 8$$

$$Equation 9$$

$$P_{m} = P_{mean} = \frac{P_{in} + P_{out}}{2}$$

where:

 Q_{out} – flowrate of gas at the outlet, V_{out} – volume of gas at the outlet, t – time, μ – viscosity of gas, L – length of the core sample, A – cross sectional area of the core sample, P_{in} – pressure of gas at the inlet, P_{out} – pressure of gas at the outlet, P_m – mean pore pressure K_g – absolute permeability of gas, K_L – Klinkenberg permeability, b – Klinkenberg slip factor, $a = K_L b$ – slope of the line on the diagram

Permeability is an intrinsic property of porous rock and is independent of the fluids flowing through it, depending solely on the rock's pore geometry (e.g., porosity, pore shape and pore size distribution). Therefore, the intrinsic permeability measured using any gas (e.g., gas1, gas2, gas3) as the pore fluid in a laboratory test should be the same as that measured with any other type of fluid. By plotting gas permeability against the mean pressure, the values of absolute permeability can be obtained from the intercepts of the K_g vs $1/P_m$ (Figure 36).

Sample saturation

The sample was saturated with a synthetic brine composed of NaCl, MgCl2 and KCl. Before flooding with brine, the tubing system was flushed with CO2 and evacuated for over 2 hours. The sample then was resaturated with brine. The outlet pressure P_{out} is set to the backpressure value and the inlet pressure P_{in} is controlled by syringe pump 1, increasing step by step with a waiting period to achieve steady-state flow. When the inlet pressure exceeds the backpressure value, the backpressure valve opens, and the brine flow is measured with a flow meter (Q_{brine}) . The sample can be considered fully saturated when the measured brine permeability k_{brine} no longer changes.

$$k_{brine} = \frac{Q_{brine}\mu_{brine}L}{A(P_{in} - P_{out})}$$
 Equation 11

Breakthrough measurement

Then the standard step-by-step test procedure (as briefly explained in chapter 3.2) was used to determine breakthrough pressure for each gas (methane, nitrogen, carbon dioxide). The test was stopped when a continuous flow of gas was detected at the outlet of the coreholder.

Gas effective permeability measurement

Gas effective permeability was measured after a continuous flow of gas was detected at **the outlet of coreholder** and **inlet pressure became stable.**

$$k_{gas.eff} = -\frac{2V_{out}\mu L}{A(P_{in}^2 - P_{out}^2)} \frac{dP_{out}}{dt}$$
Equation 12

 dP_{out}/dt is the rate of change of outlet pressure with time at constant V_{out} outlet gas volume, measured after the backpressure regulator. At the breakthrough time (when the breakthrough phenomena occurred), the outlet pressure is equal to the atmospheric pressure, and the observed pressure difference at that point represented the capillary breakthrough pressure. After continuous gas flow established the pressure at the outlet is increasing to the pressure limit defined by the backpressure regulator. Gas effective permeability can be measured whenever outlet pressure exceeds the backpressure. Effective gas permeability varies continuously with time and becomes almost constant after a long time. At this condition, no significant variations in the effective permeability were obtained with further increase in the backpressure.

Advantages of Lab Setup:

- Allows to conduct standard tests with different gases (methane, carbon dioxide, nitrogen)
- The thermostatic air bath is used to keep a constant temperature during the test. Temperature set to the reservoir storage temperature, maintaining constant temperature is important because it affects density, viscosity, interfacial tension, wettability and other key parameters.
- The use of synthetic brine helps replicate real storage conditions, as the salinity of water influences wettability, interfacial tension and contact angle. This approach ensures more reliable and accurate results.
- Reproducing of in-situ conditions by using pump 2
- Backpressure regulator is used for sample saturation and standard tests to achieve steadystate flow
- Vacuum pump is used to expel air and flush the tubing system. It enables system flushing after sample saturation and when switching to a new gas test after completing one gas test
- Measurements of absolute brine permeability k_{brine} and effective permeability of gas $k_{gas.eff}$

4.2. Case study 2

In this case study we will study the experimental setup of standard test used by Li et al. [15] to measure breakthrough pressure of carbon dioxide with the Weyburn Midale Evaporate caprock samples.

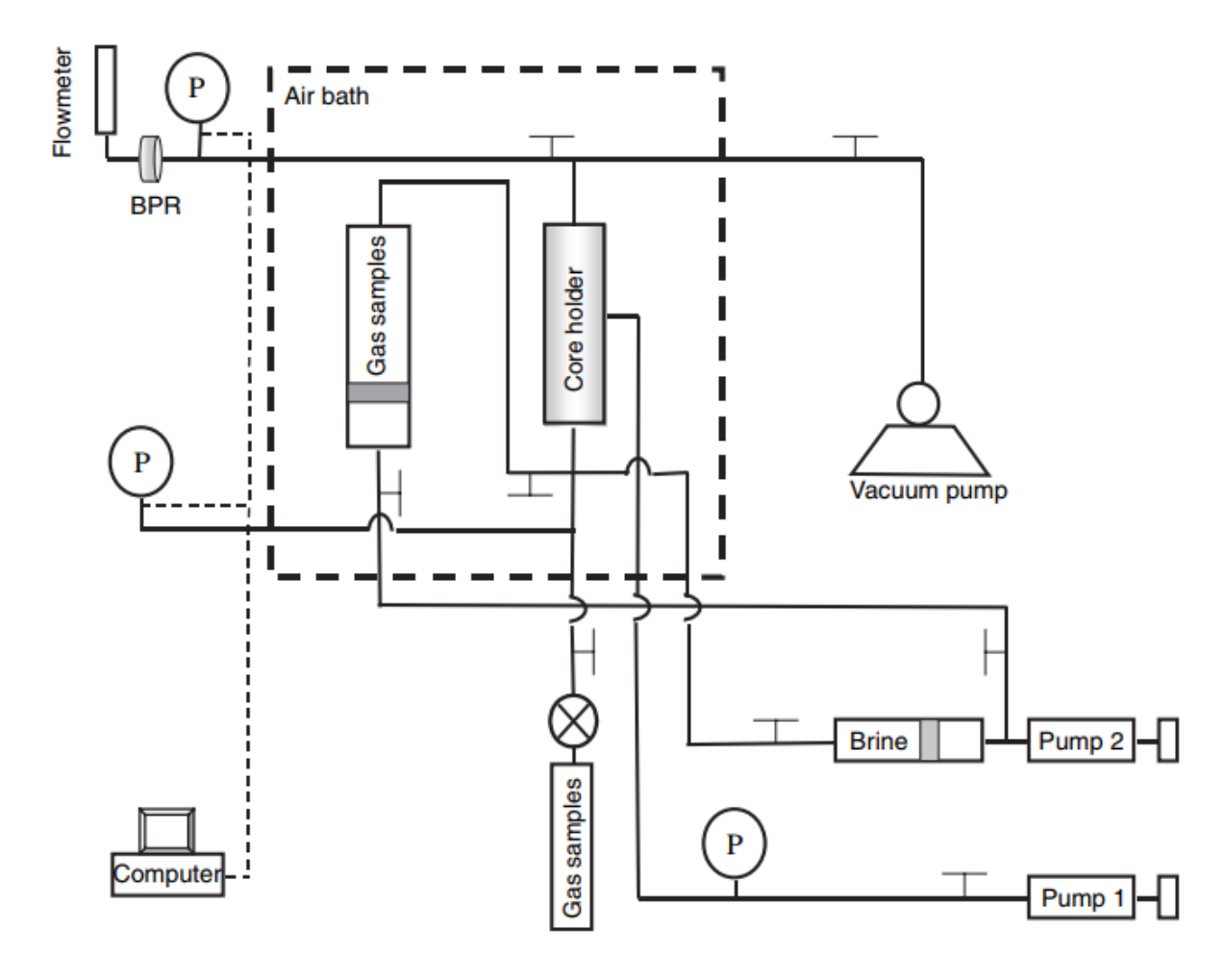


Figure 37. Schematic of apparatus for breakthrough pressure measurement [15]

The apparatus consists of:

- An air bath to keep the temperature constant during the measurement
- Pressure gauges/sensors (inlet and outlet pressures, confining pressure)
- Hassler type high pressure coreholder with a thick lead sleeve to contain the core sample. The coreholder is specialized for high-pressure CO2 displacement tests with the use of thick lead sleeves instead of the commonly used rubber sleeves to ensure a leak-tight seal around the rock samples. This avoids sealing failure caused by the effects of CO2 adsorption in rubber sleeves in a long-duration test.
- High-pressure gas sample piston cylinder to contain the test fluid sample
- High pressure **pump 1** to control the net confining pressure (the difference between the confining pressure and the injection pressure (or inlet pressure)). A net confining pressure must be sufficiently high to ensure a seal around the core sample and prevent bypassing of the gas
- High pressure **pump 2** to inject brine to saturate the core sample and to pressurize the gas sample to provide the inlet pressure.
- Vacuum pump is used to expel air from the tubing system
- Backpressure regulator (BPR) to provide the back pressure at the outlet of the core sample
- Metering capillary tube (Flow meter) with fine scales and 0.5 ml volume to measure the gas flow rate
- Two-channel, high pressure, digital Heise gauge (P) to monitor pressure

• Data acquisition system (computer) to record inlet and outlet pressures

Test procedure:

Sample Preparation

For the experiment, they used shale and anhydrite caprock samples with a diameter of 3.81 cm (1.5 inch) and a length of 5.08 cm (2.5 inch) taken from the low-porosity region of storage formation. The samples were dried and petrophysical properties were analysed. Helium porosimeter was used to measure porosity

Check for leakage in the coreholder

An equal-size metal plug to simulate zero-porosity core sample was used to test if the confining pressure is sufficient to prevent any leakage through possible channels between the sleeve and the core sample. The confining pressure is set to in-situ stress found at the depth of the storage reservoir. No leakage was occurred

Core sample saturation:

- Core sample was installed in the coreholder
- CO2 was injected at the inlet to displace air in the core sample
- Sample was evacuated to vacuum pressure for at least 2 hours
- CO2 was introduced to purge the core sample and then the evacuation was repeated once
- De-aerated formation brine was injected from the inlet until brine reached the outlet
- Confining pressure was applied for at least 12 hours to achieve steady-state brine injection
- Brine permeability was measured at the outlet
- Brine trapped in the tubings leading to the inlet was removed to ensure that gas contacted the inlet end face of the core sample

Breakthrough measurement

Then the standard test procedure (as briefly explained in chapter 3.2) was used to determine breakthrough pressure for each gas (methane, nitrogen, carbon dioxide). For the tests with nitrogen and methane the outlet of the core was at atmospheric pressure, while for carbon dioxide a constant backpressure was applied to ensure that carbon dioxide was in supercritical state during the test. At each pressure step the movement of liquid meniscus in the metering capillary tube was monitored and from this flowrate of brine coming out from the outlet was calculated. In order to be sure, that gas has not broken through at an injection pressure, the injection pressure is increased to the next level only when the flow at the outlet stops. The test was stopped when a continuous flow of gas was detected at the outlet of the coreholder.

Advantages of Lab Setup:

- Allows to conduct standard tests with different gases (methane, carbon dioxide, nitrogen)
- The thermostatic air bath is used to keep a constant temperature during the test.
- The use of formation brine for core sample saturation provides realistic reservoir condition, this approach ensures more reliable and accurate results.
- Confining in-situ pressure conditions are applied using pump 2 to simulate the stress conditions found in the reservoir storage depth
- Backpressure regulator is used for sample saturation and standard tests to achieve steady-state flow
- Vacuum pump to expel air from the tubing system ensures removal of trapped gases, enabling accurate pressure measurements.

- Measurements of absolute brine permeability k_{brine}
- Computer (data acquisition system) allows for continuous monitoring and recording of inlet and outlet pressure

Disadvantages:

- According to the schematic in Figure 37, the vacuum pump is connected to the downstream (outlet) side of the coreholder and backpressure regulator (BPR). This configuration allows flushing only the downstream tubing system, not the upstream (inlet) tubing system. Consequently, the inlet tubing for the brine injection line and gas sample line cannot be flushed directly. The only way to flush these is through the coreholder, which connects the upstream and downstream systems. To improve this, the vacuum pump should be connected to the upstream side instead of the downstream.
- The schematic also shows two gas sample cylinders: one connected to pump 2 and another with an additional pump. However, the test procedure typically involves injecting only one gas per run, using a single connection through pump 2. The second cylinder adds unnecessary complexity to the flow system without providing significant operational benefits. So, in my opinion one gas sample cylinder connected to pump 2 would be enough.

The schematic in Figure 37 was too unclear for understanding. I modified it for better clarity and comprehension, as shown in Figure 38. I recommend removing the second gas sample cylinder with its pump, improving the data acquisition system by connecting pump 2 to a computer, and connecting the vacuum pump to both the upstream and downstream tubing systems. The schematic incorporating these recommendations is shown in Figure 39.

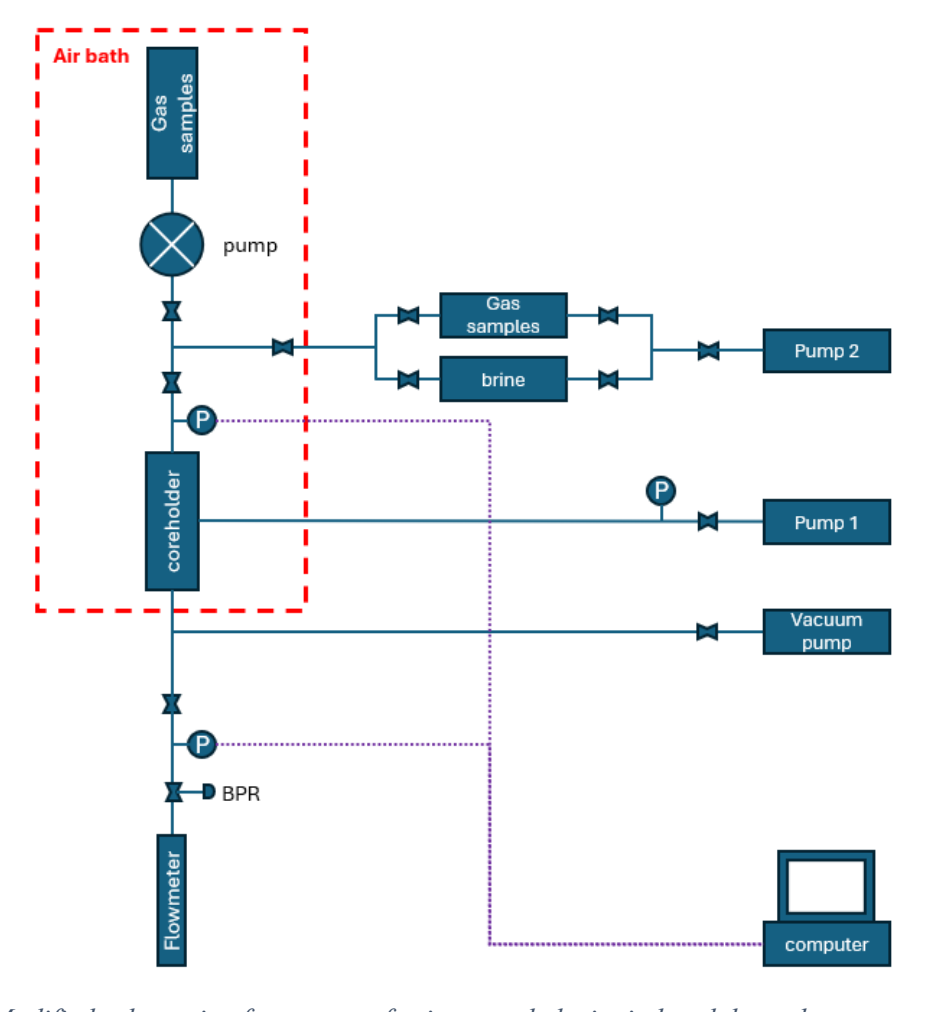


Figure 38. Modified schematic of apparatus for improved clarity in breakthrough pressure measurement

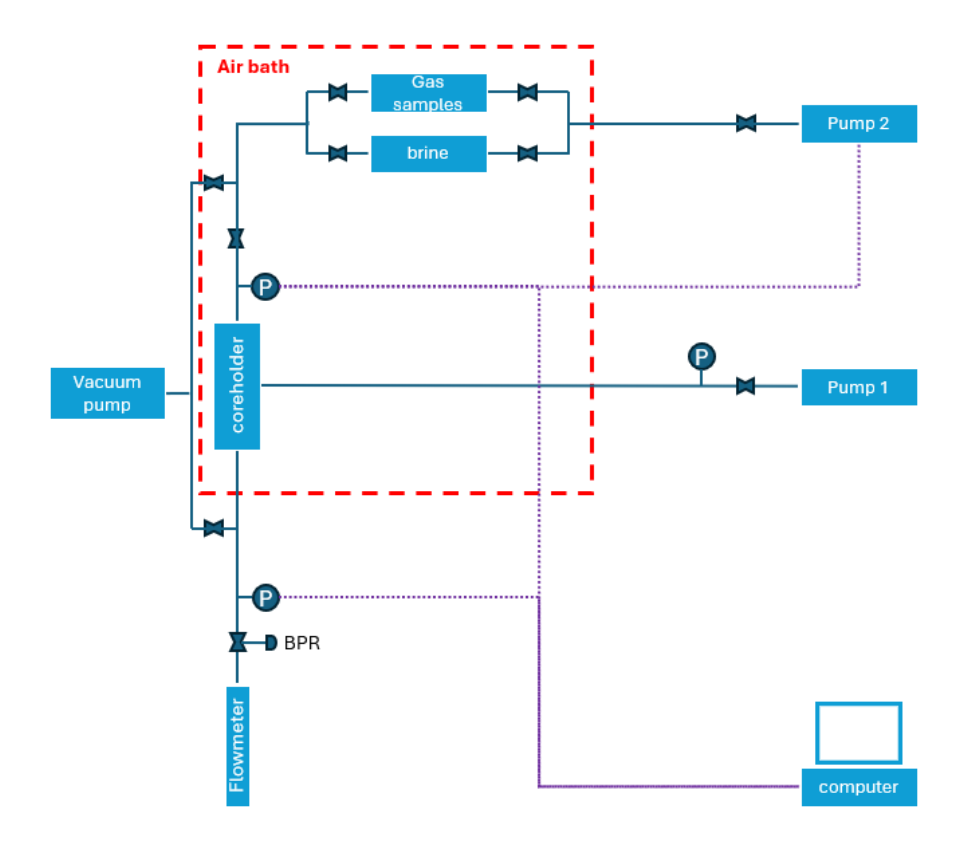


Figure 39. Schematic of apparatus with recommended optimizations for breakthrough pressure measurements

4.3. Case study 3

In this case study, we will examine the experimental setup for the standard test used by Klimkowski and Smulski [28] to measure breakthrough pressure of carbon dioxide. The schematic of the apparatus is shown in Figure 40.

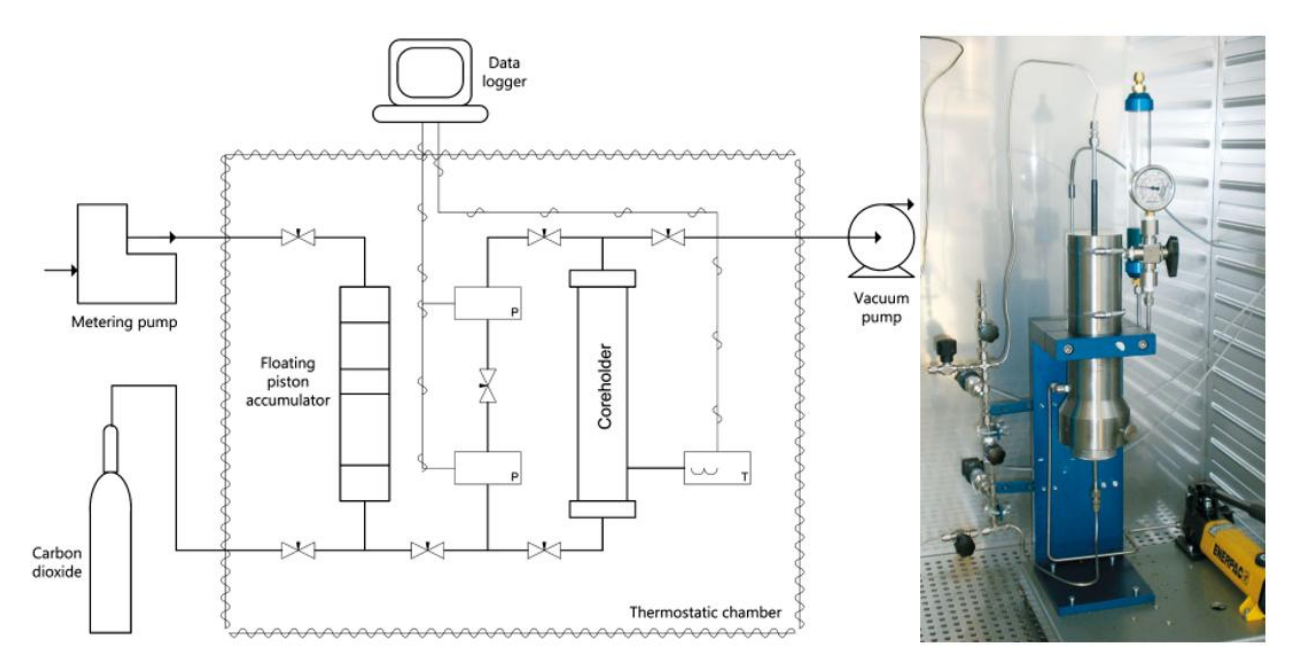


Figure 40. Schematic of Lab Setup (Left) and Hassler-Type Coreholder (Right)

The apparatus consists of:

- High pressure Hassler-type core holder
- Metering pump
- Pressure gauges (inlet and outlet pressures)
- Vacuum pump
- Temperature control
- Thermostatic chamber to ensure constant temperature during the test
- Floating piston accumulator
- Data logger to record inlet and outlet pressures and temperature

Test procedure:

Sample Preparation

Core samples with a diameter of 1 inch and a length of 1.5 inches were used. Their porosities were measured using a helium porosimeter, and their permeabilities were determined using the pressure pulse decay method.

Core sample saturation

- Core sample placed in automatic core saturator under high pressure. For the saturation of sample brine with a certain salinity was used.
- Saturated sample was placed in the viton collar and then installed in the coreholder.
- Confining pressure was applied in the coreholder to represent in-situ stress conditions
- Inlet of the coreholder was connected to the floating piston accumulator, then floating piston accumulator was filled with nonwetting fluid (carbon dioxide)

Breakthrough measurement

Then the standard step-by-step test procedure (as briefly explained in chapter 3.2) was used to determine breakthrough pressure of carbon dioxide.

Advantages of Lab Setup:

- Automatic core saturator operating at high pressure ensures effective brine saturation under representative reservoir pressure conditions.
- Thermostatic chamber maintains a constant temperature, minimizing thermal effects on fluid properties and measurement accuracy.
- Vacuum system for flushing tubing ensures clean and uncontaminated fluid pathways.

Disadvantages

- Complex fluid delivery system. The combination of a metering pump and a floating piston accumulator adds unnecessary complexity; a single integrated pump could simplify the setup.
- No outlet fluid collection system. Lack of flow measurement device at the outlet limits monitoring during breakthrough.

5. Laboratory work to measure threshold pressure

Following a comprehensive review of different lab configurations of standard test for measuring breakthrough pressure, including analysis of experimental procedures, apparatus configurations, and advantages and disadvantages, a laboratory protocol of the step-by-step test was developed for an inhouse customized laboratory setup represented in Figure 41. The experimental setup is adopted to measure the breakthrough pressure. The following section outlines a detailed procedure for conducting step-by-step test

The experimental setup is divided into four functional systems - upstream, coreholder steam, downstream and data acquisition and control system, each incorporating specific components:

Upstream system

- Syringe pump
- Injection fluid tank

Coreholder steam system

- Coreholder
- Electrical heating system
- Manual pump
- Confining fluid tank
- Pressure and Temperature sensors
- Control valves
- Tubings

Downstream system

- Receptacle, Mass balance and Video Monitoring
- Backpressure regulator (BPR)

Data acquisition and control system

Software

A syringe pump is used for the controlled injection of the gas. The syringe pump has two lines: one connected to an **injection fluid tank**, and the second line connected to the **upstream of the coreholder**. These two lines are equipped with two valves. First valve is positioned on the injection fluid tank line for the filament of the pump with injection fluid (brine or gas). Second valve is positioned on the injection line to upstream of the coreholder, it is used to regulate flow into the coreholder or isolate the syringe pump when necessary.

The core sample is placed inside the high-pressure, high temperature **coreholder**. The coreholder is equipped with an **electrical heating system** that heats two plates (heating plates) to maintain a constant temperature in the coreholder during the test. To reduce heat loss (heat dissipation) and ensure user safety, the coreholder is covered with a jacket. **Manual pump** injecting confining oil is used to create confining pressure around the core sample. Confining pressure prevents lateral flow of gas and force gas to flow through the core sample. The downstream of the coreholder is connected to a **backpressure regulator (BPR)**. The BPR is used to maintain a constant downstream pressure during the test and defines the initial pressure of the test. The <u>syringe pump</u>, which provides the upstream injection pressure and the <u>manual pump</u>, which provides the confining pressure and the BPR which provides downstream pressure and the temperature control

system, together they are used to reproduce in-situ conditions inside the coreholder during the test.

The downstream system consists of a monitoring system that helps identify the type of produced fluid and quantify its mass and flowrate. It includes a **receptacle** filled with transparent oil to collect the produced fluid, a **mass balance** and **video monitoring system**.

The system is equipped with **pressure sensors** to read pressure at the **inlet** (**P**_{inlet}) and **outlet** (**P**_{outlet}) of the coreholder, **pressure gradient** (**dP**) across the tested plug, and a pressure gauge that provides a reading of the confining pressure. These pressure sensors have a **sensitivity of ±1 psi**, ensuring reliable pressure monitoring throughout the test. **Temperature sensor** of the electrical heating system continuously measures the temperature in the coreholder. Pressure and temperature sensors, syringe pump, BPR and downstream monitoring system are connected to **data acquisition and control system**. The wetted parts of the experimental setup are made of Hastelloy to ensure its compatibility with the testing gases. A complete schematic diagram of the laboratory setup is shown in Figure 42. The specification of the lab setup is provided in Table 8.

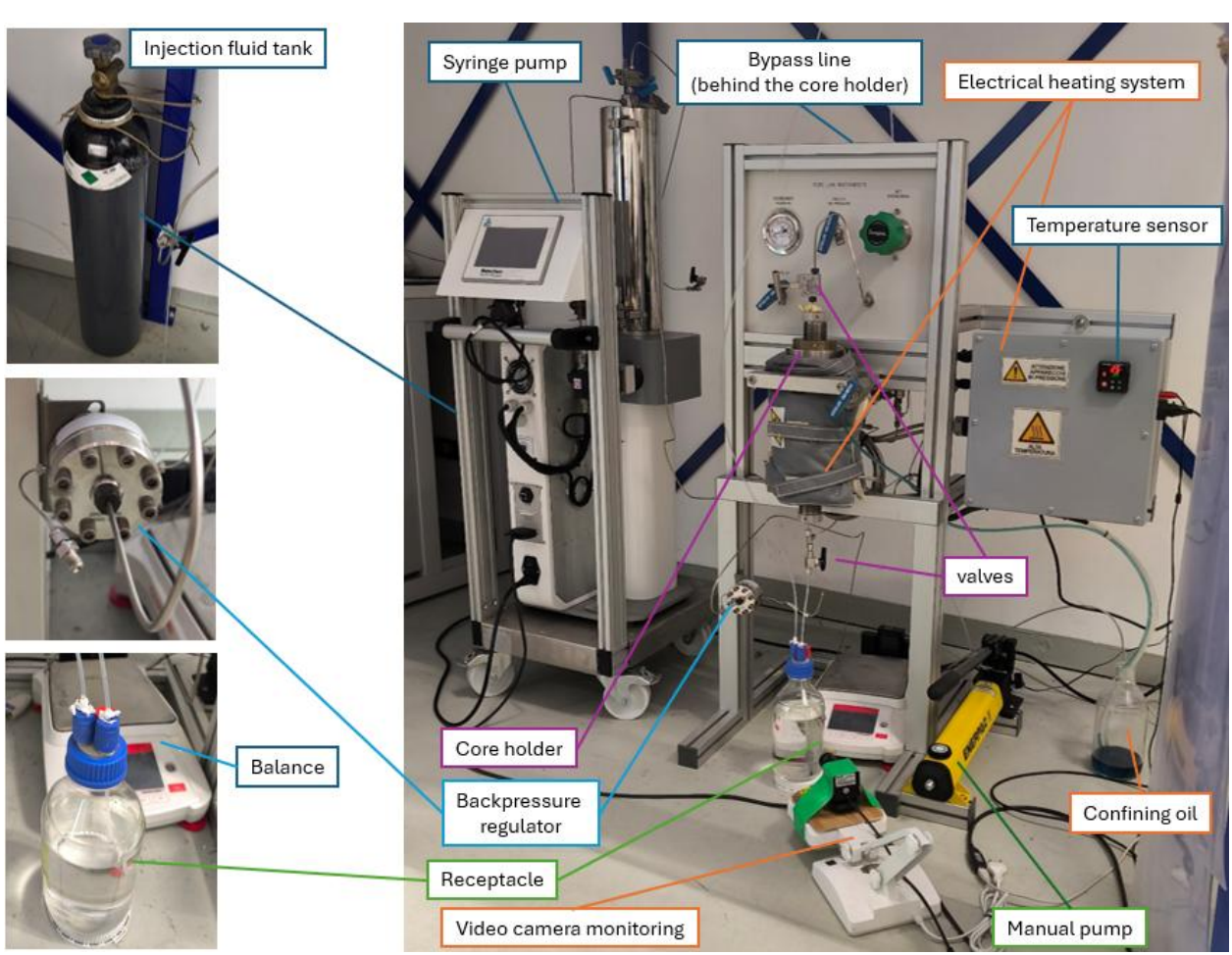


Figure 41. Experimental laboratory setup

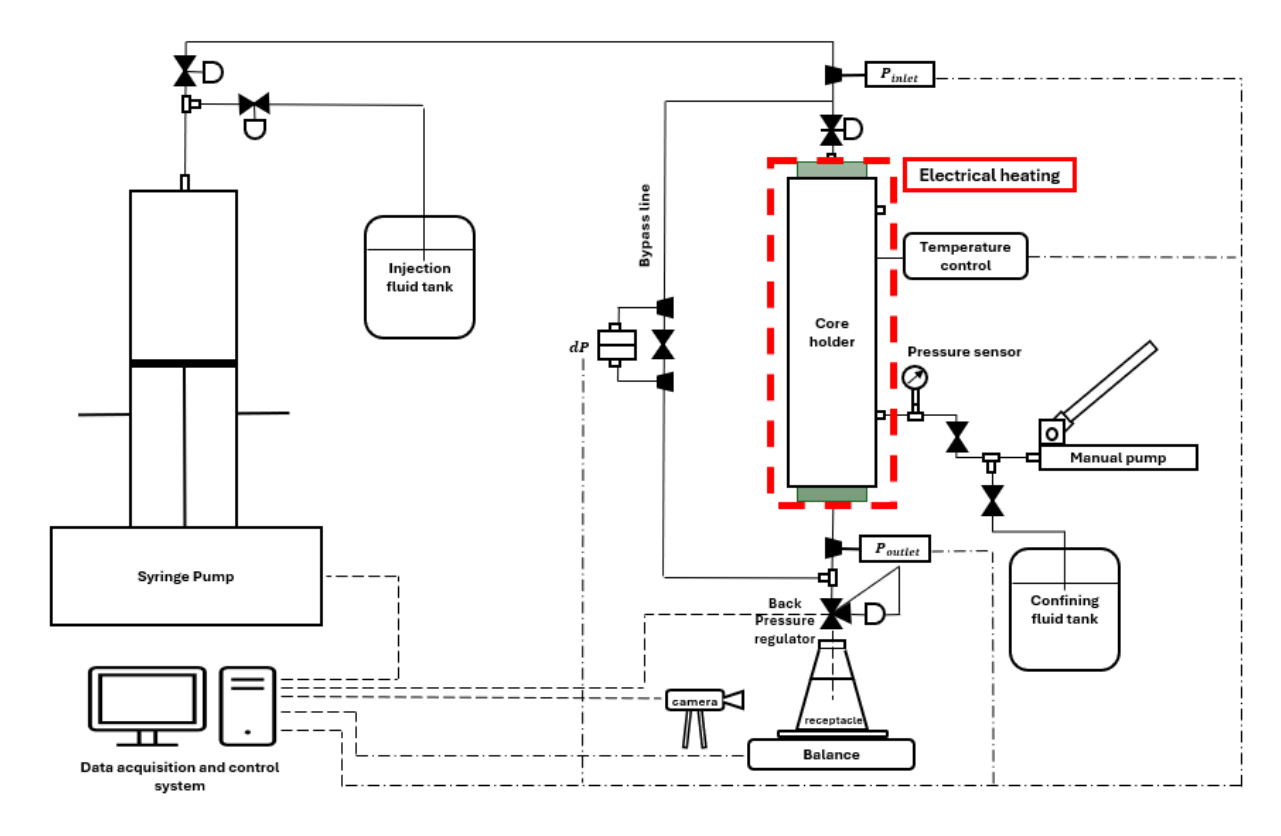


Figure 42. Schematic diagram of the laboratory setup

Table 8. Specifications of the laboratory setup

Specifications of the laboratory setup				
Operational pressure	0 - 700 bars			
Operational temperature	Ambient (20 °C) – 200 °C			
Syringe Pump Volume	500 ml			
Syringe pump Min. Flowrate	0.5 ml/min			
Syringe pump Max. Flowrate	94 ml/min			
Backpressure regulator operating pressure	0 - 200 bars			
Diameter of tubings	1/16 inch			
Accuracy of measurements				
Pressure sensors	± 1 psi			
Syringe pump flowrate	\pm 0.05 ml/min			

5.1. Detailed description of laboratory setup components

Syringe pump

The syringe pump is one the key components of the experimental setup, it is designed to enable precise and controlled injection. It operates at pressures of up to 700 bar and it has total volume capacity of 500 ml and flowrate accuracy of 0.05 ml/min. The syringe pump has three operational modes:

- Constant pressure mode, in which the pump maintains a constant injection pressure and adjusts the flowrate accordingly.
- Constant flowrate mode, where the fluid is injected at a set flowrate.
- Constant volume mode, where the pump maintains a constant volume independent of pressure and temperature

Additionally, syringe pump can also create a vacuum pressure of **-1 bar**, which allows to remove fluids from the tubings (for flushing the tubing system). Syringe pump is equipped with an integrated heating system.

Coreholder

The coreholder plays an important role in simulating subsurface storage conditions during laboratory experiments, its schematic is shown in Figure 43. The manual pump draws confining oil from a confining fluid tank and injects it into the annular space between the core sleeve and the coreholder wall through confining pressure line to create confining pressure.

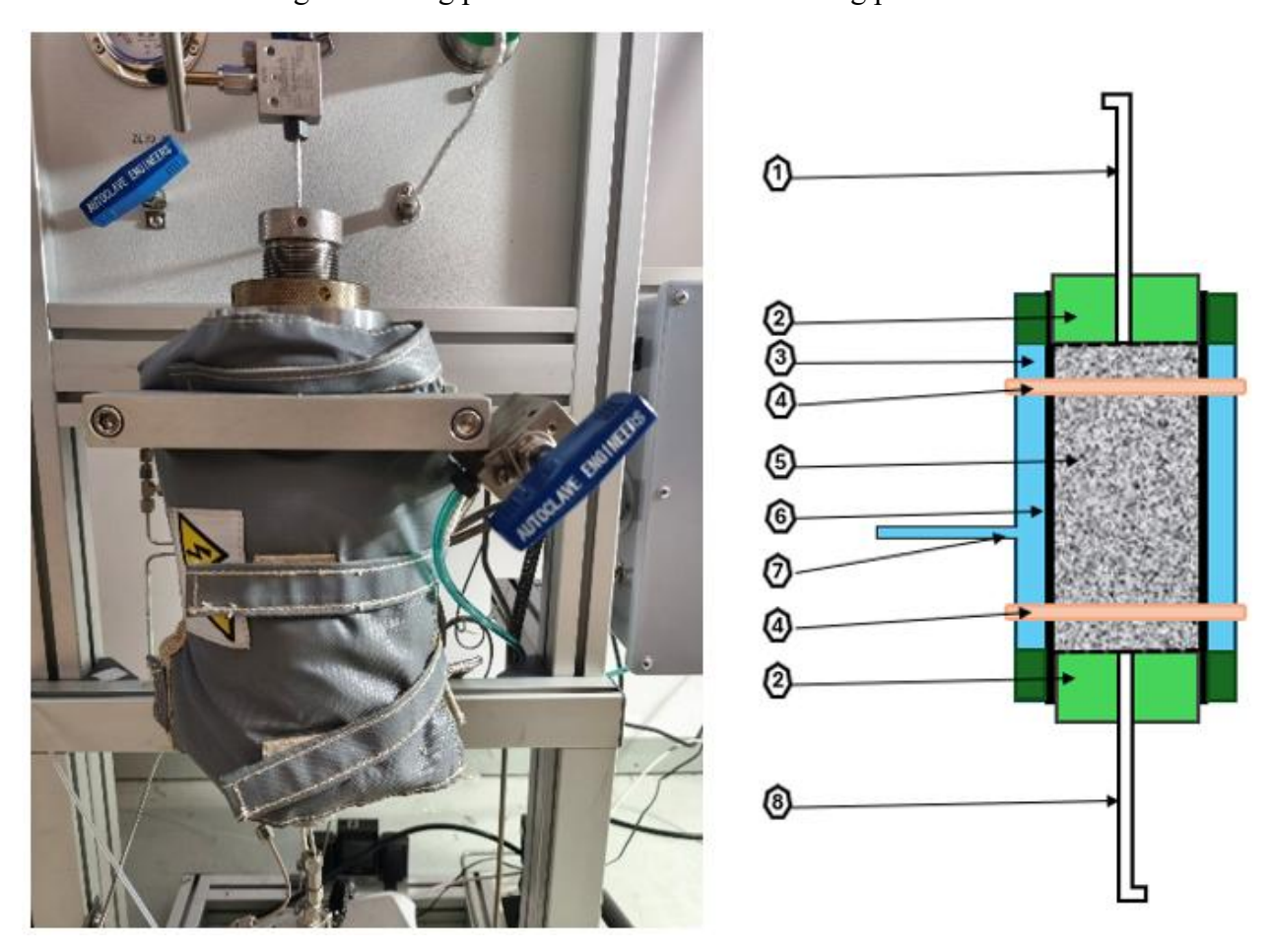


Figure 43. Schematic of the coreholder: 1) Inlet tubing 2) Sample seats 3) Confining fluid 4) Heating plates 5) Core sample 6) Rubber sleeve 7) Confining pressure line 8) Outlet tubing

Downstream monitoring system

The receptacle is a vessel filled with transparent oil that serves as an intermediate medium to visual distinguish of fluid coming out from the downstream (brine or gas). The transparent oil has a density lower than that of brine but higher than that of the gas. The receptacle is sealed with a lid and equipped with two ports (Figure 44):

• **Downstream line port:** an outlet tube from the downstream line is submerged in the transparent oil. Gas exiting the downstream line enters the receptacle, forming visible bubbles in the oil. Due to its lower density, the gas rises through the oil to the top of the receptacle while droplets fall to the bottom of the receptacle. It is used a visual confirmation of the onset of gas-induced brine displacement and gas breakthrough.

• **Ventilation line port:** A second line connects to the top of the receptacle to a ventilation system, allowing the gas to exit after rising through the oil.

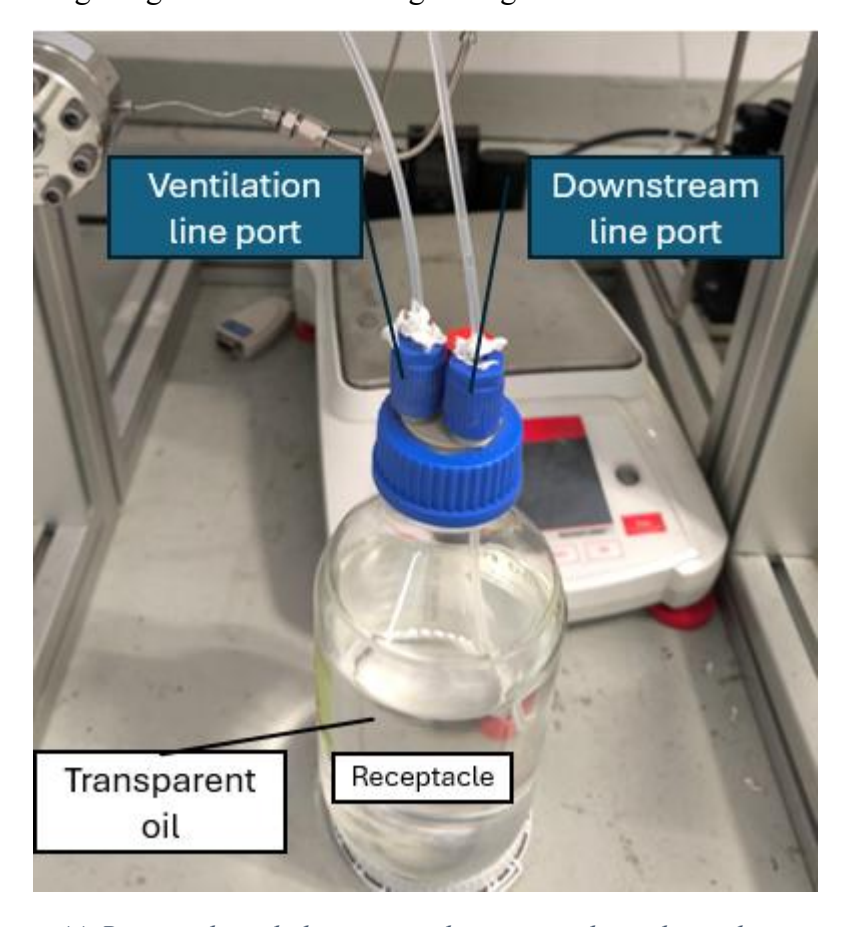


Figure 44. Receptacle with downstream line port and ventilation line port

A mass balance is used to measure the mass of brine accumulating in the receptacle. The balance is set to zero for a given weight of receptacle + transparent oil. When brine flows into the receptacle, a change of mass is detected with respect to time, the mass rate is then converted into flowrate.

The volume of brine is determined using the equation:

$$V_{brine} = \frac{\Delta m}{\rho_{brine}}$$

The brine flow rate is then determined by:

$$Q_{brine} = \frac{V_{brine}}{\Delta t}$$

where:

- Δm is the change in mass recorded by the balance (in grams)
- ρ_{brine} is the density of the brine (in g/cm3 or kg/m3)
- Δt is the time interval over which the mass change is measured (in seconds or minutes)

A **video camera** is installed at the outlet to continuously observe the fluid coming from the downstream. It detects gas bubbles and brine droplets, providing direct visual confirmation of fluid breakthrough. An oil-filled receptacle collects the displaced fluid, enhancing the separation of brine from gas. This is especially important when the volume of brine is too small for the precision

balance to detect accurately. **Together, the camera, oil-filled receptacle and balance form a combined monitoring system.** This setup ensures reliable detection of breakthrough phenomena, even when fluid volumes are very small.

Backpressure regulator (BPR)

The **backpressure regulator (BPR)** is a crucial component of the experimental system and it is responsible for maintaining a stable and constant pressure downstream of the core sample. This stability is essential for accurately reproducing reservoir pressure conditions during hydrogen breakthrough pressure testing. The BPR set point is at its downstream, once the pressure goes beyond the set point, the BPR releases the excess pressure to the receptacle in order to maintain the pressure of the line constant.

Data acquisition and control system

The laboratory setup is fully integrated with a computerized data acquisition and control system that enables continuous monitoring, precise regulation, and automated logging of critical experimental parameters. The customized software controlling the system is **SmartPLS-6 version 1.0**, whose user interface allows the operation and comprehensive control of all components. The interface features a top navigation bar with the following tabs: **Main**, **Logging**, **Test Configure**, **View Plots**, and **Help**. Below the navigation bar, a blue status panel provides real-time test information including the test date and time, logging interval, logging mode (automatic or manual), and controls to start or stop logging. The panel also displays the total elapsed logging time. All logged data are saved in files on the local computer disk for secure storage and subsequent analysis. The software interface includes a detailed schematic (Figure 45) of the laboratory setup, divided into three key sections:

- Syringe Pump: the software allows to select the aforementioned operation modes. A Start/Stop button controls the pump operation. Real-time indicators display pumps volume (ml) obtained by the piston position, flowrate (ml/min), pump pressure (psi). Control parameters are:
 - set pressure (psi) to define the desired injection pressure (in case of constant pressure control mode)
 - set flowrate (ml/min) to define the desire flowrate (in case of constant flowrate mode)
 - pumps volume (ml) to define the piston's position for a fixed volume
 - the ramp rate to define pressure increase per second.

Safety limits:

- pressure bandwidth (PbHi, psi) to define dP limits above and below the set pressure to allow for the pump to readjust pressure during transient pressure change, typically set low for gas (low compressibility fluids) and high for brine (compressible fluids), a pressure limit once reached the pump shuts down (AIPhi, psi).

The piston position and the corresponding fluid volume are also shown. Two needle valves (EV1 and EV2) are controlled via the interface **for visual purpose**: EV1 regulates the fluid source filament (either brine or test gas), while EV2 controls the injection line valve. These valves cannot be opened/closed using the software.

• Pressure/Temperature control and monitoring: the system continuously monitors inlet and outlet pressures (psig) using pressure sensors, and differential pressure (DP) of the

- tested plug. Temperature control is managed through a temperature indicator with a setpoint function.
- Mass/Flow rate monitoring: the receptacle module provides a tare function and records fluid flow rate (mL/min) and leak-off volume (mL) over user-defined logging intervals.

The system automatically logs the following parameters: date and time, elapsed time, inlet pressure, outlet pressure, differential pressure, core holder temperature, injection pump flowrate, injection pump pressure, leak-off mass, leak-off volume rate, logging mode and relative fluid volume.

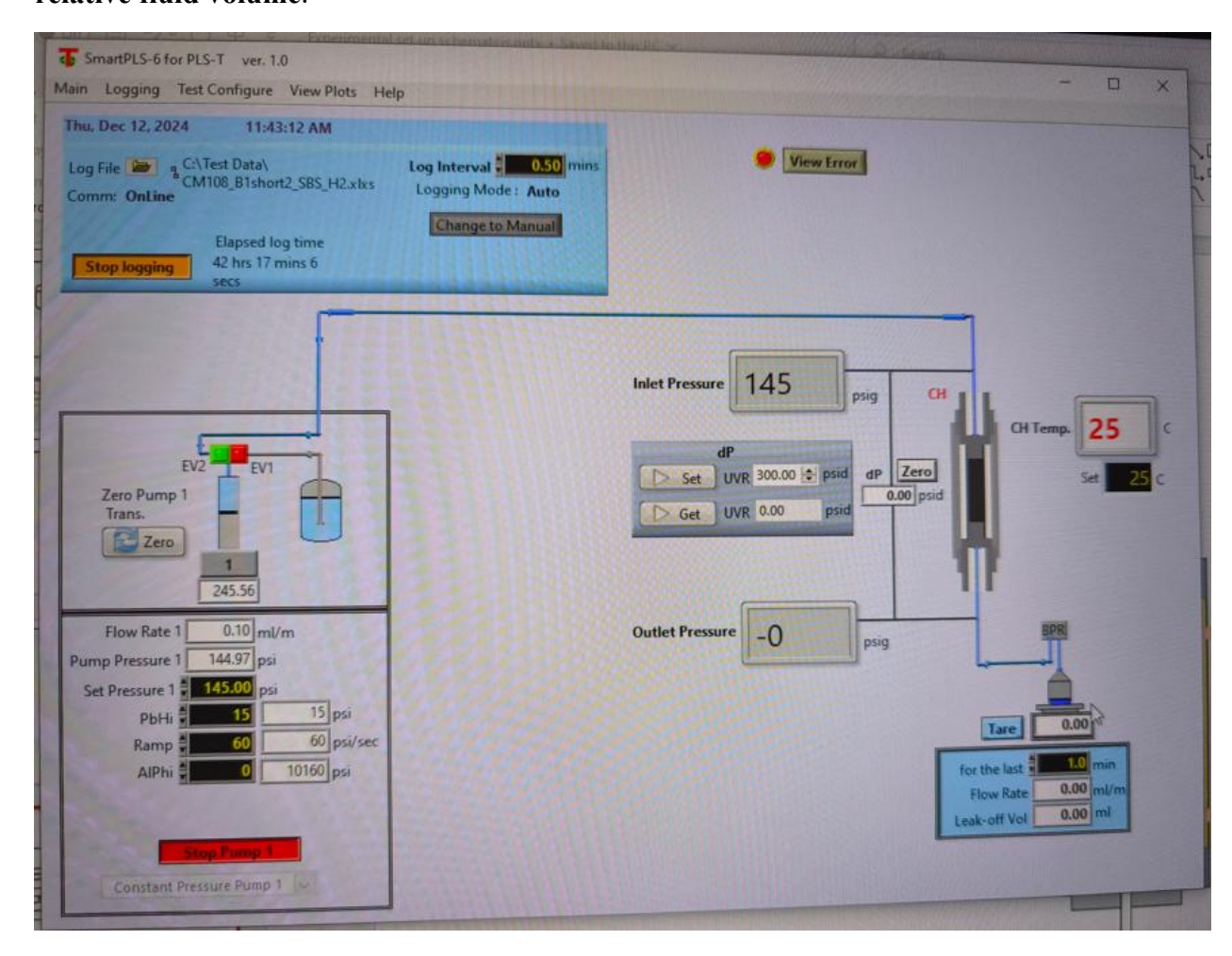


Figure 45. User interface of the customized software

Valves

Valves play an important role in the laboratory setup by enabling precise control of fluid flow and pressure during various stages of the step-by-step test. Their strategic placement allows for flexible operation, including fluid injection, isolation of system components, pressure regulation and flow path control.

There is one valve on the inlet upstream line of the coreholder and it is used to isolate the coreholder from the syringe pump.

An additional valve is placed to bypass the coreholder and connects upstream and downstream. This design allows the fluid to be redirected so that it doesn't pass through the core sample and the system can be flushed, cleaned or pressure equalized without affecting the core sample or interrupting the main experiment. This makes the system more flexible and easier to operate during the test.

For confining pressure control, the two ends of confining line are connected to two valves that are used to manage the pressure applied around the core. The first valve is positioned at the bottom of the coreholder and used to isolate the coreholder from the confining line. The second control valve is connected to the confining pump to regulate and set the desired confining pressure. Additionally, when adjusting pressure of confinement when setting the testing temperature, the second valve is kept open while the first one is slowly opened in order to release any excess pressure back to the confining pump oil tank.

A purge valve is positioned on the coreholder and connected to the confining space. It is used to vent air that might accumulate inside the confining space after continuous use of the experimental setup.

Tubings

The Hastelloy tubing system has the standard 1/16-inch diameter. The tubing system is exposed to the ambient temperature causing heat and temperature loss during the test, to minimize this temperature loss the tubing is wrapped with insulation.

5.2. Test procedure

Test preparation

To obtain realistic and reliable breakthrough pressure measurements, it is essential that the caprock sample remains intact and free from heterogeneities such as microfractures (fissures) or pre-existing failure planes. The presence of internal microfractures may allow gas to easily find the less resistant flowpath and bypass the rock matrix and break through immediately at the beginning of the test, resulting in unrepresentative results that do not characterize the true sealing efficiency of the caprock. Therefore, a detailed understanding of the sample's structure and integrity is important. We should have information about the petrophysical parameters of the core sample like porosity, permeability, length, diameter, mineral composition etc.

Based on the coreholder's specifications, the standard dimensions of the caprock samples used in our tests include a diameter of **1.5 inches**, with varying lengths. For samples shorter than 3 inches, **custom-designed extensions** are mounted to stabilize the sample during testing and to ensure proper sealing and alignment within the coreholder.

Reproducing in-situ conditions

The confining pressure applied during the test is equal to the tectonic stress value at the depth where the caprock sample was taken and the temperature is equal to the in-situ temperature. Accurate replication of these conditions is essential to ensure the relevance and reliability of the experimental results, as these parameters affect the breakthrough pressure magnitude. Confining pressure and temperature are case-specific values and depend on the core sample.

We put the fresh core sample into the coreholder and begin applying confining pressure. Before starting this, we ensure that there is no air in the annular space of the coreholder. To remove any air, we pressurize the annular space using manual pump and then slightly open the purge valve to purge the air. Once we see that the confining fluid has filled the annular space, we slightly open

the purge valve to push out all the air from the coreholder and then we close the purge valve. Once we are sure that there is no air, we can set testing condition: confining pressure and temperature in the coreholder. To achieve this condition, we gradually increase the temperature by regulating the confining pressure in the coreholder. Manual pump injects confining oil at confining set pressure value and set temperature value. At the beginning the temperature inside the coreholder is ambient temperature and confining pressure is set confining pressure value. Because the annular space volume is constant, the pressure in the coreholder changes with temperature. We start pressurizing at ambient temperature in the coreholder with a set confining pressure value. We wait for some time for the pressure equilibrium to be established, if there is no change in confining pressure, we increase temperature in the coreholder by temperature increment and monitor the confining pressure. If the confining pressure increases above the set value, we open the purge valve to release the excess pressure and wait until the pressure stabilizes again to set value at this temperature. This procedure is repeated until we reach testing conditions in the coreholder. We increase the temperature we wait and monitor the pressure in the coreholder and if it is higher than set value, we release the pressure until it is set value and keep doing this until we reach testing conditions. We do this procedure because, if we directly set testing conditions there is high risk that core sample fails. Sudden increase in confining pressure can alter the internal pore structure of the core sample, affecting porosity and permeability which in turn directly influence the breakthrough pressure magnitude. Moreover, there is a high risk of fracturing the sample and to prevent this we confine core sample gradually.

Check Equipment Integrity

Before starting the step-by-step test it is essential to confirm that all components of the experimental setup are fully operational and properly secured. A thorough visual inspection and functional check should be conducted to ensure the reliability and accuracy of the measurements. This includes verifying:

- Proper operation of the syringe pump, pressure sensors, valves, BPR and the data acquisition and control system, ensuring that each component responds accurately and consistently with its specifications.
- Verification of the integrity of all tubing and fittings, which is critical given the high-pressure environment and the use of reactive test gases such as hydrogen. All tubing connections must be inspected for mechanical wear, corrosion and correct fitting engagement. Fittings should be torqued according to manufacturer specifications to avoid under- or over-tightening, which can result in leaks. Any leakage not only affects the accuracy of pressure readings and flow measurements but may also cause premature or false indication of breakthrough, compromising the reliability of the results.
- Secure sealing of the coreholder and associated tubing to ensure that test conditions remain stable throughout the experiment.

The step-by-step test should only be started after confirming that the system is free from any mechanical or operational issues.

Test with the fresh sample.

In our standard workflow we run the test with fresh samples directly taken from the storage site, meaning that they have original saturation with formation brine. The reason why we use fresh

samples is because generally caprocks are rich in clay mineral and clay swells when it comes in contact with low-salinity brine (swelling) and there is a modification of the internal pore matrix structure (porosity and permeability change), which directly affects breakthrough pressure magnitude. We try not to saturate the core sample and use a fresh sample in order to keep the chemical balance of clay molecules with brine, and then we try to run the test. Another reason why we use a fresh sample is that generally the full saturation of a sample can take a long time in the laboratory; depending on the core sample, the saturation can take 1 month or more. We fill the syringe pump with hydrogen and start injection. We ran the test with the fresh sample and we failed, because at the beginning of the injection we detected gas bubbles at the downstream indicating breakthrough phenomena. And the pressure corresponding to this phenomenon was much lower than expected breakthrough pressure for the core sample. This may be due to one of the following reasons: either the core sample is not fully saturated or it has fissures (microfractures).

It is maybe because of the evaporation of some brine from the core sample, thus affecting the saturation of the core sample as it is not fully saturated. For this reason, we will saturate the core sample with synthetic brine having the same salinity as the formation brine. The reason why we use a representative synthetic brine is for two reasons:

- To avoid the swelling of the clay (this concerns only clay samples)
- The threshold pressure is sensitive to brine salinity, a synthetic formation brine from which the tested plug was retrieved is recommended in order to obtain a representative breakthrough pressure value

If we resaturate the sample and run the test and obtain the same value of breakthrough pressure as before saturation, it indicates that the core sample contains fissures (microfractures).

Saturation of the core sample

First of all, we try to purge all the hydrogen from the tubing system, because the first step-by-step test failed. Then we fill the syringe pump with the synthetic brine and we start the saturation of the sample. Saturation of the sample may also be performed if there are no fresh samples or the sample is dry or being reused.

For the saturation of the sample, the syringe is initially isolated from the core holder, and the pump piston is set to dead volume mode (Figure 46). The valve on the injection line is then opened, and the line is connected to the brine tank. The pump begins to draw brine into the system, ensuring the syringe is completely filled.

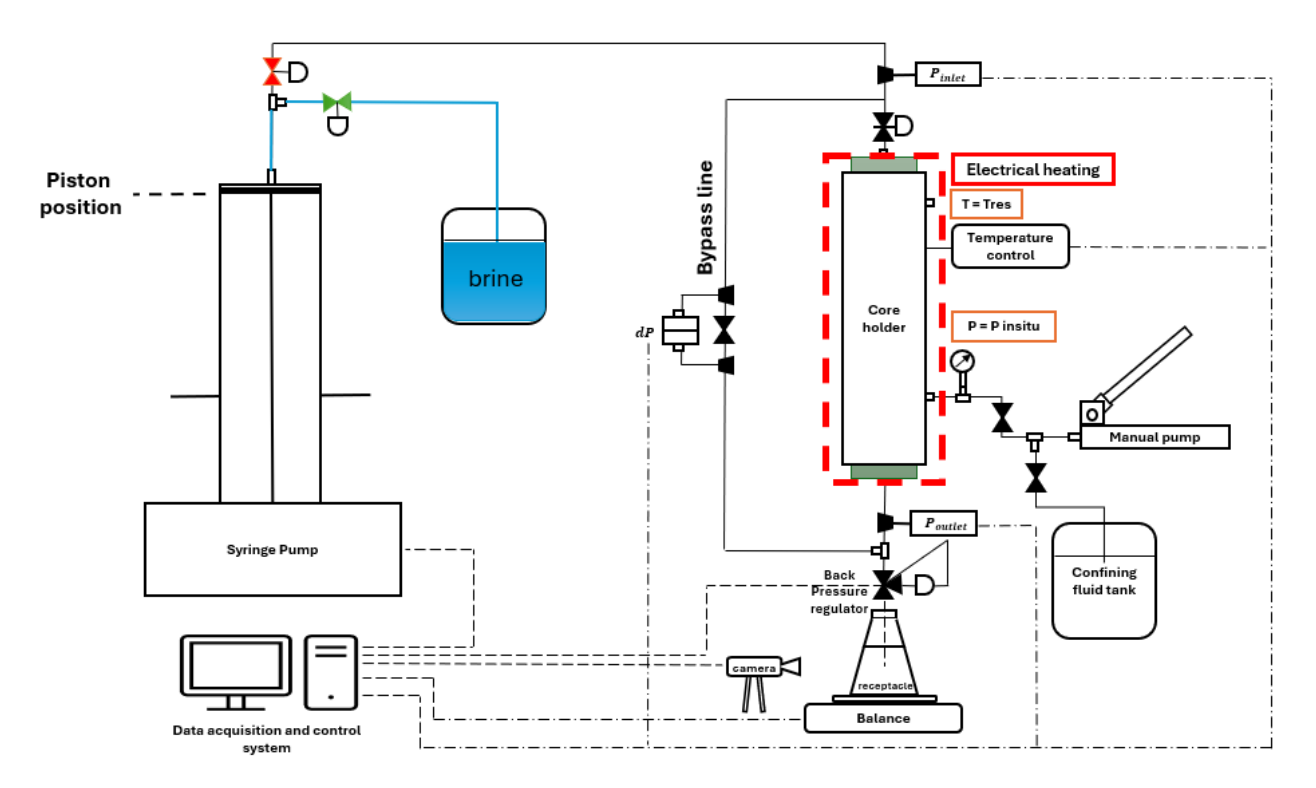


Figure 46. Pump filament with brine phase. Red valve is closed, green valve is open, and blue tubing lines indicate the presence of brine

After the syringe pump is filled, the injection line valve is closed and the upstream valve of the syringe pump is opened, while the bypass line is closed. Brine injection into the core sample then begins at a low flowrate to promote gradual and complete saturation of the porous structure. Injection continues until brine is detected. The syringe pump operates in constant pressure control mode, maintaining a stable injection pressure while continuously delivering brine through the upstream inlet of the coreholder into the core sample (Figure 47). Throughout the process, the syringe pump provides real-time data on the remaining brine volume in the syringe pump.

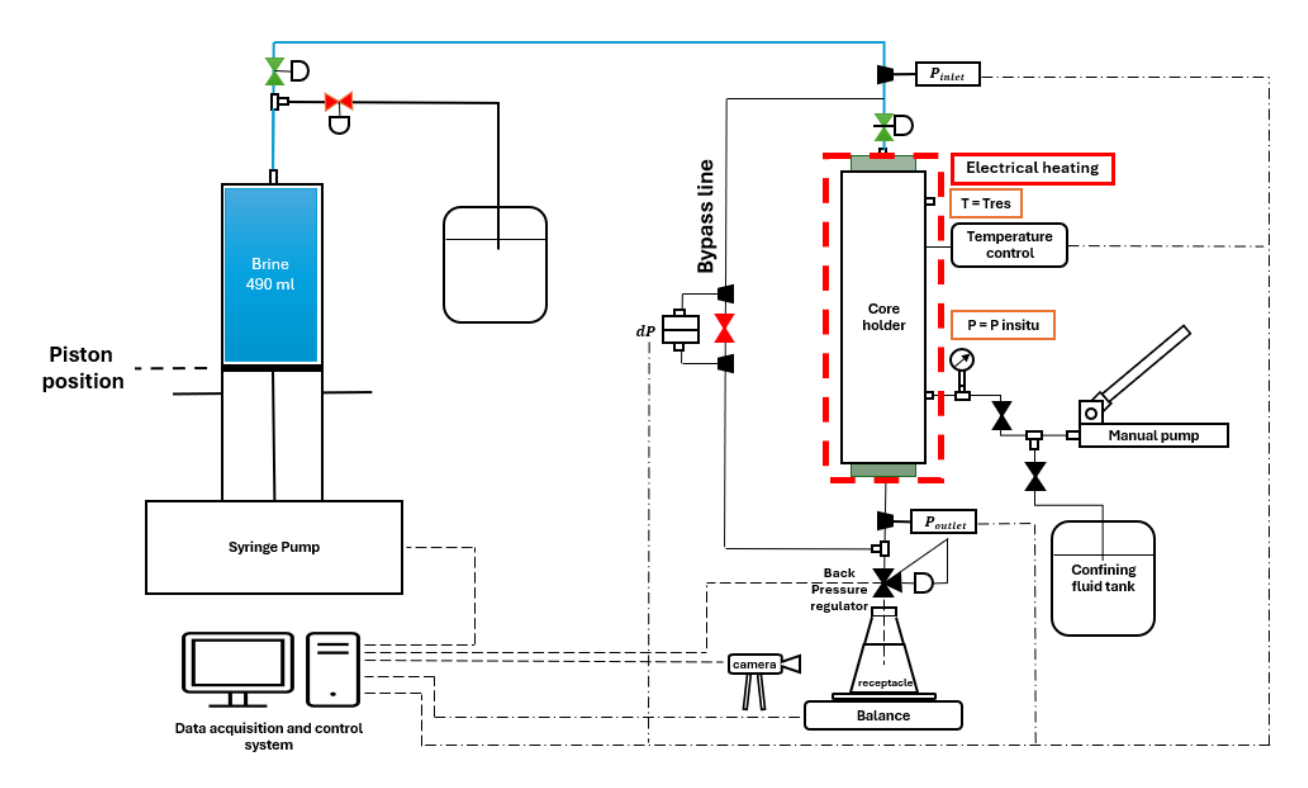


Figure 47. Sample saturation phase. Red valves are closed, green valves are open and blue tubing lines indicate the presence of brine

At this stage, no fluid was detected at the downstream outlet of the coreholder indicating that the core sample is still undergoing saturation. The injected brine displaces air within the pore spaces and air bubbles begin to appear at the outlet.

As saturation progresses, at a certain point small droplets of brine begin to emerge at the downstream outlet. However, this does not indicate that the saturation process is complete, this just means that brine has found the pathway to the bottom. Due to the heterogeneous nature of the rock, the core sample contains different pore throat sizes that require varying pressure differentials for complete saturation. Smaller pores demand a higher-pressure differential (ΔP) to displace trapped air. Consequently, at this stage, the flow at the outlet alternates between air and brine, with an increasing fraction of brine over time. The process continues until a point is reached where only brine flows from the outlet, with no visible air bubbles. This stage indicates the maximum achievable saturation of the core sample under laboratory conditions. It is important to note that 100% saturation cannot be achieved, as there is no direct method to confirm complete brine saturation in low-permeability caprock samples. To further ensure saturation, the pressure is increased by an additional pressure (which is case specific) after observing stable brine flow at the outlet. This ensures that any remaining air is fully displaced. The system is maintained under these conditions for 48 to 72 hours to allow to reach a representative brine saturation of the sample.

Leakage detection and prevention

During the saturation phase, it is important to regularly check the experimental setup for any brine leaks. Because brine is visible and wet, the leak identification is relatively simple. Each connection and joint in the system is inspected by either touching it directly or wrapping absorbent tissue paper (e.g., Scottex) around it. If the tissue become wet, a leak is present. A major challenge arises with inaccessible void spaces inside the core holder, especially upstream of the core holder, as the portion above the sample seat is hollowed out and is inaccessible, which cannot be visually

inspected. To detect leaks in these areas, tissue paper is carefully inserted into the voids and left for about five minutes. If the tissue remains dry, it confirms that no leakage is occurring (Figure 48).







Figure 48. Use of tissue paper to detect brine leakage at inaccessible void spaces within the coreholder and at tubing joints during the saturation phase

Post saturation brine removal and tubing cleaning phase

Following the saturation phase, it is essential to thoroughly remove all remaining brine from the tubing system. Residual brine left in the tubing can lead to salt precipitation, possibly clogging the line. Moreover, for the injection of gas, the tubing must be free of any contamination like salt precipitation or brine, this would not allow simulation of gas-brine displacement, as injecting gas will contact residual brine inside the tubing and spend part its energy to displace this residual brine, leading to pressure losses (pressure drop) and thus leading to wrong threshold pressure measurements. Therefore, a systematic flushing and cleaning procedure is important to maintain equipment performance and ensure the reliability of the measurements.

The cleaning procedure begins by closing the inlet valve to isolate the core holder from the pump. The bypass valve is also closed. The upstream valve of the pump is then opened, and the pump is switched to vacuum mode to create a vacuum pressure of approximately -1 bar. This negative pressure assists in extracting the brine from the tubing network. If the pump is partially filled, the piston position provides an indication of the remaining brine volume in the system. The pump is then instructed to expel the brine completely, discharging it through the outlet line into a collection vessel for potential reuse (Figure 49).

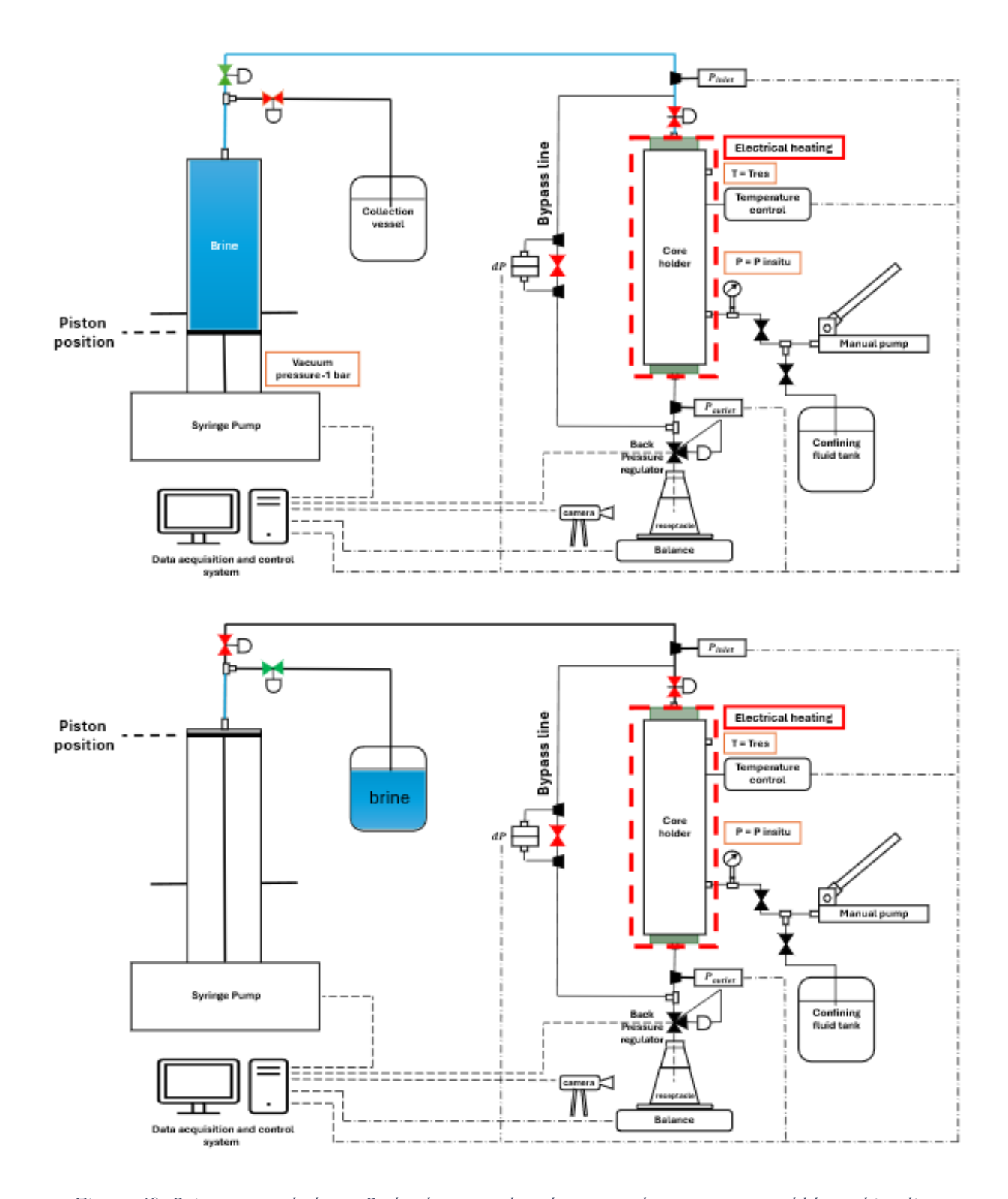


Figure 49. Brine removal phase. Red valves are closed, green valves are open and blue tubing lines indicate the presence of brine

To mitigate the risk of salt precipitation within the tubing, the system is flushed with distilled water to displace and dilute any remaining high salinity brine droplets. The pump is refilled with distilled water and operated to circulate the water through all lines and components. After this initial flush, the system is again evacuated using vacuum mode to remove the distilled water. This flushing and purging cycle is repeated multiple times to ensure complete removal of brine and any salt deposits. Each cycle enhances the cleanliness of the system. By rigorously following this cleaning phase, the system is ensured to be free of brine and suitable for the next phase of the experiment.

Breakthrough pressure measurement phase

Once the core sample has been fully saturated with brine, we proceed to fill the syringe pump with hydrogen and start the step-by-step test. For this the syringe pump is filled with hydrogen gas, and it is then connected to the upstream (Figure 50). The initial conditions of the test simulate in-situ conditions. To begin the test, we open bypass valve and set the BPR to the initial test pressure (P_0). The tubing system is filled with hydrogen gas, ensuring that both the inlet and outlet of the coreholder are maintained at the same pressure (Figure 51). Once this condition is established, we close bypass line to isolate the downstream from upstream. At time zero, the inlet (P_0) and outlet (P_0) pressures are equal and the pressure difference (P_0) is zero (Figure 52).

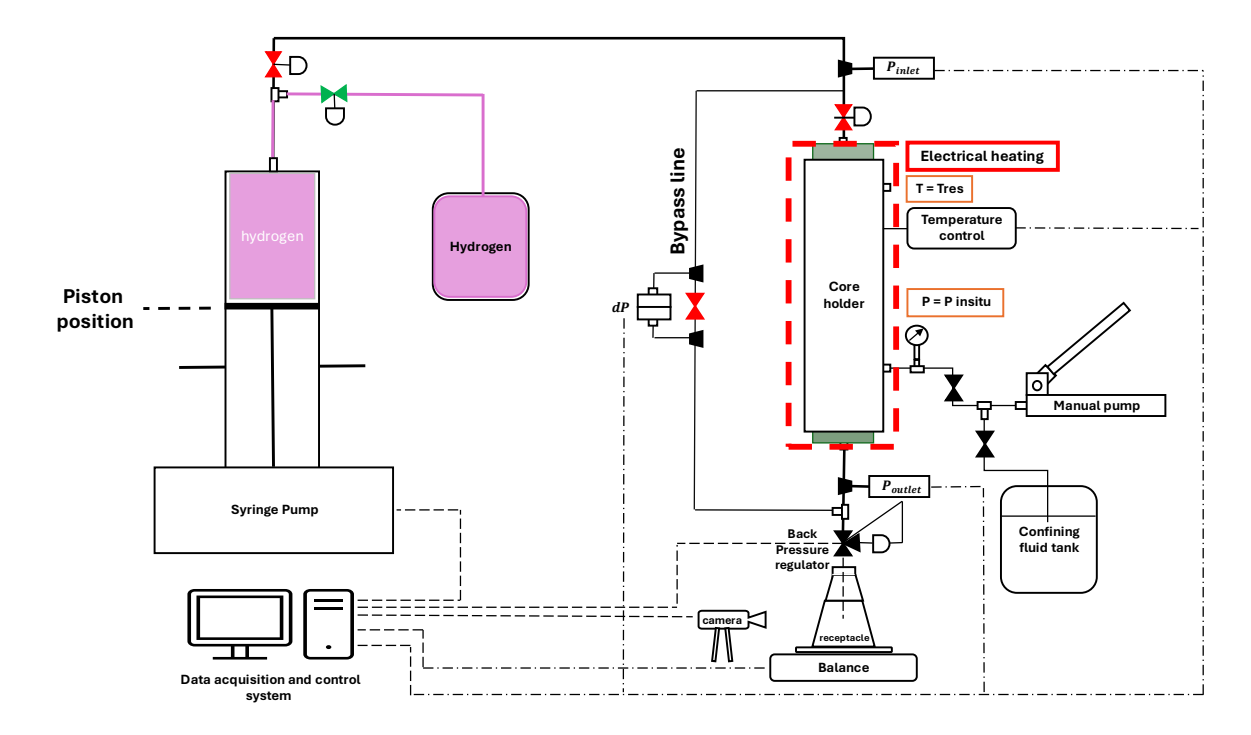


Figure 50. Pump filament with hydrogen phase. Red valve is closed, green valve is open, and purple tubing lines indicate the presence of hydrogen

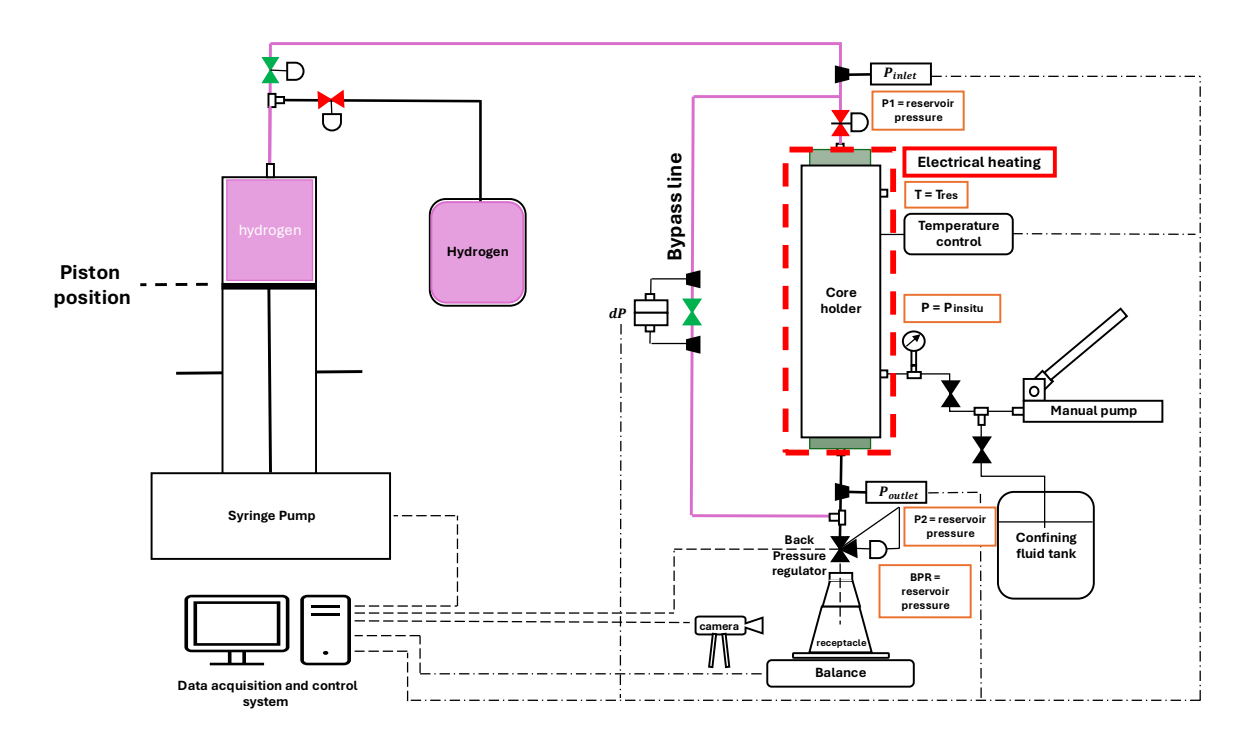


Figure 51. Applying initial reservoir conditions, bypass line is open.

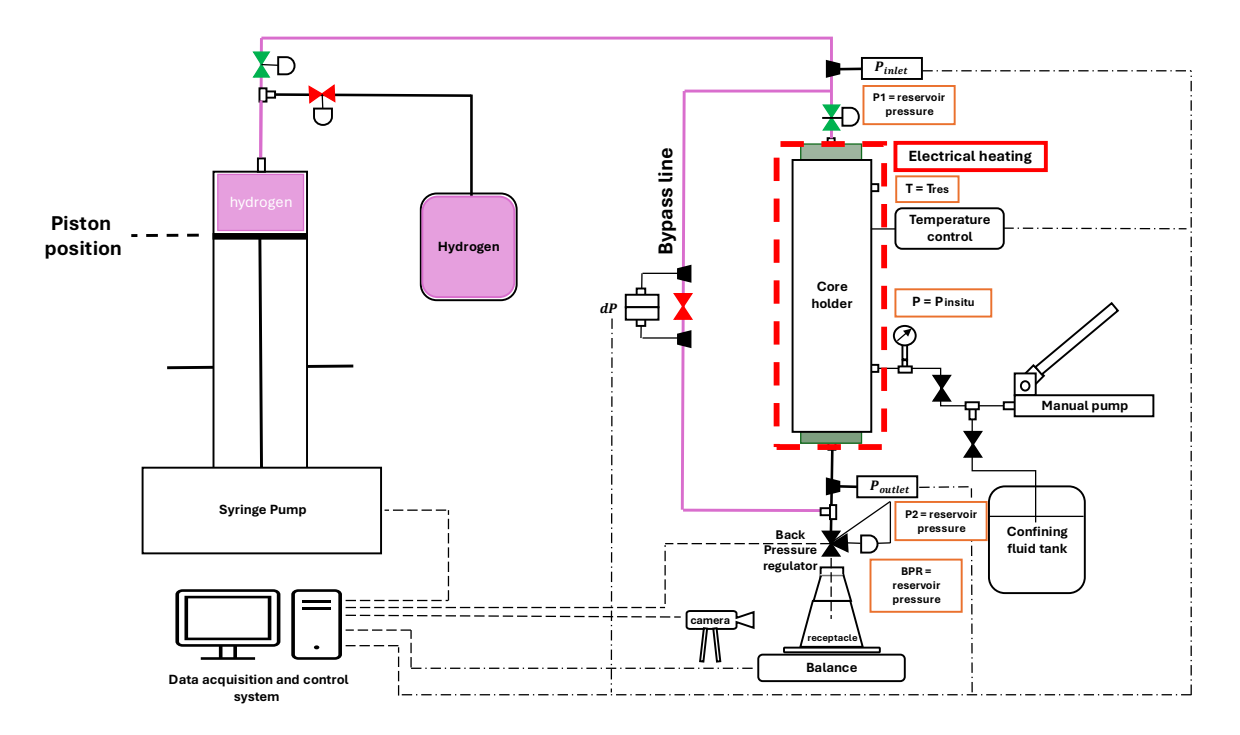


Figure 52. At time 0, the system at initial reservoir conditions, inlet and outlet pressures equal to reservoir pressure. BPR set to reservoir pressure. Delta P is zero, bypass line is closed.

After each pressure increment, the system was checked for hydrogen leaks. For this purpose, either gas detection foam or an electronic gas detector was used (Figure 53). The gas detection foam was sprayed over potential leak points, such as connections and fittings, where the presence of gas leak would be indicated by bubble formation. While for the gas detector, its sensor nozzle would be aimed at these points and indicate the gas concentration in the air in ppm.







Figure 53. Hydrogen leak detection using the bubble method and gas detector at high-risk locations including coreholder inlet and outlet, pump joints and tubing connections

The test begins by pushing the piston and applying an initial pressure differential (ΔP), which is case specific. The pressure is gradually increased in ΔP increments, and we monitor the system for any changes. Pressure increment plays important role in the test, the smaller pressure step increment gives higher accuracy and higher duration, while bigger pressure step increment gives overestimation of breakthrough pressure.

The waiting time between each step is determined by various criteria. One of the primary indicators is the volume reading from the piston. If the volume of hydrogen injected into the core does not change despite the pump maintaining constant pressure, it suggests that gas is not yet entering the sample. Since caprock core sample has very low permeability, it may take longer time to reach capillary equilibrium, some days or even weeks. Therefore, we use increasingly longer time steps. Coupled with that we monitor volumetric variation of the pump upstream. If no variation in volume is observed within this time frame, it indicates that we can proceed to the next step, where the pressure is incrementally increased by ΔP increments. We continue this process until we observe a measurable change in volume, which indicates that gas has started to enter the sample. The flowrate accuracy of 0.05 ml/min when conducting test with low permeability caprock samples the syringe pump can read flowrate change above 0.05 ml/min. but in case of ultra-low permeability caprock samples the flowrate can be very low below 0.05 ml/min and syringe pump cannot read this, for this reason we measure volumetric variation in every 5 minutes and then convert it into flowrate for relative permeability measurements.

If the syringe pump has injected all the hydrogen and we still haven't reached the breakthrough phenomenon, we can fill the pump with hydrogen and continue the injection. For this, we isolate the coreholder from the syringe pump, then the dead volume upstream to the coreholder will maintain the pressure at the inlet constant. The pump's pressure is then reduced in order to prepare for gas intake from the tank and increase its volume as it has reached 0 ml before end of the test. Once the pump is recharged, we close the tank line and increase its pressure back the current pressure step of the test. Then we connect it again to the dead volume and proceed with increasing the inlet pressure to reach the following step.

The entry of gas is monitored using a video camera, which allows us to visually confirm the displacement of brine. As the gas displaces the brine inside the sample, we observe the brine droplets produced into the receptacle. The appearance of brine at the outlet is a clear indicator that drainage has started, which can potentially signify **the entry pressure**. However, it is important to

recognize that brine displacement does not necessarily correlate directly with the entry pressure. This is because the sample may not be 100% saturated, and the gas may penetrate and displace brine in certain regions of the sample without visible signs of displacement at the outlet.

Once brine displacement is observed, we continue to wait until there is no further brine flow, typically for 24 hours, to ensure that the system has reached a stable condition. At this point, we proceed to the next pressure increment and repeat the process. This cycle continues until we observe the presence of gas bubbles at the outlet, indicating that the gas has successfully penetrated the sample. The appearance of gas bubbles signifies that we have reached the breakthrough pressure, which is the point at which the gas has established a continuous flow path from the inlet to the outlet (Figure 54).

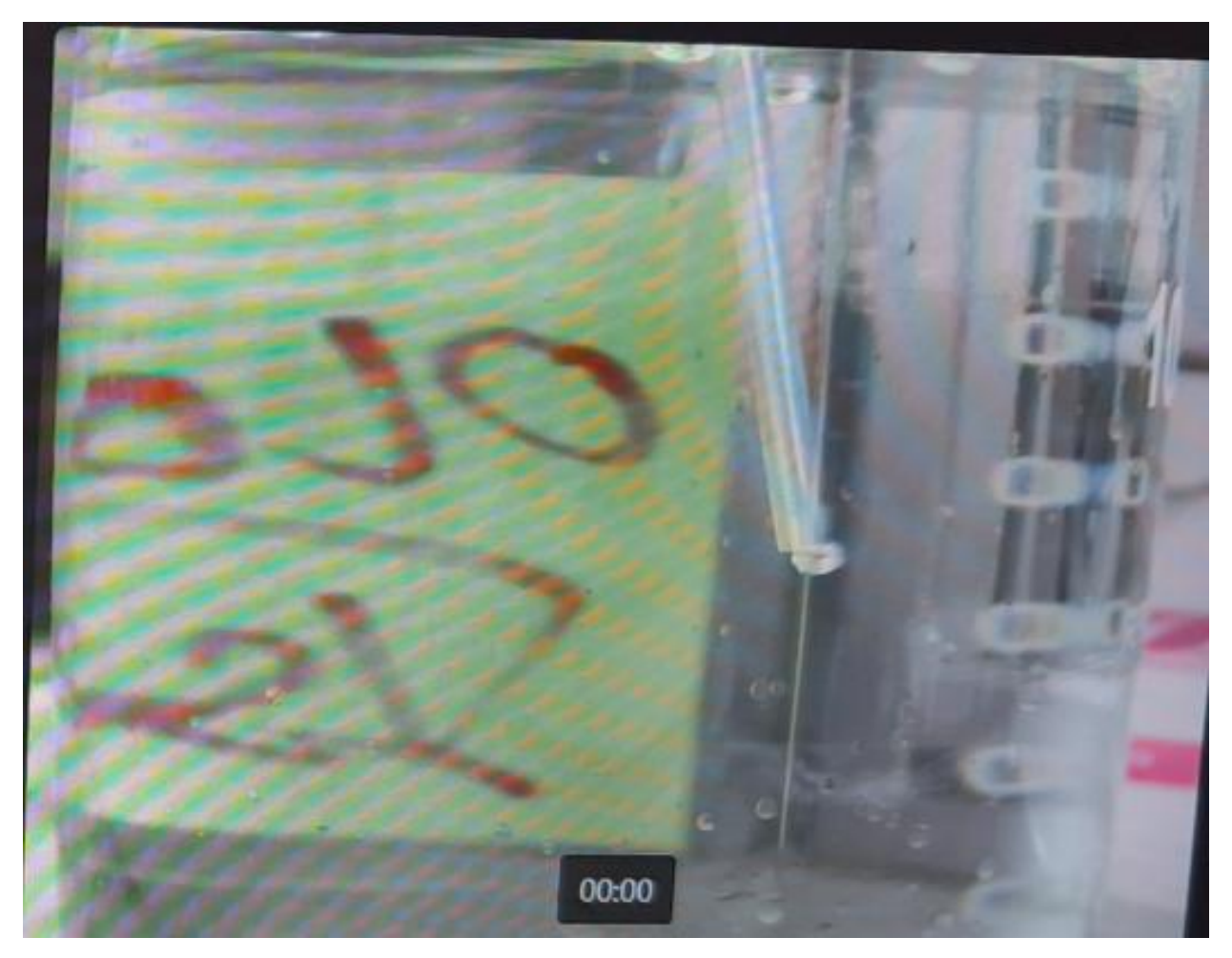


Figure 54. Gas bubble appearance at the receptacle indicating gas breakthrough

Upon confirming the breakthrough pressure, the test is complete, and we document the results. The **breakthrough pressure** is considered the pressure at which gas begins to flow continuously through the sample.

Measurement of gas relative permeability

After reaching the breakthrough pressure we continue to increase the gas pressure equivalent to two pressure steps and apply that pressure gradient for 48 hours to ensure that no additional brine is displaced from the sample. As the saturation of brine in the core must be constant for accurate measurements of gas relative permeability. At this point, we can measure the relative permeability

to gas (Krg). It is important to note that the measurements may be influenced by the Klinkenberg effect (see Figure 36), which occurs due to gas slippage in tight caprocks. This effect can cause the measured permeability to differ from the true absolute permeability. To account for this, we perform permeability measurements at different gas flowrates and differential pressures (ΔP). By increasing the differential pressure, we may observe different Krg measurements based on different ΔP .

Main advantages of the experimental setup

- Allows to conduct **step-by-step test with different gases** (hydrogen, methane, carbon dioxide, nitrogen), as the system components are made of **Hastelloy** steel.
- Receptacle and camera are complementary to the balance. Camera is used to monitor the presence of fluid coming out at the outlet. The balance is meant to measure the mass variation over time and then convert it into flowrate, but when we test certain types of core samples, for example ultra-low permeability caprock samples, the leak of brine is very limited at the outlet, and the sensitivity of the mass balance cannot read it. Also, because the test takes months, we don't know when the brine production starts. To observe this, we use receptacle with a camera. The receptacle is filled with transparent oil, and the reason is that if we fill it up with water and the brine starts to be produced, we cannot see and distinguish it because the density of the brine (coming out from the coreholder outlet) and the water in the receptacle are almost the same. What we do instead is fill it with transparent oil to clearly see and detect brine production (droplets), because brine is denser than oil and by gravity it will go down and we can see it clearly. In case if it is gas, the gas will go up. This is the advantage of our laboratory setup.

Limitations

Despite the many advantages of our laboratory setup, several limitations were identified during the experimental procedures that could potentially affect the accuracy and reliability of the results. Addressing these limitations through targeted improvements is essential for enhancing experimental performance and data quality.

- **Manual operation of valves.** While the syringe pump operation is controlled by software, the valves require manual adjustments and limits quick intervention in case of emergency unless an operator is physical present in the laboratory.
- The confining pressure gauge can only be ready in presence, limiting the monitoring precision
- Limited accessibility for leak repair in coreholder design. While leaks can be detected during testing, the current coreholder design does not allow sufficient physical access to the inlet and outlet joints for timely maintenance or corrective action. As a result, any detected leaks cannot be addressed without interrupting or stopping the experiment. This limitation poses operational challenges, potentially affecting test continuity and data reliability.
- Temperature fluctuations and their impact on the accuracy of experimental results. Although both the coreholder and the syringe pump are equipped with temperature control systems, the tubing that connects them remains exposed to ambient temperature. Despite the fact that tubing has insulation to decrease heat dissipation, the tubing still has heat loses to the ambient, particularly during day and night. This is particularly problematic during long-duration tests, where upstream pressure is increased and the system is left to stabilize over several days. Because when we are testing at high temperature the coreholder set at that temperature, the pump is set at that temperature, but the tubing is not set to that temperature,

because it is in contact with ambient, there is some heat dissipation. And because the pump is set to constant temperature, the volume inside the pump will decrease slowly. The pressure is constant, but the volume is changing. The operator is reading the volume change, and the operator cannot differentiate whether this volume decrease is related to the temperature difference or if some gas has entered the sample.

5.3. Recommendations

- Implement Active Electrical Heating for Tubing Insulation. Despite the fact that tubing has insulation, there are still some heat losses. To minimize temperature fluctuations and stabilize pressure throughout the experiment, it is recommended to insulate the tubing system using active electrical heating. Active electrical heating refers to the use of electrically powered heating cables or tapes wrapped around the tubing to maintain a uniform temperature along its length. The active electrical heating for tubing insulation can be integrated with the existing electrical heating system currently used for coreholder heating. By preventing heat loss to the surroundings, active electrical heating helps preserve fluid properties and minimizes pressure variations caused by ambient temperature changes, resulting in more consistent and reliable experimental conditions.
- Redesign and improve the coreholder assembly. Modify the coreholder to provide better access and visibility to inlet and outlet joints by introducing modular end fittings (modular design). This can be achieved by incorporating transparent sections or accessible inspection points, facilitating easier and more frequent leak checks and maintenance. A modular design would allow local access to the inlet and outlet joints, enabling targeted maintenance or replacement of component without dismantling the entire system. Improved leak detection will enhance system integrity and the accuracy of the results.
- Upgrade software for full automation of control valves. Develop or integrate software that allows remote and automated operation of control valves in addition to the pump. Automation of these components will reduce the risk of human error and increase control precision.
- Install an additional BPR in the confining line of the coreholder to automatically control the confining pressure in the coreholder during confining phase at different temperatures. The BPR can be set to the desired confining pressure and monitored and controlled with data acquisition and control system. When we start pressurizing gradually the coreholder, BPR will automatically regulate pressure and keep it at set confining pressure value. This will allow to minimize human error, as the process was controlled manually by operator before, and ensure more efficient and safe confinement of the core sample.
- Use nitrogen gas for the flushing of the tubing system after it has been flushed several times with distilled water. The distilled water removes any salt particles from the tubing system, however, after water flushing a thin film of water may remain on the internal surface of the small-diameter tubing (1/16 inch) due to interfacial tension (capillary effects). Subsequent flushing with nitrogen helps to remove this residual water film and dry the tubings completely, ensuring stable and accurate pressure conditions during the test. The reason why we should use nitrogen is that it is preferred over air because it is inert and does not react with hydrogen, CO₂, or other gases used in the experiments, whereas air contains oxygen, which could lead to oxidation or unwanted reactions. Inert gas flushing is standard practice for sensitive gas systems. Although air could be used in non-reactive scenarios, it carries a higher risk of contamination or oxidation. In our case, either nitrogen or air can be used because of tubing made of Hastelloy, but as standard practice we suggest using nitrogen.

The modified laboratory setup incorporating the recommendations is shown in Figure 55. The tubing system has been upgraded with an active electrical heating system, enabling consistent temperature control throughout the duration of the experiment. This modification is critical for minimizing pressure fluctuations due to ambient temperature changes, thereby enhancing the stability and reliability of pressure-sensitive measurements. Additionally, an extra backpressure regulator (BPR) has been installed in the confining line. Together, these modifications significantly improve the operation of the lab setup, decreases human errors and improve accuracy and reliability of the breakthrough pressure measurements.

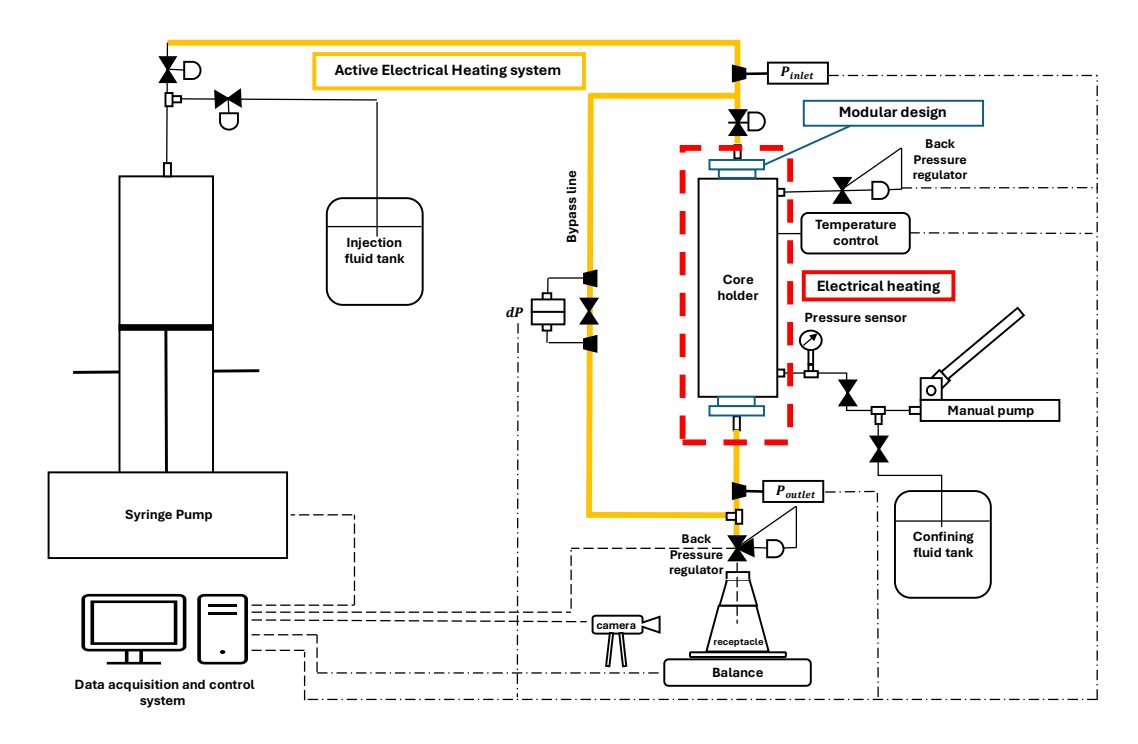


Figure 55. Modified diagram of the laboratory setup

6. Conclusion

This thesis presents a comprehensive investigation into laboratory methods for evaluating the sealing efficiency of caprocks through capillary breakthrough pressure measurements. A detailed review of existing experimental approaches was conducted, focusing on both direct and indirect methods. Among these, the Standard Test, also known as the Step-by-Step test, was identified as the most representative and reliable method for assessing caprock sealing efficiency under various gas exposures.

Building on this foundation, the core contribution of this work lies in the development and implementation of a standardized laboratory protocol tailored specifically for the Step-by-Step test. This protocol was designed to ensure accuracy, repeatability, and applicability to multiple gases, including hydrogen, which is of growing importance in UHS research. The customized laboratory setup was critically evaluated and optimized through technical improvements in temperature control, pressure stability, and system automation, resulting in enhanced measurement reliability.

The outcomes of this research provide a robust and practical methodology for measuring capillary breakthrough pressure, which is crucial for selecting suitable underground hydrogen storage sites,

defining operational parameters and minimizing leakage risks. By establishing a clear and standardized procedure, this work advances the development of safe and efficient UHS technologies, contributing to the broader adoption of hydrogen as a clean energy solution.

Bibliography

- [1] U. Nations, «Paris Agreement,» 2015.
- [2] Z. Kai, H. Liu, J. Liangliang, J. Shu, Y. Ruyang, C. L. Hon, X. Congjiao and C. Zhangxin, "The role of hydrogen in the energy transition of the oil and gas industry," *Energy Reviews*, vol. 3, no. 4, 2024.
- [3] O. D. Kwamena, A. William, R. Hamid and M. Mohamed, "Underground Hydrogen Storage: Transforming Subsurface Science into Sustainable Energy Solutions," *Energies*, vol. 18, no. 3, p. 748, 2025.
- [4] Statista, "Forecast Hydrogen Storage Capacity Worldwide," [Online]. Available: https://www.statista.com/statistics/150032%209/hydrogen-storage-capacity-forecast-global/.
- [5] N. G. H. Company, "NEOM Green Hydrogen Company," [Online]. Available: https://nghc.com/.
- [6] Z. Lingping, V. Stephanie, E.-K. Jonathan, E. Lionel, S. Mohammad, S. Joel, D. Jeremie, G. Ausama and X. Quan, "Role of geochemical reactions on caprock integrity during underground hydrogen storage," *Journal of Energy Storage*, vol. 65, 2023.
- [7] S. M. Nasiru, H. Bashirul, A. S. Dhafer, A.-A. Amir, M. R. Mohammed and Z. Ehsan, "A review on underground hydrogen storage: Insight into geological sites, influencing factors and future outlook," *Energy Reports*, vol. 8, pp. 461-499, 2022.
- [8] W. Jinkai, W. Rui, W. Mingzhen, B. Baojun, X. Jun and L. Yuhan, "A comprehensive review of site selection, experiment and numerical simulation for underground hydrogen storage," *Gas Science and Engineering*, vol. 118, 2023.
- [9] L. Guangyao, Y. Wei, C. Zhangxin, L. Zhong, L. Benjieming, D. Peng, Z. Chen, L. Wanqing and Q. Haotian, "Technical challenges and opportunities of hydrogen storage: A comprehensive review on different types of underground storage," *Journal of Energy Storage*, vol. 114, 2025.
- [10] D. Shadfar, A.-S. Mohammed, A. W. David, O. L. Promise, M. Mohammad and S. R. Valeriy, "Underground hydrogen storage: A review of technological developments, challenges, and opportunities," *Applied Energy*, vol. 381, 2025.
- [11] Inkosas, "Corrosion-resistant alloys. Hastelloy C-276 Alloy," [Online]. Available: https://www.inkosas.cz/download/niklove-slitiny/hastelloy-c-276.pdf.
- [12] EMERSON, "Chemical Compatibility of Elastomers and Metals," [Online]. Available: https://documentation.emersonprocess.com/intradoccgi/groups/public/documents/reference/d351798x012_06.pdf.
- [13] F. Ahmed и A.-Y. Ahmed, «Geomechanical integrity and geochemical reactions of shale caprocks for hydrogen storage: A comprehensive review,» *Fuel*, т. 400, 2025.
- [14] Y. Chen, Y. Xinran, L. Peijin, S. Xijie, H. Weimin, L. Yuxing, C. Zhangxing, L. Cuiwei and W. Keliu, "From micro to macro: A comprehensive review for underground hydrogen storage technologies and challenges," *Renewable and Sustainable Energy Reviews*, vol. 224, 2025.

- [15] M. D. Z. L. S. H. H. Q. E. N. S. Li, "Gas breakthrough pressure for hydrocarbon reservoir seal rocks: Implications for the security of long-term CO2 storage in the Weyburn field," *Geofluids*, vol. 5, no. 4, pp. 326-334, 2005.
- [16] P. Bin, Y. Xia, J. Yang and I. Stefan, "Underground hydrogen storage: Influencing parameters and future outlook," *Advances in Colloid and Interface Science*, vol. 294, 2021.
- [17] H. Milad and S. Behnam, "Understanding caprock integrity in underground hydrogen storage: A geochemical study of mineral alteration and sealing efficiency," *International Journal of Hydrogen Energy*, vol. 154, 2025.
- [18] X. Yi, L. Jia, L. Xin, W. Songhe, M. Zongyuan, Z. Shaowei and J. Xuanye, "Influence mechanism of brine-gas two-phase flow on sealing property of anisotropic caprock for hydrogen and carbon energy underground storage," *International Journal of Hydrogen Energy*, vol. 48, no. 30, pp. 11287-11302, 2023.
- [19] V. Rocca, Sealing efficiency of cap cork, P. d. Torino, Ed., Turin, 2024.
- [20] S. S. B. M. K. A. Hildenbrand, "Gas breakthrough experiments on fine-grained sedimentary rocks," *Geofluids*, vol. 2, no. 1, pp. 3-23, 2002.
- [21] T. Wu, P. Zhejun, L. D. Connell, B. Liu, X. Fu and Z. Xue, "Gas breakthrough pressure of tight rocks: A review of experimental methods and data," *Journal of Natural Gas Science and Engineering*, vol. 81, no. 103408, 2020.
- [22] W. Purcell, "Capillary Pressures Their Measurement Using Mercury and the Calculation of Permeability Therefrom," *Journal of Petroleum Technology*, vol. 1, no. 2, 1949.
- [23] S. Schlomer and B.M. Krooss, "Experimental characterisation of the hydrocarbon sealing efficiency of cap rocks," *Marine and Petroleum Geology*, vol. 14, no. 5, pp. 565-580, 1997.
- [24] B. Andreas and A.-H. Alexandra, "Predicting capillary of mudrocks," *Marine and Petroleum Geology*, vol. 45, pp. 208-223, 2013.
- [25] Thomas L.K. и Katz D.L., «Threshold Pressure Phenomena in Porous Media,» *Society of Petroleum Engineers Journal*, т. 8, pp. 174-184, 1968.
- [26] J. M. L. P. B. P. Egermann, "A fast and accurate method to measure threshold capillary pressure of caprocks under representative conditions," in *International Symposium of the Society of Core Analysis*, Trondheim, Norway, 2006.
- [27] R. Amirsaman, A. T.-N. Seyyed, K. Elnaz and K. Mosayyeb, "A laboratory study on capillary sealing efficiency of Iranian shale and anhydrite caprocks," *Marine and Petroleum Geology*, vol. 66, no. 4, pp. 817-828, September 2015.
- [28] D. Viberti, Fluid Mechanics in Porous Media, Turin: Politecnico di Torino, 2022, pp. 30-35.
- [29] K. Lukasz and S. Rafal, "LABORATORY METHOD TO MEASURE SEALING CAPACITY OF CAPROCKS," *Archives of Mining Sciences*, vol. 57, no. 2, pp. 471-481, 2012.